Volume 6, No. 5

December, 1960

THE SOVIET JOURNAL OF

ATOMIC ENERGY

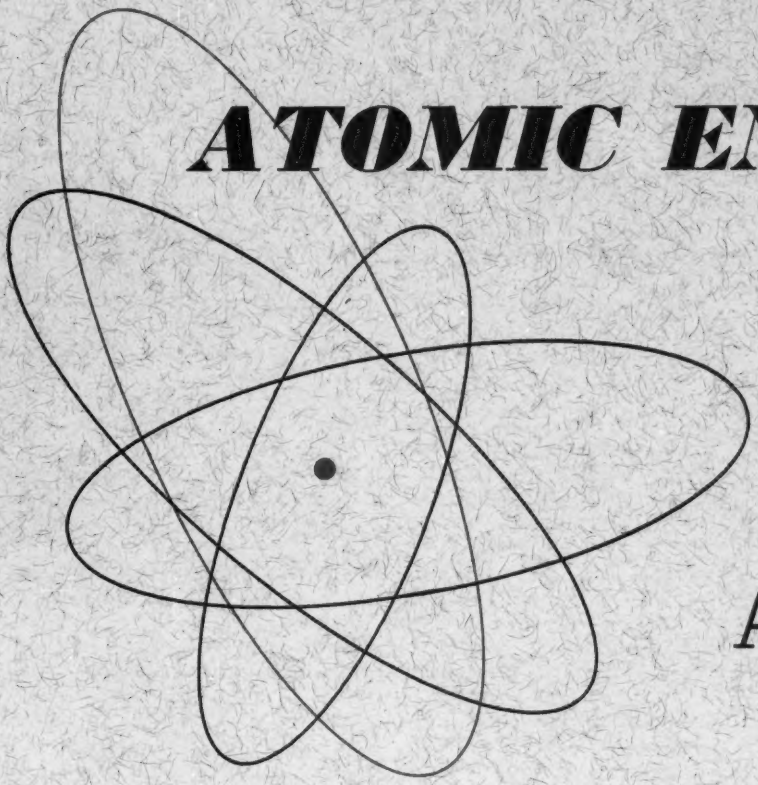

Атомная энергия

TRANSLATED FROM RUSSIAN

CONSULTANTS BUREAU

Now available . . . an insight into the Soviet problems and achievements in . . .

PRODUCTION of ISOTOPES

The eighteen papers which comprise this volume were originally read at the All-Union Scientific and Technical Conference on the Application of Radioactive Isotopes, Moscow, 1957. The reports consider the problems and achievements of Soviet scientists in the production of radioactive isotopes by irradiation of targets in Soviet reactors and cyclotrons. Not only is this work of significance to producers of isotopes, but many of the papers will prove useful to isotope users as well.

The Development of Isotope Production in the USSR.
Certain Aspects of the Production of Radioactive Isotopes in a Nuclear Reactor.
Production of Radioactive Isotopes in a 10-Mev Deuteron Cyclotron.
Determination of Product Yields in Nuclear Reactions.
Spectrochemical Methods of Analyzing High-Purity Materials Used in Reactor Construction and for the Production of Radioisotopes.
Quantitative Spectral Determination of Impurities in Radioactive Preparations.
The Production of Alpha-, Beta-, and Gamma-Sources Using Oxide Films on Aluminum and Its Alloys.
Stable Isotopes Enriched by the Electromagnetic Method.
Ultrahigh-Temperature Ion Source for Electromagnetic Separation of Isotopes of Elements in the Platinum Group.
Inhomogeneous-Field Mass-Spectrometer for Analysis of Light-Element Isotopes.
The Relative Abundance of Palladium and Germanium Isotopes.
Some Problems in the Theory of Isotope Separation.
Separation of Isotopes of Light Elements by Diffusion in Vapors.
A Diffusion Column for the Separation of Isotopes.
A Fractionating Column for Preparing BF_3 Enriched in the Isotope B^{10}.
An Investigation of the Separation of the Stable Isotopes of Light Elements.
The Separation of Carbon Isotopes.
Low-Temperature Methods for Separating Helium Isotopes ($He^3 - He^4$).

1959 durable paper covers 136 pp. $50.00

c b CONSULTANTS BUREAU
227 WEST 17th STREET NEW YORK 11 N. Y.

EDITORIAL BOARD OF ATOMNAYA ÉNERGIYA
A. I. Alikhanov
A. A. Bochvar
N. A. Dollezhal
D. V. Efremov
V. S. Fursov
V. F. Kalinin
A. K. Krasin
A. V. Lebedinskii
A. I. Leipunskii
I. I. Novikov
(Editor-in-Chief)
B. V. Semenov
(Executive Secretary)
V. I. Veksler
A. P. Vinogradov
N. A. Vlasov
(Assistant Editor-in-Chief)
A. P. Zefirov

THE SOVIET JOURNAL OF

ATOMIC ENERGY

A translation of ATOMNAYA ÉNERGIYA, a publication of the Academy of Sciences of the USSR

(Russian original dated May, 1959)

Vol. 6, No. 5 December, 1960

CONTENTS

	PAGE	RUSS. PAGE
Half a Century of a Great Book. The Fiftieth Anniversary of the Publishing of "Materialism and Empirocriticism," by V. I. Lenin. L. A. Druyanov	363	509
Laureates of the Lenin Prize for Construction of the 10 Bev Synchrophasotron	366	insert
Application of Sorption and Solvent-Extraction Processes in the Hydrometallurgy of Uranium. B. S. Kolychev	368	513
Chemical Behavior of Mo^{99} Formed by the Irradiation of Uranium Oxide with Slow Neutrons. L. V. Shiryaeva and Yu. M. Tolmachev	381	528
Dissociation of the UF_6 Molecule under the Action of Fragments from Fission of the Uranium Nucleus. V. A. Dmitrievskii and A. I. Migachev	385	533
Radiation Vulcanization of Fluorine Copolymers. F. A. Galil-Ogly, T. S. Nikitina, T. N. Dyumaeva, A. S. Novikov, and A. S. Kuz'minskii	391	540
On an Approximate Method for the Homogenization of a Heterogeneous Reactor. V. V. Smelov	396	546
Complete Symmetry and Isotropic Spin Conservation in the Nonleptonic Decay of Hyperons. Gyo Takeda and M. Kato	404	556
Letters to the Editor		
The Problem of the Use of Organic Compounds as Moderators in Nuclear Reactors. B. G. Dubovskii and M. N. Lantsov	411	563
Calculation of Heat Generated in a Shutdown Reactor. T. N. Zubarev and A. K. Sokolov	413	564
Dilatometric Studies of Rolled Uranium Rods. L. V. Batenin, A. N. Rudenko, and B. V. Sharov	414	565
Radioactivation Determination of Beryllium. Kh. B. Mezhiborskaya	416	567
Radiation Changes of Some Physical Properties of Graphites with Different Degrees of Graphitization. Yu. N. Aleksenko and L. E. Kakushadze	417	568
Total Cross Section of Np^{237} in the 2–10,000 ev Energy Region. Yu. V. Adamchuk, S. S. Moskalev, and M. I. Pevzner	420	569
On the Existence of Light Nuclei with Large Neutron or Proton Excess. A. I. Baz'	422	571
Detection of Slow Neutrons by the Capture γ Rays of Cadmium during Measurements of the Moisture Content of Organic and Inorganic Soils by the Neutron Method. V. A. Emel'yanov and V. E. Nesterov	424	573
Measurement of the Hard Portion of the Neutron Spectrum in a BR-5 Reactor by Use of an Ionization Chamber Containing He^3. A. I. Abramov and M. G. Yutkin	427	575
Yields of Ru^{103} and Ru^{106} on Fission of U^{235} and Pu^{239} by Fast Neutrons. M. A. Bak, S. S. Bugorkov, T. A. Il'inskaya, Yu. G. Petrov, K. A. Petrzhak, V. M. Solntsev, A. V. Sorokina, and V. N. Ushatskii	429	577
Neutron Energy Dependence of Removal Cross Sections of H_2O, B_4C, C, Fe, and Pb. D. L. Broder, A. A. Kutuzov, and A. P. Kondrashov	431	578

Annual subscription $75.00
Single issue 20.00
Single article 12.50

Copyright 1960 Consultants Bureau Enterprises, Inc., 227 West 17th St., New York 11, N. Y.
Note: The sale of photostatic copies of any portion of this copyright translation is expressly prohibited by the copyright owners.

CONTENTS (continued)

	PAGE	RUSS. PAGE
Average Energy of β Particles at Various Depths of an Atmosphere-Equivalent Medium. V. P. Kasatkin	434	581
New Positron Activities in Neutron-Deficient Isotopes of Lutetium, Ytterbium, and Holmium. A. V. Kalyamin, I. Ya. Levenberg, and V. A. Yakovlev	435	582
Annular Shielding of Chromatographic Columns in Work with Radioactive Isotopes. A. A. Goryunov	436	582
On the Equilibrium Shift between Radon and Its Decay Products in the Air Stream. Yu. P. Bulashevich and N. P. Kartashov	438	584
Propagation of Co^{60} Radiation in the Air Above the Earth. O. I. Leipunskii and V. N. Sakharov	440	585
News of Science and Technology		
[Start-up of a Reactor for Heat Supply and Generation of Electric Power		588]
[The Utilization of Critical Yield in American Nuclear-Reactor Engineering. Source: Nucleonics 16, No. 12, 39 (1958)		591]
[Nuclear Reactors of the Western European Nations		595]
Alloys of Uranium with Platinum Series Metals	443	599
[High Radiation Level. Hydrocyclone Centrifuging Removes Homogeneous Reactor Fission Products. Source: Chem. Engr. Progr. 54, No. 2, 79 (1958)		602]
[The "Atomic Industrial Forum" Association		603]
Brief Communications	445	603
Information and Bibliography		
Terms and Definitions	447	605
New Literature	447	605

NOTE

The Table of Contents lists all material that appears in Atomnaya Énergiya. Those items that originated in the English language are not included in the translation and are shown enclosed in brackets. Whenever possible, the English-language source containing the omitted reports will be given.

Consultants Bureau Enterprises, Inc.

HALF A CENTURY OF A GREAT BOOK

L. A. Druyanov

(The fiftieth anniversary of the publishing of "Materialism and Empirocriticism," by V. I. Lenin)

The book "Materialism and Empirocriticism" was written by V. I. Lenin in the period of political reaction which had set in in Russia after the defeat of the 1905 Revolution.

The book, in the form of a militant Communist Party philosophy, was a brilliant and creative development of Marxism. Written half a century ago, it has not only not become dated, but,to a certain extent,has grown more timely. It belongs to the number of those infrequent productions of human genius whose value does not disappear with time.

A real revolution took place in natural science in the nineteenth and the beginning of the twentieth centuries, which destroyed the traditional views of many scientists. Discoveries were made of X rays and radioactivity; an experimental proof of the existence of the electron was obtained; the quantum hypothesis, the special theory of relativity, etc., were formulated. These discoveries undermined the belief of scientists in the truth of the so-called mechanistic picture of the world, in the universality of the laws of mechanics, in the indivisible and indestructible atom, etc.

At the same time that they widened and deepened the notions of physicists about the structure of matter and the forms of its motion, of space and time, etc. these discoveries in physics pointed out the narrowness and limitations of the philosophical basis of the old physics, i.e., metaphysical and mechanistic materialism, to which the overwhelming majority of scientists spontaneously adhered. The new data of science would not fit within the framework of this form of materialism, which had become obsolete. The only philosophy which in essence could help analyze the achievements of natural science and interpret them correctly was dialectical materialism. However, scientists lived under circumstances which (to use Lenin's expression) repelled them from Marx and Engels and threw them into the embrace of the trivial state philosophy in which empirocriticism* flourished. The breakdown of metaphysical materialism and the outlook on nature which was based on it was taken by them as the breakdown of materialism in general.

These scientists – Lenin called them "physical" idealists – came to see in physical concepts and theories, not the reflection of a material world, but "hieroglyphs" working hypotheses, "symbols," etc. They decided that matter can disappear and be transformed into energy ("energetism"), that space and time causality and the regularity in nature are not objective.

The departure of part of the naturalists from materialism and their idealistic treatments of discoveries in physics caused a crisis in physical science – the crisis of the philosophical foundation of natural science.

By applying the standpoints of Marxist gnosiology to an analysis of the achievements of natural science, Lenin gave a philosophical explanation of the discoveries in physics. He refuted the idealistic conclusions which the empirocriticists attempted to attach to natural science, and showed scientists the real ways out of the difficulties which had accumulated in science and from the crisis in the philosophical foundations of physics.

Lenin showed that the achievements of science confirmed the materialistic doctrine of objective space and time, of causality, the regularity of nature, and contained no foundations for idealistic conclusions in these categories. Lenin wrote: "The materialistic basis of the spirit of physics, as in the whole of contemporary physical science, will overcome each and every crisis; but only by the continual replacement of metaphysical materialism by dialectical materialism" (Coll. Works, vol. 14, p. 292).

During the last few decades the vigorous progress of physics has continued. Quantum physics, the theory of relativity, the theory of elementary particles, and many other divisions of theoretical physics have been formulated. Artificial radioactivity, chain nuclear fission reactions, thermonuclear synthesis, and many other phenomena have been discovered.

These successes of physics have again confirmed the correctness of dialectical materialism and the correctness of the philosophical generalizations made by Lenin in his book. In capitalist countries, however, the philosophical battle around new discoveries in science still continues, and as before, the basic questions of the world outlook stand at the center: the questions of the objective reality of the external world, of space and time, of causality, and of the connection between matter and motion. As a result, the theoretical analysis of the achievements of science

*A philosophy of "critical experience" (a variety of subjective idealism); idealistically distorting the concept of "experiment" and reducing it to the sum of human experience, and reducing the objects of the material world about us to a complex of sensations; the combination of the elements of a subjective experiment. – Ed.

in the book, "Materialism and Empirocriticism," has completely retained its value up to the present day.

Thus, Lenin wrote that the abstract mathematical character of physics, in losing the graphic nature inherent in classical physics, is one of the gnosiological causes of the rise of "physical" idealism: "The approach to such uniform and simple elements of matter, the laws of motion of which permit of a mathematical treatment, brings about the neglect of matter by the mathematicians. 'Matter disappears,' and only equations remain" (Coll. Works, vol. 14, p. 294). Contemporary physics has risen to a still greater degree of abstraction. The complex mathematical apparatus which scientists use enables one to percieve more deeply and fully the regularity of physical processes. Nevertheless, a number of physicists assert that contemporary science develops as if only on the basis of theoretical mathematical methods, and not on the basis of experiment. Statements in such a spirit were made, for example, by the late English physicist A. Eddington, and also the German scientist K. Weizsacker. The latter asserts in his book "History of Nature," that the world will be perceived exclusively with the aid of mathematics, without experiment, and concludes that the truth is finally found in God.

The conception of matter formulated by Lenin is still exceptionally important in understanding the accomplishments of contemporary physics. This concept has been verified and made more concrete by the new discoveries of the scientists, however individual foreign physicists, erroneously identifying the philosophical concept of matter with its representation in classical physics, are negating the reality of the elementary particles. The Austrian physicist A. March, for example, regards the elementary particles as if they were "unsubstantial" structures. He attempts to prove that the progress of physics manifests itself as a process of "desubstantialization" of microobjects. March draws the conclusion that the "spirit of materialism" and the "materialistic way of thinking" in contemporary physics are "suffering a collapse" (Arthur March, Das neue Denken der modern Physik. Hamburg, 1957, pp. 120-122).

The eminent German physicist W. Heisenberg also proposes that the microobjects are only mathematical structures, and not particles of matter. Similar statements are frequently made by other physicists. For example, P. Bridgman regards physical reality as being the "totality of operations"; P. Jordan asserts that it is the "totality of experimental results", etc.

Lenin wrote that each attempt to take away motion from matter unavoidably leads to a distortion of science and to its idealistic interpretation. Several foreign physicists are presently trying to revive the idea of "energetism." Incorrectly interpreting the law relating mass and energy, the mutual conversion of particles of matter, the phenomenon of the mass defect, and several others, they speak of the transformation of matter into energy and of the "materialization" of energy. W. Heisenberg, for example, asserts that the basic substance of all that exists is energy, not matter.

Lenin pointed out that the theoretical misfortunes of "physical" idealists are explained by their lack of knowledge of dialectics and their inability of analyze dialectical antinomies, whose presence in nature started their natural discoveries. Examples of such antinomies are the simultaneous presence of wave and particle characteristics in microobjects, of statistical and dynamical regularities, discontinuity and continuity of physical processes, etc. A metaphysical consideration of these contrasts frequently leads some physicists to idealistic conclusions.

Thus, N. Bohr, W. Heisenberg, and several other scientists, in attempting to interpret the peculiar particle-wave properties of microobjects from the standpoint of classical physics, introduced the idealistic principle of complementarity, from which they drew the conclusion that space-time and causal descriptions mutually conflict.

Another idealistic statement made by several contemporary physicists (W. Heisenberg, P. Dirac, P. Bridgman, et al.) and by philosopher-idealists is that the data of quantum mechanics indicate the absence of determinism in microprocesses. The basis for such conclusions is the statistical character of this science. The negation of determinism in microprocesses is the result of the incorrect identification of determinism in general with mechanistic determinism. Lenin wrote: "The truly important theoretical- perceptual question which separates the philosophical tendencies is what degree of accuracy has our description of causal connections achieved ..., and in whether the source of our perceptions of these connections are objective regularities in nature, or properties of our mind....." (Coll. Works, vol. 14, pp. 146-147).

The indeterministic conception of quantum mechanics and the principle of complementarity were thoroughly demolished and refuted in the works of Soviet scientists, in particular in the works of V. A. Fok and D. I. Blokhintsev. These scientists, assuming different positions in treating the basic aspects of quantum theory, nevertheless arrived at the same opinion concerning the necessity of overhauling the philosophical views of N. Bohr, W. Heisenberg, et. al., from a viewpoint of dialectical materialism. Indeterminism was also exposed to criticism from a number of foreign physicists: D. Bohm, J. Vigier, Zh. Vassel†, L. de Broglie et al.

Like other theories of present-day physics, the theory of relativity is the object of a struggle between materialism and idealism. Misrepresenting this theory, the physico-idealists attempt, for example, to interpret the relativity of lengths and time intervals which are established by the special theory of relativity as their nonobjectiveness, drawing therefrom a conclusion about the arbitrariness and conditionality of the scientific picture of the world. In reality, the dependence of space and time on the motion of matter, their continuous connection with each other, is an ob-

† Transliteration of Russian. – Publisher's note.

jective fact established by experiment which in no way depends on the will of an observer.

The physico-idealists are attempting to use the general theory of relativity to construct various cosmological models of the Cosmos: the closed Cosmos, the finite Cosmos, the expanding Cosmos, etc. The model of the expanding Cosmos, which uses as its basis the phenomenon of the red shift of the light in the spectra of extragalactic nebulae, enjoys wide popularity among the idealists. The author of this model, the Belgian mathematician J. Le Maître, maintains that the universe is a bounded and spatially finite sphere whose radius is continually increasing because of galactic dispersion. Le Maître and other fideists concluded from this that this process possesses a beginning in time and that, consequently, a creater of the Cosmos exists; they even "calculated" that the act of creation occurred about $2 \cdot 10^9$ years ago. It is natural that similar conclusions are maintained by the clericalists, the adherents of neo-Thomism,‡ and other enemies of science.

The scientist-materialists showed that such conclusions do not follow at all from the theory of relativity and are the result of arbitrary assumptions and extrapolations. Present-day physics conclusively proves the correctness of the teaching of dialectical materialism concerning space and time. The attempts of the idealists to use the achievements of science for conclusions in the spirit of fideism suffer invariable failure.

Lenin wrote: "There is nothing in the universe other than matter in motion, and moving matter can move in no other way than in space and in time. Human notions of space and time are relative; but from these relative notions absolute truth accumulates, and these relative notions, in developing, proceed in the direction of absolute truth, and approximate it. The variability of human concepts of space and time in no way disprove the objective reality of both, just as the variability of scientific concepts of the structure and forms of the motion of matter does not contradict the objective reality of the external world" (Coll. Works, vol. 14, pp. 162-163).

Thus, the struggle between materialism and idealism is carried on in present-day physics as it was half a century ago. However, by virtue of the fact that socialism has become a world system, and Marxist-Leninist philosophy is acquiring more and more popularity among scientists of the capitalist countries, many contemporary scientists (for example, M. Born, L. de Broglie et al.) who previously took idealistic positions in physics, are beginning to come out against idealism. In particular, the step taken by L. de Broglie in renouncing his idealistic views which he had held for 25 years is significant. It is characteristic that N. Bohr spoke out in favor of a deterministic interpretation of quantum physics in one of his latest articles ("Usp. Fiz. Nauk" 67, vol. 1, pp. 37-42, 1959). J. Bernal, J. Haldene, and other scientists in the capitalist countries are defending dialectical materialism in natural science.

All of this essentially strengthens the front of the leading science (the position of materialistic natural science), and confirms Lenin's conclusions about the necessity of dialectical materialism in natural science, whose basis provides the means by which the crisis in physics can be surmounted. Lenin's "Materialism and Empirocriticism" is, as before, an effective weapon in the battle against contemporary idealistic philosophy and contemporary "physical" idealism.

---

‡ The official philosophical doctrine of the Catholic Church reviving the theologic-idealistic system of the medieval scholastic Thomas Aquinas. — Ed.

LAUREATES OF THE LENIN PRIZE FOR CONSTRUCTION OF THE 10 BEV SYNCHROPHASOTRON

A great achievement of Soviet science and engineering is the creation of the largest apparatus in the world for the study of elementary particles and their interactions – the 10 billion ev synchrophasotron, the operation of which is based on the principle of autophasing, discovered by Academician V. I. Veksler.

The synchrophasotron is intended for the acceleration of "elementary" particles of matter and for imparting ultrahigh energies to them, which is necessary for the further study of the atomic nucleus. The largest atomic machine has tremendous size and operates with unusual precision. The weight of the annular electromagnet of the synchrophasotron is 36 thousand

V. I. Veksler

L. P. Zinov'ev

N. A. Monoszon

D.V. Efremov

E. G. Komar

A. M. Stolov

tons, and its outer diameter is about 70 meters. The pressure in the vacuum chamber, inside of which the accelerated particles move, is decreased to one billionth of an atmosphere.

The particles of matter rotate in the synchrophasotron millions of times in a magnetic field increasing with time, thereby augmenting their energy by degrees. In a period of 3.3 seconds, these particles

make four and a half million revolutions and travel a distance of a million kilometers, approaching the velocity of light.

For the solution of this extremely difficult scientific and engineering problem, the Lenin prize was awarded to Academician V. I. Veksler; Chief of the Division of the Laboratory of High Energies of the Joint Institute for Nuclear Studies, L. P. Zinov'ev; Assistant Chief of the Board for the Utilization of Atomic Energy of the Council of Ministers of the USSR, D. V. Efremov; the Workers of the Scientific Research Institute E. G. Komar, N. A. Monszon, and A. M. Stolov; Academician A. L. Mints; Senior Scientific Associates of the Radiotechnical Institute of the Academy of Sciences of the USSR, T. A. Vodop'yanov and S. M. Rubchinskii; Senior Scientific Associate of the P. N. Lebedev Physical Institute of the Academy of Sciences of the USSR, A. A. Kolomenskii, V. A. Petukhov, and M. S. Rabinovich.

A. L. Mints

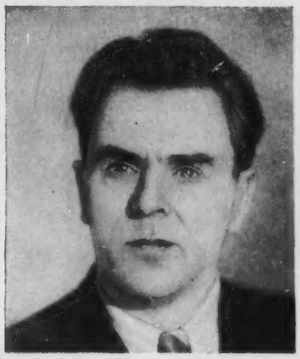

F. A. Vodop'yanov

S. M. Rubchinskii

A. A. Kolomenskii

V. A. Petukhov

M. S. Rabinovich

(From an article by Academician A. N. Nesmeyanov which appeared in the newspaper "Pravda" on April 22, 1959).

APPLICATION OF SORPTION AND SOLVENT EXTRACTION PROCESSES IN THE HYDROMETALLURGY OF URANIUM

B. S. Kolychev

This article is a review of those reports presented at the Second International Conference on the Peaceful Uses of Atomic Energy (Geneva, 1958) which dealt with sorption- and solvent-extraction processes in the hydrometallurgy of uranium. It is shown that these methods have been adopted on a relatively wide scale in the industries of the USA. The various forms of application of sorption are discussed, particularly the new processes of uranium recovery by sorption from pulp. Two main classes of extraction solvents are considered: organophosphorus compounds and amines, and the influence of various factors on solvent-extraction processes is also discussed. Examples are given of the application of sorption and solvent-extraction processes in ore-processing plants, and general conclusions are drawn.

At the second Geneva Conference, more than 40 reports dealt with problems of the hydrometallurgy of uranium. Nearly three-quarters of these reports describe the main trends in the processing of uranium ores: acid leaching of uranium, followed by its sorption-or solvent- extraction recovery from the resulting solutions or pulps, and carbonate leaching of uranium, followed by precipitation of rich concentrates by various methods.

This proportion of reports reflects in some degree the extent to which these methods have been adopted in the industries of the USA. According to the data presented at the Second Geneva Conference, concerns employing carbonate leaching in the USA provide ~ 28 of the total output of uranium concentrates; sorption processes, 37%; and solvent extraction processes, 35%.*

For this reason, the present review of the reports covers the two principal branches of the hydrometallurgy of uranium: sorption and solvent extraction.

Uranium Recovery by Sorption

Sorption processes are of considerable importance in the hydrometallurgy of uranium ores.

The recovery of uranium from pulps by means of the RIP process (discussed for the first time in reports of the First Geneva Conference) is dealt with in Report No. 500†, describing the operation of a plant at Moab, Utah. Concentrated sulfuric acid was added to the ore crushed to 28 mesh, together with a solution of $NaClO_3$ as oxidizer. The addition of the acid was regulated so as to give a pH = 1.4–1.6 in the slimes after classification. With a lower pH value, the final product would be purer, but the capacity of the resin lower. With a higher pH value, the total capacity is increased but more rapidly for iron then for uranium. The sulfuric acid consumption was 13 kg per ton of ore for each per cent of calcium carbonate. Experience showed that the leaching temperature should not be less than 50°C, since in summer when maintained at that level, recovery is 95%, while in winter at 25°C it is only 88%.

Thick pulps cannot be used in the RIP process. In the classification of pulp preparatory to sorption, the sp. gr. is taken as 1.06, corresponding altogether to only 7% solids, while particle size should not exceed 325 mesh for the following reasons:

This dilution and particle size prevent cementing of the resin into a rather compact mass;

The fraction above 325 mesh is difficult to wash out of the resin before elution;

Particles above 325 mesh clog the baskets, increasing the resistance and resulting in breakage of the baskets or lifting machinery.

The resin is contained in cubic baskets (1.8 m sides) made of stainless steel and covered with network. The baskets are moved up and down in the pulp freed from sand.

"Permutit SKB" and "Rohm and Haas KhE-123" resins are mainly used in the process. These resins have been developed for the RIP process and are made in a grain size of -10 to +20 mesh. The complete recovery of the uranium takes ten hours of sorption with four baskets in each stage. In ten stages, more than 99% of uranium can be recovered with a loading of 56 g U_3O_8/liter of resin.

The uranium occurs in solution mainly in the form of a complex of trisulfate $UO_2(SO_4)_3^{-4}$ and disulfate $UO_2(SO_4)_2^{-2}$. Sorption takes place in accordance with the equation $4RNO_3 + UO_2(SO_4)_3^{-4} \rightarrow R_4UO_2(SO_4)_3 + 4NO_3^-$ where R signifies the resin.

The plant has two sections of 14 stages each, with four baskets in each stage. A basket contains 1080 liters of resin Four stages are for elution. A nitric acid solution with pH = 1.2 is used for elution, the ratio to the

* An article by R. Kennedy, Mines Mag. 47, 9, 22 (1957) is of interest, since it points out that plants using sorption processes in the first half of 1957 formed 61% of the total capacity of ore-processing concerns in the USA, while those using solvent-extraction processes formed only 8%.

† The Report numbers given are the numbers of the reports presented at the Second International Conference on the Peaceful Uses of Atomic Energy, 1958.

total volume of resin being 5.85:1. The eluant contains about 9g U_3O_8 / liter in the form of trisulfate ion.

Precipitation is by gaseous ammonia, a pH = 3.4 – 3.8 being maintained in the first reaction tank; one of 4.6 – 4.8 in the second tank; and one of 7.0 in the third tank. The concentrate pulp is thickened in a rubber-lined thickener. The overflow is filtered in frame presses and the underflow in vacuum drum filters. Nitric acid is added to the filtrate which is then returned to elution. After washing and filtration on the vacuum drum filters, the cake is pulped and pumped to an oven for drying to 0.2 % moisture content. The concentrate containing 80% U_3O_8 is packed in drums each containing 320 kg. Report No. 500 gives the dimensions of the basic equipment.

Report No. 1113 deals with the analysis of the characteristics of ion-exchange resins and the influence of poisons on the effectiveness of the resins. The principal resin employed in South Africa is the product of the copolymerization of styrene and divinylbenzene followed by chloromethylation and the introduction of trimethylamine as active exchange group (of the type of IRA-400).

It was found that an increase in the percentage of divinylbenzene in the resin increased the strength of the resin, its selectivity for uranium, and the capacity per unit volume of wet resin, but,at the same time, there are difficulties in introducing a large number of active groups into the lattice, which makes it impossible to increase the capacity further. It has been found that more than 7% divinylbenzene should not be added.

Primary amines as active group (weak base anion exchangers) have a weak affinity for the uranyl sulfate complex, the affinity increasing through secondary to tertiary amines. For that reason, it is perferable to use resins with primary ammonium bases as active groups of the type

$$-CH_2-\underset{\displaystyle CH_3}{\overset{\displaystyle CH_3}{\overset{|}{\underset{|}{N}}}}-CH_3\ \Big]^{+}\ Cl^{-}\ .$$

For increasing the surface, the resin is used in the form of grains of a size of -20 to +50 mesh. The spherical form increases the mechanical strength of the resin.

In Report No. 1113 the cost of the individual stages is analyzed; methods are given for determining the effectiveness of each stage, and the effect of various poisons on the action of the resins is discussed. The last question is considered in greater detail in Report No. 101, which is an account of the work done by the Teddington Laboratory (England). The report deals with problems concerning the nature and mechanism of adsorption and the poisons of sorbents encountered in actual practice. Strong base anion-exchange resins are principally concerned, as used in the sorption cycle with pH = 1.8, and also in elution 0.1 M HNO_3 + 1 M NH_4NO_3 or 0.1 M H_2SO_4 + 1 M NaCl. Poisons may be permanent and nonpermanent. Permanent poisons are substances which are adsorbed irreversibly, and nonpermanent poisons are those which, having a higher affinity than uranium, reduce the capacity of the sorbent for uranium, but which can be later eluted. There is no sharp line of demarcation between them. Permanent poisons are thiocyanates, polythionates, cobalt cyanide, silicates, and compounds of molybdenum.

The action of thiocyanates is the result of the following factors:

Strong base anion-exchange resins have a greater affinity for thiocyanates than for uranium, which causes the capacity for uranium to be reduced. (This effect could be greater if the uranium were not partly sorbed in the form of a complex with the thiocyanate.);

The thiocyanate uranium complex is held more strongly by the resin than the two uranium complexes and remains on the resin even after complete elution of the uranium.

Cyanides of cobalt and thiocyanides act in approximately the same way. These compounds are of particular importance for South African plants, where the chief raw material is well known to consist of the tailings from gold extraction.

Poisons of another type are the solids (Report No. 1113) formed on the surface of the resin granules (for example,elemental sulfur formed as the result of the decomposition of polythiocyanates) or inside them (polymerized SiO_2). SiO_2 in solution is in the form of $SiO_2 \cdot nH_2O$ in molecular but not ionic form. These molecules do not diffuse back, which prevents the penetration of other ions into the resin granules and reduces the capacity of the resin. The degree of influence of SiO_2 varies. Some resins tolerate up to 20% of SiO_2 without appreciable change in their properties, whereas with some, the capacity is appreciable reduced even after 5%.

In South Africa, this type of poisoning is successfully counteracted by the use of regeneration, carried out by washing the resin with a 5% solution of NaOH. The latter must be used with care, since it produces degradation of the active groups; for example,degradation of quaternary ammonium bases to tertiary, secondary, and primary bases, which rapidly reduces the affinity of these groups for the uranyl sulfate complex.

Report No. 1553 of Argentine experts is a description of laboratory work on the application of ion exchange to the treatment of Argentinian ores from Malargue (Mendoza)

The composition of the ore is not given, but evidently it is fairly rich in uranium, since the solutions obtained after acid decomposition contained 4 g/liter U_3O_8. A standard scheme was tried out for the recovery of uranium from clarified sulfuric acid solutions. Dowex 2-X 8 resin with a particle size of 50 - 100 mesh was used.

The most interesting part of Report No. 1553 may be considered to be the description of a rapid method for the determination of very small amounts of uranium in the presence of ions of other metals. For this, the fact employ-

ed was that iron, copper, vanadium, and other metals are more strongly absorbed by strongly acid cation exchangers than is uranium. The strongly acid cation exchanger used was Dowex 50-X 12. An amount equaling 0.5 ml of the sample under test with 0.5 ml of water was passed through small columns containing 1 ml of resin, followed by elution by a 0.4 M solution of ammonium sulfate in sulfuric acid of a concentration of 3.5 g/liter. For the quantitative determination of uranium, a sample of between 2.5 and 4.5 free volume was used (the free volume being the volume between the grains of sorbent, equal to 0.4 of the volume of sorbent), which also contained the bulk of the uranium. The uranium was determined colorimetrically in the sample. The columns could be used repeatedly after regeneration by a 6 N hydrochloric acid solution, followed by flushing with a 0.4 M ammonium sulfate solution in sulfuric acid.

Report No. 1412, delivered by Spanish experts, also describes an investigation to select the conditions for using ion exchange in the recovery of uranium from sulfuric acid solutions produced in the treatment of ores from Venta de Cardena (Spain).

The work was conducted on a large laboratory scale using a system of 4 columns having an internal diameter of 2.6 cm and a height of 1.5 m. The object was not to discover new relationships, but to determine the optimum parameters of the process. Report No. 1412 is profusely supplied with numerical data and graphic material.

Report No. 1719 by Hungarian scientists also concerns laboratory investigations on the recovery of uranium from Hungarian ores by means of ion exchange. Some of the basic stages of the treatment of the ores are studied in the report.

Evidently the ores investigated were high carbonate ores, since leaching was by soda solutions containing 3-5 % Na_2CO_3 and 1-1.5% $NaHCO_3$. At 90°C and with ore crushed to a fineness of 70μ, it was possible to obtain in 75 min 90-92% recovery of uranium in solution. It was found advantageous to introduce the oxidizer, $KMnO_4$, 10 min before leaching was complete, probably because by that time the air used for stirring had already oxidized the more readily oxidizable constituents.

Hungarian resins of the type of "Mekeon RA," consisting of structurally different quaternary ammonium bases, were used for the ion exchange. The resins were used at a pH value of up to 12. Their capacity when saturated with synthetic solutions of uranyl tricarbonate was 94 mg U/ml. No aging was found with these solutions; after a thousand cycles, the capacity was reduced by only 6%.

RIP and ion-exchange processes in a fluidized bed were also tested, but the scale of the experiments for the last-mentioned process was very small.

Report No. 484 mentioned (without giving any data) the application of the process of sorption of uranium from carbonate solutions produced in the alkaline leaching of the ash of uranium-bearing coals.

Report No. 1096 by Australian specialists describes an attempt to develop a new method of sorption from pulps, and gives an account of the sorption process carried out in a column with a pulsating bed of sorbent. Before being fed to the column, the pulp was subjected to classification in hydrocyclones in several stages, and contained fractions of approximately 300 mesh.

The actual sorption process was carried out as follows. The pulp was fed to the column from below and was passed through the bed of IPA-400 or IPA-410 resin which had a grain size of from 10 to 20 mesh (Fig. 1, Report No. 1096). The resin was prevented from being entrained by the pulp by a 30-mesh strainer, placed in the upper part of the column. Blockage of the strainer by resin was prevented by gentle, slow pulsation of the entire flow by means of a pneumatic system. A suspended bed of resin was formed, comparable to the bed of ore in a jigging machine. This bed was not turbulent and gravitational segregation took place in it; the heavier, loaded resin settling rapidly to the bottom where it encountered the fresh pulp, whereas the exhausted pulp, on the contrary, encountered the lighter, fresh resin above. The principle of a counterflow process was thus preserved.

The loaded resin together with the pulp was removed from the bottom and fed to a 30-mesh strainer, where it was separated from the pulp, which was returned to the column. After being washed, the resin was subjected to elution, which also took place in a pulsating bed. After elution, the resin was fed to the top of the column. Pulsation in the column was effected at a speed of 2 sec upwardly, 1 sec change in direction, 3 sec downwardly, 1 sec change in direction. The maximum diameter of the test column was 1.3 m and the height of the resin layer was 1.8 m.

The pulp fed to the column had a content of solids of 15 to 35%, in which this process differs advantageously from the RIP process adopted in the USA. The starting solution contained 0.5 to 3.5 g U_3O_8/liter. The mean velocity of the ascending pulp stream was 18 m/hr. The loading was 25 to 56 g U_3O_8/liter of resin. In the eluted resin, the concentration was 4 to 14 g U_3O_8/liter with an extraction of 99.8% of U_3O_8 from the solution.

Report No. 1096 gives calculations of the economics of the individual stages of the process.

The Soviet Report No. 2063 described work on the recovery of uranium from natural water. Of all the communications on the hydrometallurgy of uranium, this report aroused the greatest interest and the largest number of questions were asked in connection with it.

Report No. 2063 described a technological scheme for the recovery of uranium from natural water with an extremely low uranium content, not exceeding on the average 60 mg per 1 m^3 of water. It was found that the best results with regard to the recovery of uranium are given by salts which are hydrolized by the natural alkalinity of the water with the formation of flocculent precipitates of hydroxides.

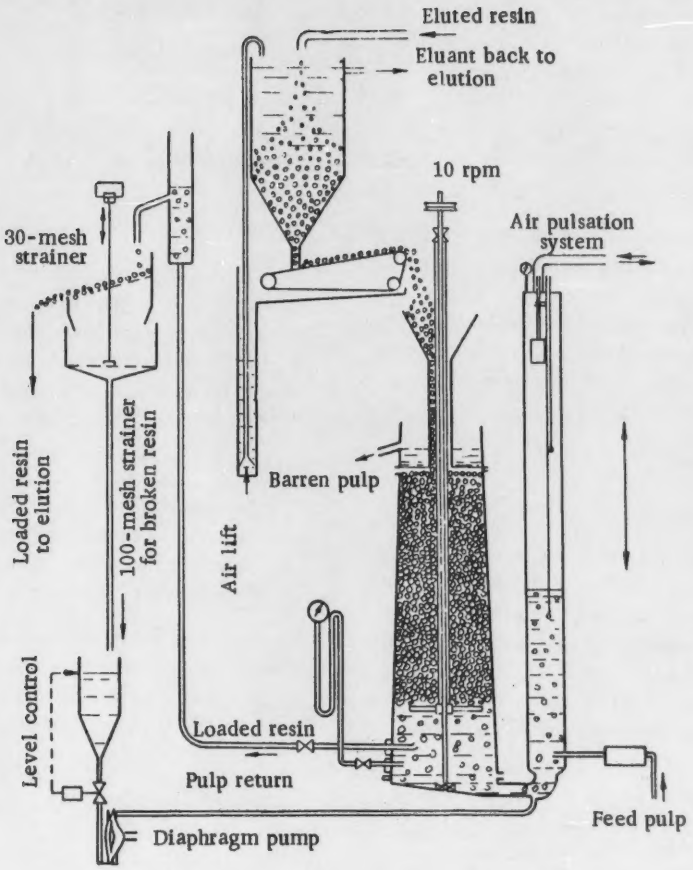

Fig. 1. Adsorbtion column with pulsating bed of sorbent utilized on experimental apparatus.

The mechanism of uranium recovery in this process comprises chemisorption, physical adsorption on the surface of colloidal particles, and the capture of uranium-containing suspensions. Chemisorption appears to be decisive. By means of such a method, it is possible to recover 80-90% of all the uranium contained in the water.

The main problem is the careful separation of the suspension of hydrozides from the enormous bulk of water by means of clafifiers. The cost of the uranium in this casewill be determined almost entirely by the cost of the electric power required for pumping; since for the production of 1 kg of uranium, 20-40 thousand m^3 of water must be pumped, depending on the initial content.

Recovery of Uranium by Solvent Extraction

The extensive application of extraction from solutions obtained in the treatment of ores has been the result of considerable research work on the choice of selectively acting solvents, and of a study of the mechanism of solvent extraction and the influence of the structure of the solvent on its extractive properties.

Extraction processes are not new in the uranium industry, since they have been used for the refining of uranium and for the treatment of reactor fuel. The ethers and ketones used for these purposes, however, could not be employed for the extraction of uranium from industrial solutions obtained in the treatment of ores. These solvents, which extract uranium nitrates satisfactorily, have a low extraction power for uranium sulfates. Sulfuric acid is mainly used in the processing of ores. The first problem facing investigators was, therefore, to find a good solvent for uranyl sulfate.

Report No. 509 is a lengthy survey covering almost 60 papers by American scientists.

As a result of tests on some hundreds of organic compounds of widely differing categories, a number of repre-

sentatives of long-chain alkylamines and several organophosphorus compounds of both acid and neutral character were selected for practical application.

The investigations show that, like ion-exchange resins, alkylamines can extract uranium from sulfate solutions:

$$(R_3NH)_2SO_{4(org)} + UO_2(SO_4)_2^{-2}(aq) \rightleftharpoons$$

$$\rightleftharpoons (R_3NH)_2UO_2(SO_4)_2\ org + SO_4^{-2}(aq).$$

The formula for the uranyl organic complex in this equation is arbitrary and has not been definitely established.

Like weak base resins, amines are ineffective at high pH values, but solutions of quaternary ammonium bases, as shown in Report No. 509, like strong base ions, extract uranium from carbonate solutions‡:

$$2(R_4N)_2CO_{3(org)} + UO_2(CO_3)_3^{-4}\ (aq) \rightleftharpoons$$

$$\rightleftharpoons (R_4N)_4UO_2(CO_3)_{3\,(org)} + 2CO_3^{-2}(aq)$$

The analogy continues in stripping processes, since uranium is extracted from solution in the organic phase by solutions of chlorides or nitrates as employed in the elution of strong base anion-exchange resins. Since stripping involves two liquid phases (not a liquid-solid phase as in elution), carbonate solutions can be used for such a process. In that case the extracted iron is precipitated and can be separated from the solutions before the precipitation of the uranium.

Report No. 509 also considers other problems.

Choice of solvent

It has been found that most amines can be used in the form of a 0.1 M solution in kerosene. Longchain alcohols can be added to improve the separation of the phases.

Selectivity

Selectivity varies sharply according to the structure of the solvent: it increases from the primary amines to tertiary amines, and also according to the degree of branching of the organic chain. Selectivity increases in a particularly marked manner with branching of the chain in a position close to the nitrogen atom (Table 1).

Loss of solvent in the aqueous phase

Because of the large volumes of processed solutions, even a low solubility of the solvent in water can be of considerable importance. These losses increase with increase in length of the organic chain. Usually they amount

‡In an article by W. Clifford, E. Bullwinkel et al., J. Amer. Chem. Soc. 80, 12, 2959 (1958), there is a reference to the fact that the process takes place satisfactorily in the presence of 8-hydroxyquinoline.

TABLE 1 Selectivity of Amines as a Function of Their Structure (0.1 M amine; approximately 1 M SO_4; pH = 1)

Metal ion	Extraction coefficient*				
	1°	2°Str	2°M Br	2°H Br	3°
MgCa, Mn(II), Fe(II), Co(II), Ni(II), Cu(II), Zn, Al, Cr(III), V(II)	< 0.1	<0.01	<0.01	<0.01	<0.01
Fe(III)	40	<0.5	<0.5	<0.1	<0.01
Rare earths	20	—	<0.1	<0.01	<0.01
Ti(IV)	20	5	–	0.2	<0.1
Th (0.5 M SO_4)	>5000	—	>500	2-15	<0.1

Remarks:

1° Branched primary amines (for example Amine 21F81, Primene JM-T);

2°Str Straight-chain secondary amines (e.g., dilaurylamine);

2°M Br Moderately branched secondary amines (e.g., ditridecylamine);

2°H Br Highly branched secondary amines branching close to nitrogen atom (e.g., Amine S-24, Amine 9D-78);

3° Tertiary amines with long straight or moderately branched chains (e.g., trilaurylamine, tri-isooctylamine, butyldilaurylamine.

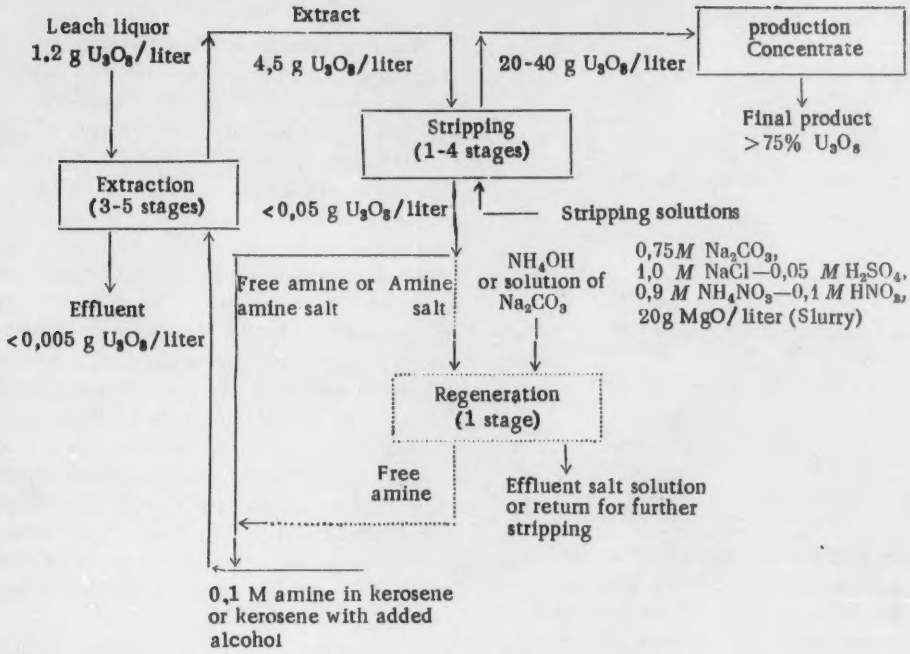

Fig. 2. Basic flowsheet of Amex process.

to 0.015 kg of solvents per 1 kg of uranium extracted from a solution containing 1 g U/liter.

Solvent loss due to entrainment, evaporation, spillage, etc. amount to 0.05% of the original quantity used. The cost of the usual amines (such as, for example, tri-iso-octylamine, Amine 9D-178, Amberlite LA-2**) is 2.2-3.3 per kg.

The basic flowsheet of the Amex process follows (Fig. 2, Report No. 509).

According to the information given in Report No. 509, a productive plant utilizing solvent extraction by means of amines has been constructed for 300 tons per day at Port Radium (Canada) and for 750 tons per day at Mexican Hat (Utah). The former uses mixer thickeners and the latter, Podbelniak centrifugal machines. A plant with a capacity of 3000 tons per day is being built at Ambrosia Lake (New Mexico) and one of 200 tons per day at Lakeview (Oregon). Both will use mixer thickeners.

The solvent extraction process using amines as solvent can be used for the separation of uranium and thorium. Amines having a chain branched close to the nitrogen atom are good solvents for uranium, and those with a chain branched far from the nitrogen atom are solvents for thorium. At plants where sorption is used for the recovery of uranium, the thorium can be extracted in a second cycle using straight-chain primary or secondary amines.

The possibility of separating uranium and vanadium has been confirmed in laboratory conditions.

The extraction of uranium from industrial solutions can also be carried out by means of organophosphorus compounds, in particular alkylphosphoric acids. These problems are discussed fully in Report No. 1550, which describes systematic investigations of organophosphorus compounds as extractants for uranium in industrial processes. The result of these investigations has been the wide-scale application of extraction by dialkylphosphoric acid (Dapex process), in particular di(2-ethylhexyl) phosphoric acid (D2EHPA), which is available commercially and has acceptable technical characteristics.

All types of organophosphorus reagents can be combined in the following system, which includes acid and

---

**By Amine 9D-178 or Amberlite LA-2(LA-1) are understood secondary amines with a strongly branched chain of the type

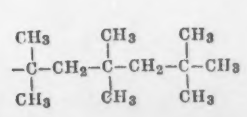

or a mixture of their homologues with 12-15 carbon atoms.

neutral reagents:

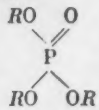
Trialkylphosphates

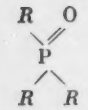
Trialkylphosphine oxide

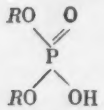
Dialkylphosphoric acid

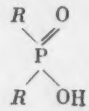
Dialkylphosphinic acid

Alkyldialkylphosphinate

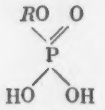
Monoalkylphosphoric acid

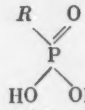
Monoalkylphosphonic acid

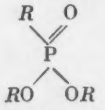
Dialkylalkylphosphonate

The acids take part in the extraction process in the same way as cation exchange resins, exchanging their hydrogen ion for an ion of the extracted metal. The reagent in a hydrocarbon medium is evidently associated in the dimeric molecules

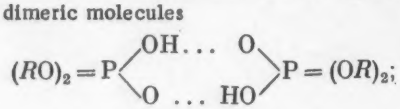

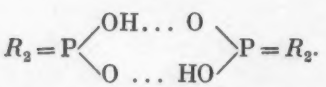

Larger aggregates were found for monoalkyl compounds. Since the reagent is dimeric in the solvent, it forms in the extraction of UO_2^{++} a complex containing four dialkylphosphoric groups. Generally, the number of dialkylphosphoric groups is twice as large as the cation charge.

The authors of Report No. 1550 state that in the class of organophosphoric acids, the extraction power decreases with increase in branching of the alkyl chain close to the phosphorus atoms, as is shown by Table 2.

For organophosphoric acids, the extraction coefficient as a rule decreases with increase in dielectric constant of the diluent. The selectivity of phosphoric acids is lower than in the case of secondary and ternary amines. Acids having straight or only slightly branched chains (for example, isoctyl) extract a larger quantity of aluminum. Branched chains tend to reduce the extraction power for aluminum. Other metals: calcium, magnesium, zinc, trivalent chromium, divalent iron, copper, nickel, and manganese are extracted to an insignificant degree. Low, but nevertheless noticeable, extractability is observed in the case of quadrivalent vanadium, hexavalent molybdenum, and the rare earths, and a much greater extractability in the case of trivalent iron, titanium, thorium, and other quadrivalent metals. To diminish the extraction of trivalent iron, it must be reduced to divalent iron, even if by means of iron scrap.

Compounds such as R_3PO, $R_2(RO)PO$, $R(RO)_2PO$ resemble tributylphosphate in properties.

The extraction power for uranium is reduced from phosphines through phosphinates to phosphates. Phosphines are capable of extracting uranium from sulfate and phosphate liquors, for which tributylphosphate is completely ineffective. Nitrates have a higher extractability which decreases rapidly through chlorides to sulfates. An important consequence of the high extractability of nitrates is the considerable increase in the extraction of uranium by neutral alkylphosphorus compounds from sulfate or chloride solutions when comparatively small amounts of nitrate are added to them.

TABLE 2 Variation of Extraction Coefficient of Organophosphoric Reagents. (Aqueous phase: 0.5 M SO_4; pH = 1; 0.004 M U (VI). Initial organic phase: 0.1 M, extractant in the solvent stated. Ratio of aqueous phase to organic phase equal to 1; t = 25°C)

Reagent	Extraction coefficient	
Dialkylphosphoric acids	Carbon tetrachloride	Kerosene
n-octyl	90	450
3,5,5-trimethylhexyl	40	260
2-ethylhexyl	17	135
2-ethyl-4-methylpentyl	–	90
2-propyl-4-methylpentyl	–	60
Octyl-2	11	—
Diisobutylmethyl	2	10

TABLE 3 Effect of Impurities on the Extraction Coefficient. (Aqueous phase: 0.5 M SO_4; pH = 1; 0.004 M U (VI). Initial organic phase: extractant in the solvent stated. Radio of aqueous phase to organic phase equal to 1; t = 25°C)

Reagent	Concentration, M	Extraction coefficient	
		Reagent without addition	in combination with 0.1 M D2EHPA
Di(2-ethylhexyl) phosphoric acid.	0.1	135	–
Phosphates:			
tri-n-butyl.	0.1	0.0002	470
tri-2-ethylhexyl . . .	0.1	0.0002	270
Phosphinates:			
n-butyl di-n-butyl. .	0.1	0.002	3500
n-butyl di-n-hexyl...	0.1	0.002	3500
Phosphine oxides:			
tri-n-butyl.	0.05	0.0025	7000
tri-n-octyl.	0.1	0.06	3500
tri-2-ethylhexyl. . . .	0.1	0.02	650

Dialkylphosphoric acids have the important property of considerably increasing the extraction power in combination with neutral phosphorus compounds, the extraction coefficient becoming much higher than for each of the components separately (Table 3). This property is inherent only in dialkylphosphoric acids; the extraction power of monoalkylphosphoric acids and alkylphosphinic acids is even diminished. This synergetic effect is known only for uranium. For the other metals mentioned in this report, it is either absent or produces the opposite effect.

Report No. 1550 also refers to the possibility of separating different metals (including rare-earth metals) by solvent extraction.

The basic flowsheet for extraction by organophosphorus compounds (Dapex process) is shown in Fig. 3 Report No. 509. Extraction by phosphoric acids is not recommended for solutions of high iron content, since the cost of reduction will be high.

The process of solvent extraction by means of organophosphorus compounds is in use at plants in Shiprock, New Mexico (500 tons per day), Grand Junction, Colorado (350 tons per day), Rifle, Colorado (1000 tons per day) and Grannison, Colorado (200 tons per day). A plant which will use this process is under construction at Riverton, Wyoming (500 tons per day).

The Dapex process can be successfully used also for the extraction of uranium from eluate liquors. A plant with a planned output of 300 tons per day is now being equipped in Edgmont South Dakota.

All but one of the plants mentioned use mixer-settlers.

Some reports described the operation of individual plants using solvent-extraction processes, or the technology of processing one ore or another by means of solvent extraction. For example, Report No. 511 describes the operation of one of the new plants in Salt Lake City, Utah, processing various ores obtained from the states of Utah, Colorado, and Wyoming.

In the technical scheme as carried out at this plant, some interest attached to the separation of the ores processed into "difficult" ores, requiring a high concentration of acid, and "easy" ores, requiring a moderate concentration of acid. In order to utilize the residual acidity from the first two stages of processing the difficult ores, the easy ores are fed directly to a third acid-leaching stage. This results in some economy in acid consumption. To reduce the iron and precipitate the heavy metals, hydrosulfide is added in the last leaching stage; for clarifying the liquors after the acid decomposition of the ores, thickeners are used here as at the majority of American plants, Separan being added at each thickening stage as flocculant.

Extraction is carried out by means of a 0.1 M solution of dodecylphosphoric acid in kerosene, and stripping is by means of concentrated 10 M hydrochloric acid, which is regenerated during evaporation to approximately 90%. The evaporation equipment is made of resistant plastic of the Teflon type. The final product contains about 90% U_3O_8. According to statements by the authors of Report No. 511, the plant in Salt Lake City cost 1.5 million dollars, whereas the undertaking without the use of solvent

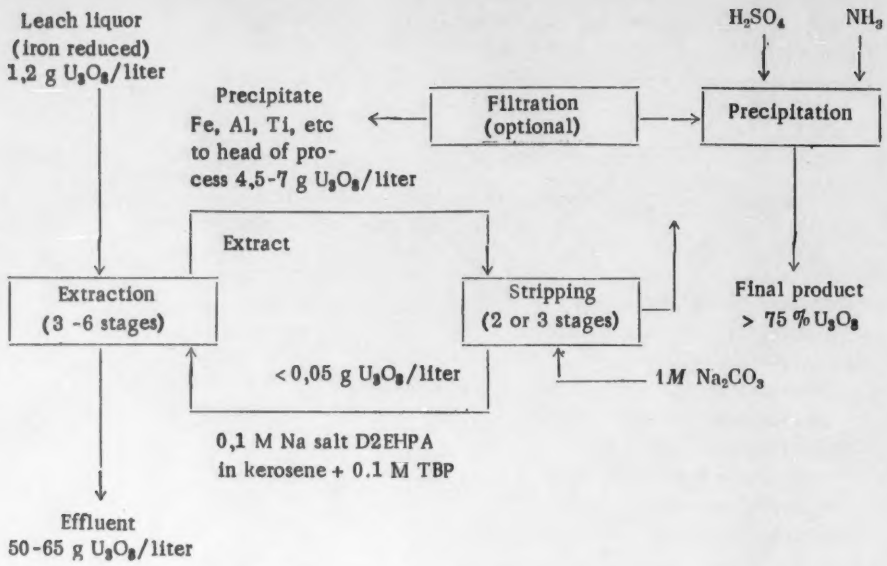

Fig. 3. Flowsheet of Dapex process.

extraction cost about 6 million dollars. Report No. 511 gives the dimensions and types of the main forms of equipment.

Report No. 501 describes the choice of conditions for carrying out the simultaneous extraction of uranium and vanadium from solutions obtained in the processing of roasted ores from the Colorado Plateau. It was found that the best extractant is a combination of amines and alkylphosphoric acids, usually employed for the extraction of uranium. Alkylphosphoric acids are good extractants for uranium, and amines of the aliphatic series extract pentavalent vanadium; but in the presence of chlorides, contained in considerable quantities in the liquors after chloride roasting, they are poor extractants for uranium.

Kerosene with tributylphosphate is recommended as diluent. The addition of tributylphosphate permits stripping by carbonate solutions without the formation of a third layer. The best results were given by a mixture of 0.2 M solution of a ternary amine of the aliphatic series with a 0.1 M solution of alkylphosphoric acid (in particular di(2-ethylhexyl) phosphoric acid or heptadecylphosphoric acid). The extraction coefficient of this mixture is higher than that of each solvent separately, but the mechanism of its action is still unexplained. The flowsheet, Fig. 4 Report No. 501, shows the distribution of uranium and vanadium in the extraction and stripping stages.

Japanese scientists presented Report No. 1361 on the search for a technique of processing the low grade ores (0.05 - 0.1 % U_3O_8) from the Ningyo-Toge deposits, discovered in 1955, in the Tottori Prefecture. They found that for the direct production of uranium tetrafluoride of high nuclear purity it is best to use a two-stage extraction using organic solvents, with intermediate electrolytic reduction of the uranium.

In contrast to the standard methods employed in the USA and Canada, for the reduction of iron, in Japan clarified liquors are processed by a portion of the solutions obtained after electrolytic reduction and containing quadrivalent uranium. The reduction of iron is thus entirely due to electrolysis. According to statements of the authors of Report No. 1361, this method of reducing the iron diminishes the possibility of emulsion formation in the subsequent extraction, as is frequently found in the case of reduction by steel shavings.

The solution thus processed is passed to extraction by a 0.1 M solution of di(2-ethylhexyl) phosphoric acid in kerosene, followed by stripping with a 10% soda solution. The stripped solutions, containing 30 g/liter of uranium, after acidification, are subjected to electrolytic reduction for converting hexavalent uranium into the quadrivalent form. The quadrivalent uranium is recovered by extraction with an organic solvent of increased molar concentration, and after treatment with 20% of hydrogen fluoride is precipitated in the form of uranium tetrafluoride. All the impurities not removed in the preceding operation are separated well in this stage. The tetrafluoride could also be precipitated from the aqueous phase, but the product would then be much less pure, necessitating the introduction of additional purifying stages. After filtration, drying, and igniting, a product of very high nuclear purity was obtained. The experiments are currently being continued.

Special interest is afforded by Reports No. 497 and 496 of American scientists, since the work described in them was carried out with the object of developing processes for

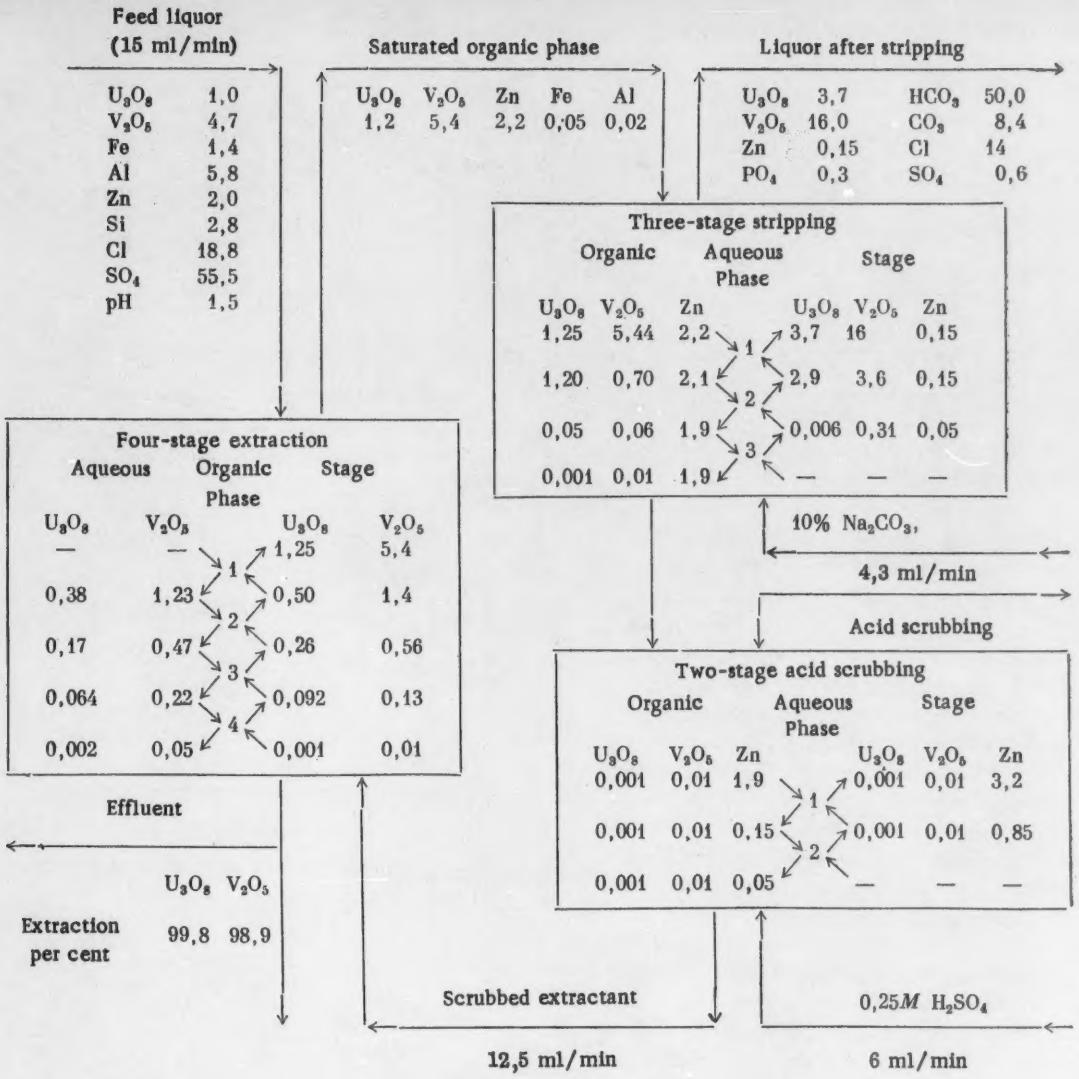

Note: All contents shown in grams per liter.

Fig. 4. Flowsheet showing distribution of uranium and vanadium.

solvent extraction from pulps of different densities. Amines cannot be used for extraction, because of the formation of stable emulsions in the presence of even small amounts of solids, and the resulting high loss of extractant. At the same time, tests on an experimental apparatus have shown that alkylphosphoric acids may be employed as reagents just as effectively for pulps as for clarified solutions. Solvent entrainment decreases with a decrease in the thickness of the pulp; and, in the opinion of the authors of Report No. 497, when the content of solids becomes less than 5%, the economy of eliminating the clarifying process exceeds the cost of a solvent loss.

Report No. 497 gives the results of a study of the possibility of reducing solvent loss when working with thick pulps. Pulps require a higher ratio of organic to aqueous phase than do clarified solutions. In most cases, for the solvent extraction of pulps, the mixers employed for clarified solutions can be used. All attempts to use pulsed columns resulted in the formation of stable emulsions. The best results in regard to solvent entrainment were obtained with a turbomixer-settler, the action of which will be gathered from Fig. 5 (Report No. 497). The tests were carried out in a laboratory form of turbomixer-settler, 15 cm in diameter and 35 cm in height. Its capacity was

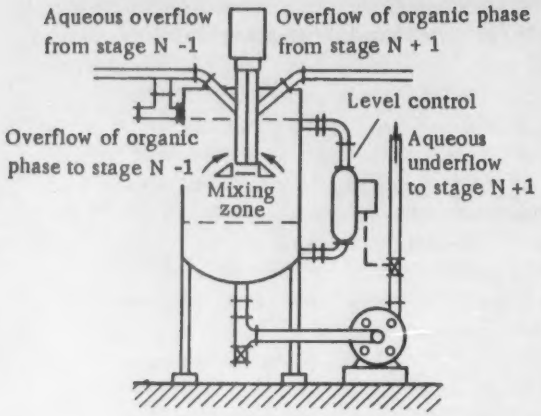
Aqueous overflow from stage N -1
Overflow of organic phase from stage N + 1
Level control
Overflow of organic phase to stage N -1
Aqueous underflow to stage N +1
Mixing zone

Fig. 5.
Diagram of a turbomixer-settler.

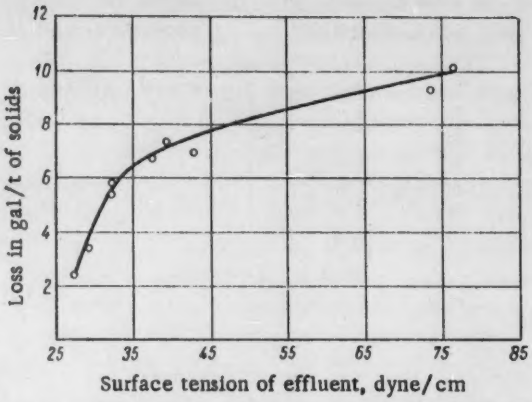

Fig. 6. Loss as a function of surface tension of effluent.

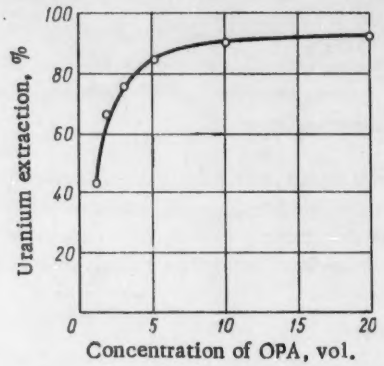

Fig. 7. Uranium extraction as a function of the concentration of OPA.

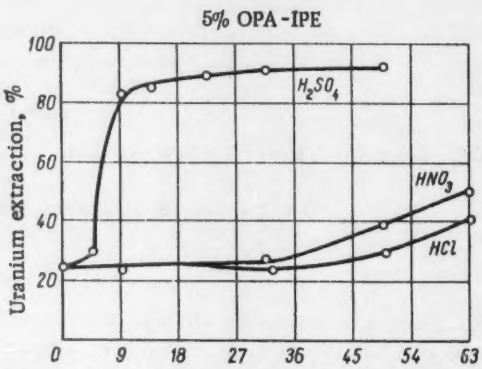

Fig. 8. Uranium extraction as a function of the type of acid.

100 ml/min using pulps obtained in the processing of Colorado Plateau ores with sulfuric acid. The reagent was 0.1 M solution of monododecylphosphoric acid in kerosene. The entrainment of reagent at a mixer speed of 500 rpm was 25-40 liter/t of solids. On increasing the speed to 800 rpm, the entrainment was almost doubled. Visual study of the effluent by which the organic solvent was entrained showed that the organic phase was dispersed in it in the form of a spherical particles 15-150 μ in diameter, and only very little of it was adsorbed on the surface of the solid particles. This was also confirmed by the fact that after centrifuging of the pulp containing 30 liters of entrained solvent per ton of solids, less than 2 liters of organic solvent remained in the solid phase.

If after separation, the pulp is diluted with water, the sand and slurry settle and the organic phase is separated, due to which the entrainment is reduced by several times. Addition of hydrophile surface-active substances to the pulp before contact with the organic solvent diminishes the entrainment, as is shown by Fig. 6 (Report No. 497).

Forty-five surface-active agents were tried and some of them (for example, ammonium lignin sulfonate) reduced the entrainment of solvent by half. On subsequent dilution of the pulp with water, entrainment was reduced to about 3/5 liter/t of solids. Report No. 497 shows that by correct choice of equipment, dilution of effluent pulp and addition of surface-active substances, it is possible to reduce solvent entrainment, but the figures obtained cannot as yet be regarded as economically acceptable.

Very interesting is the attempt to combine solvent extraction with acid decomposition. This work is described in Report No. 496.

During extraction of the pulp, when the ores are brought into contact with the acids before extraction, the acid consumption on the whole remains the same as in the normal processes, since the conditions of acid decomposition are not altered. Matters are different if the acid decomposition is combined with solvent extraction. In this case, concentrated sulfuric acid is added previously to the diluted extractant or to the mixture of extractant and crushed ore. Different types of extractants, the influence of concentration and type of diluent on the uranium extraction, the amount of acid and the ratio of extractant and ore during contact in leaching were studied under laboratory conditions. The

extractants investigated were isooctylphosphoric acid (OPA) containing both mono- and diesters, and also monododecylphosphoric acid and monoheptodecylphosphoric acid. No substantial difference was found between their extraction powers.

Uranium extraction rapidly increases with increase in the concentration of isooctylphosphoric acid, then the rate of increase in extraction diminishes and after 10% concentration practically does not alter (Fig. 7, Report No. 496).

Figure 8 (Report No. 496) shows the effect of different inorganic acids on uranium extraction. In the processing of high carbonate carnotites by sulfuric acid with a 5% solution of OPA in isopropyl ether (IPE), the acid consumption was 9-13.5 kg/t of ore. For the extraction of 85% of the uranium in the aqueous process, about 160 kg of sulfuric acid must be used. The consumption of other acids in the case of combined extraction-leaching is not appreciably diminished. Such reduction in sulfuric acid consumption is due to the fact that during processing, the carbonate grains become coated with an insoluble film of gypsum, while the uranyl sulfate formed is dissolved by the organic solvent, and the freshly formed surface of the mineral is again exposed to the action of acid. If other acids are used, the calcium salts formed are soluble.

In the extraction-leaching process, the medium should be kept acid, otherwise the discard pulp cannot be washed completely free from extractant by the diluent, due to the formation of calcium alkylphosphates, insoluble in organic solvents.

The recovery of uranium is increased if ethers and ketones are used as diluents. Although methyl ethyl ketone gives the best recovery of uranium, isopropyl ether is less soluble in water, which makes it a better diluent. Kerosene is also not very soluble in water, but, if it is used, thickening is not so good and the loss of isooctylphosphoric acid is increased. The ratio of the phases also has an influence on the good recovery of uranium. Provided there is good contact, 2 mg of 5% solution of extractant is sufficient for 1 g of ore.

Crushing to 50 mesh is adequate for good extraction of carnotite ores. The process described in Report No. 496 is applicable only for secondary ores; maximum economy is obtained when processing high carbonate ores. The process is also promising for ores whose pulps are difficult to thicken and filter. For ores containing uraninite, satisfactory recovery was not effected by this process. These investigations are as yet being carried out under laboratory conditions.

There were no other reports submitted to the Conference in dealing particularly with the solvent-extraction process in the treatment of uranium ores. Solvent extraction as an auxiliary method of recovering uranium from solutions obtained was mentioned in some reports describing the choice of technical scheme for ores from specified deposits. For example, the French Report No. 1225 describes a method of chemical benefication of low grade ores for subsequent processing by different methods (including solvent extraction), based on the following principles:

1. fractional neutralization of solutions, after sulfuric acid leaching of low grade ores, with lime for the precipitation of the uranium in the form of an intermediate concentrate, sufficiently rich in uranium (10-20 %), the waste liquors being purified at the same time;

2. repeated processing of this concentrate by simple methods for the production of a solution permitting the precipitation of well-known uranate, or repeated processing in a nitric acid medium for extraction by tributylphosphate with the object of producing uranium of nuclear purity.

Fractional precipitation was carried out in two stages: a first precipitation in the limits of pH = 2.7 for removing maximum impurities, in particular iron (the risk of the precipitation of uranium phosphate, precipitating before the uranyl, was eliminated by the addition where necessary of trivalent iron); after separation of the first precipitate by filtration, the second precipitation was carried out at a pH = 6.5-7.0, resulting in a 10-20% concentrate containing 5-20% Fe_2O_3, 20% CaO, and 5-20% Al_2O_3. If dehydration has been effected by filtration, the first neutralization can be carried out directly in the pulp, which reduces somewhat the number of operations. In the case of decantation, neutralization cannot be carried out in the pulp, since the higher pH value would impair the precipitation conditions.

After lengthy studies, the authors of Report No. 1255 decided that acid leaching is preferably carried out as follows. The intermediate concentrate is mixed with sulfuric acid or iron sulfate and is roasted at 150-400°C, after which it is treated with the return nitrate liquors. There is good recovery of uranium with slight extraction of impurities. The filtered solution, after the addition of nitric acid, is passed to extraction by tributylphosphate. After extraction, the aqueous phase is neutralized by lime; the precipitate of impurities is discarded, and the solution is returned to leaching.

Such a chemical method of processing the solution with separation, by filtration in an acid medium, of the precipitated impurities and with separation of an intermediate concentrate appears to be cumbersome and uneconomical.

Report No. 230 deals with a study of the leaching of uranium from the low grade pegmatitic deposits of northern Saskatchewan in Canada (0.08% or less uranium).

Attempts to enrich these ores by flotation failed to give any satisfactory results. This is partly due to the fact that as a rule, uranium minerals are not very suitable for flotation, and partly to the fact that in many ores they are intimately bound up with the gangue. Recovery of uraninite from the pegmatites of above 83-85% was impossible, the yield being 20-22% and the ratio of enrichment 3.5-4.

In leaching the uranium, 75 kg of sulfuric acid is consumed per ton of concentrates, Recovery is about 95%. Referred to the ore, this yield represents 80% for an acid consumption of 15 kg/t. More economical figures were obtained from direct processing of the ores. For example, leaching with sulfuric acid at a temperature of 25°C gave a recovery of about 90% of uranium after 24-48 hours, depending upon the method of leaching adopted; the acid consumption was 9-18 kg, with or without the addition of an oxidizer. The iron present in the ore was evidently sufficient to ensure the requisite oxidizing effect.

Different leaching methods did not give greatly differing results, although a somewhat higher recovery was obtained by the use of percolation.

The recovery of uranium from the solutions obtained was by solvent extraction. The best results (99.9% recovery) were obtained with three-stage and four-stage counterflow extraction using a 0.1 M solution of the amine 9D-178 (amine LA-1) in kerosene, the ratio of solution to extractant being 4:1.

The principal conclusion which can be made from the review is that there is a fairly pronounced trend towards dispensing with processes of separating solids from liquids and towards the recovery of uranium directly from pulps, since even counterflow decantation processes, not to mention filtration, have quite a considerable weight in the over-all economy of uranium technology.

The second conclusion is that there is some disappointment in the RIP process (in the technical form usually adopted in the USA) in view of the bulkness and mechanical complexity of the equipment and the impossibility of using thick pulps. This is clear from the report describing the operation of the Moab plant, and also from the endeavors to develop new processes of sorption from pulp; for example, the process of ion exchange in a pulsating bed of resin††.

The third point which merits attention is the attempt to develop a technology of combining leaching with solvent extraction for attaining maximum reduction in acid consumption and increasing the uranium recovery.

It is also not without interest to note the almost complete rejection of filtration for the separation of solids after ore leaching, and the extensive adoption of counterflow decantation using flocculants.

These trends may be regarded as decisive in the development of sorption and solvent-extraction processes in the technology of uranium production.

Received February 7, 1959

---

††See also the article by E. Rau, Mines Mag. 47, 9, 39 (1957) on the counterflow recovery of uranium from pulps in special apparatus, in which contacting of the resin and pulp as well as their separation is effected.

CHEMICAL BEHAVIOR OF Mo^{99} FORMED BY THE IRRADIATION OF URANIUM OXIDE WITH SLOW NEUTRONS

L. V. Shiryaeva and Yu. M. Tolmachev

In this paper we examine the problem of extracting Mo^{99} from irradiated samples of U_3O_8 and UO_2, fired in vacuum and in a stream of argon from 400 to 1200°. The relation of the per cent of Mo^{99} extracted to temperature and time of firing was demonstrated.

The activation energy for removing Mo^{99} from uranium oxide grains for some sections of the curves was calculated on the basis of the relations obtained between the logarithm of the value of Mo^{99} extraction and the inverse absolute temperature.

The results of experiments on the extraction of Mo^{99} from neutron irradiated preparations of U_3O_8 and UO_2 fired in a stream of hydrogen and oxygen are given in [1].

In the present report we describe the results of experiments with preparations of U_3O_8 and UO_2, which were fired in vacuum and in a stream of argon after irradiation. The starting U_3O_8 and UO_2 preparations and the procedure for leaching Mo^{99} from the samples after they had been heated were the same as in [1]. For samples fired at a high temperature, the Mo^{99} remaining after leaching was also determined.

Experiments involving firing in vacuum (10^{-2} mm Hg) were performed in the following way. Special quartz tubes were first degassed at 700°C for 1 hour. Then, after the preparations of irradiated oxides had been placed in them, the tubes were pumped out and sealed. The samples in the tubes were fired in a furnace at temperatures of 400-1200°C for 1.5 hr. Approximately half of the tube was placed within the furnace while its sealed end was outside the furnace and cooled with water. The MoO_3 which volatilized from the oxide powder during firing condensed in the cooled end of the tube. After cooling, the tube was cut in half. The MoO_3 which had distilled into the cold end of the tube was washed out with dilute NaOH solution. A carrier solution of ammonium molybdate was added to the solution obtained and, after the usual purification, lead molybdate was isolated.

Figure 1 (a, b) gives the relation of the per cent of Mo^{99} extracted to firing temperature of U_3O_8 and UO_2 in vacuum and argon and, for comparison, in hydrogen and oxygen.

The extraction values plotted on the ordinate equal the sum of Mo^{99} leached and volatilized (Fig. 1 a and b). The curves for Mo^{99} extraction from U_3O_8 fired in hydrogen and oxygen almost coincide (Fig. 1 a). The greatest extraction was observed at 1200°C (70%). However, the highest curve is that for extraction from U_3O_8 fired in argon.

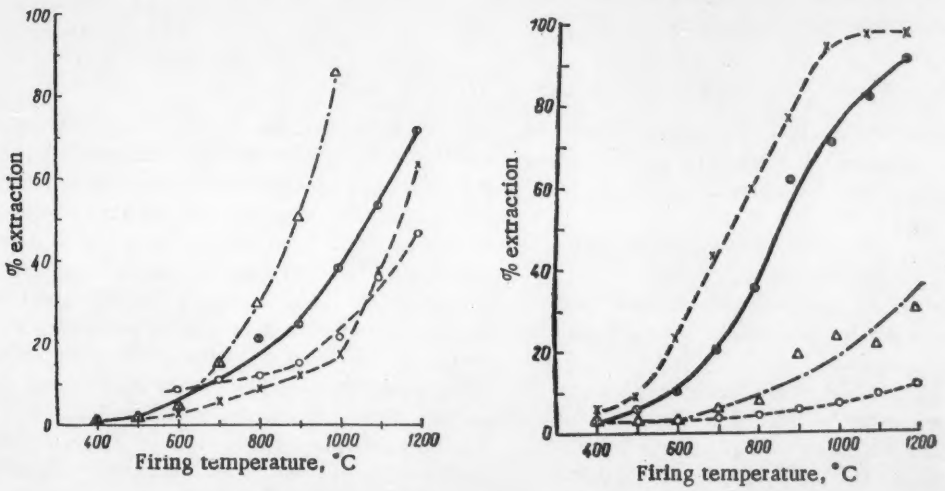

Fig. 1. Relation of per cent of Mo^{99} extracted from U_3O_8 (a) and UO_2 (b) to firing temperature: x – in oxygen; O – in hydrogen; ⊗ – in vacuum; Δ – in argon

Volatilization of Mo^{99} During Firing

Medium	Firing temperature of U_3O_8, °C				Medium	Firing temperature of UO_2, °C			
	900	1000	1100	1200		900	1000	1100	1200
Argon	0*	17*	16*	23*	Argon	Not determined	0*	0*	0*
Vacuum	0,1	1,2	7,3	22	Vacuum	Not determined	0,2	1	7,8
Oxygen	1*	1,5*	6*	12*	Oxygen		8*	12*	30*

*The values were determined by the difference between the starting activity of molybdenum and the activity remaining in the sample.

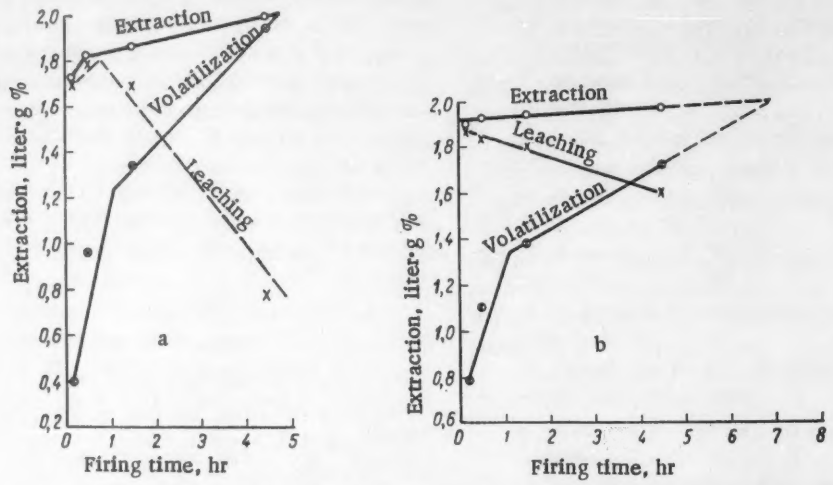

Fig. 2. The relation of the logarithm of the per cent of Mo^{99} extracted from U_3O_8 (a) and UO_2 (b) to firing time in vacuum; Temperature 1200°C.

Mo^{99} extraction from UO_2 (Fig. 1 b) proceeded differently: least molybdenum was extracted from preparations fired in hydrogen and most from preparations in vacuum and oxygen.

The table gives data on the volatilization of Mo^{99} at high U_3O_8 and UO_2 firing temperatures.

Volatilization of Mo^{99} was noticeable in vacuum only at high temperatures, and it was somewhat greater from U_3O_8 than from UO_2.

Figure 2 (a,b) gives data on the change in the logarithm of the percent of Mo^{99} extracted in relation to the increase in U_3O_8 and UO_2 firing time in vacuum at 1200°C.

A large part of the Mo^{99} accumulating on the surface of the grains of the oxide powder came from inside the grains, and this process occurred at a high rate at the beginning. In the first ten minutes of firing in vacuum at 1200°C, 50 and 80% of Mo^{99} accumulated on the surface of the grains of the U_3O_8 and UO_3 powders, respectively; almost all this molybdenum was leached by subsequent treatment. Then the rate of Mo^{99} accumulation on the grain surface fell. With an increase in firing time, the amount of Mo^{99} remaining inside the oxide grains decreased, but part of it volatilized from the grain surface. An extrapolation of the curves shows that 100% of the Mo^{99} was sublimed during the firing (1200°C) of urano-uranic oxide for 5 hr and uranium dioxide for 7 hr in vacuum.

Using the data given in Fig. 1 (a,b), we plotted the relation of the per cent of Mo^{99} extracted to the inverse absolute firing temperature $1/T$ (Fig. 3 a and b) in semilogarithmic coordinates.

If one assumes that the degree of extraction (elimination) of Mo^{99} from the grains of oxide powder that we determined depended to a considerable degree on diffusion processes, then the activation energy of these processes may be calculated from the slope of the lines corresponding to them. The values of these energies are given in kcal/mole in circles beside each line (Fig. 3 a and b).

Discussion of Results

In interpreting the relations obtained one should consider several factors: the chemical and physical properties of uranium oxides and their phase conversions, the chemical and physical properties of molybdenum and its oxides, the effect of firing time and temperature, the interaction of uranium and molybdenum oxides with hydrogen and oxygen, and also the fact that the U_3O_8 and UO_2 samples were not degassed before irradiation. The oxygen contained in the irradiated preparations (mainly due to sorption) may oxidize the Mo^{99} formed during fission. It is quite probable that the formation of molybdenum oxides occurred as a result of the interaction of hot Mo^{99} atoms with oxygen as well as during the subsequent heating.

The presence of an inflection in the curve (Fig. 3b) showing the relation of molybdenum extraction from uranium dioxide that had been fired in hydrogen to temperature may be explained hypothetically as follows. Firing in hydrogen produced no changed in the composition and lattice of UO_2. The temperature at the intersection of the two straight sections of the curve is 1070°K and probably corresponds to the Tammann loosening temperature of the oxide lattice [2]. It is 0.43 of the absolute melting point of UO_2, which equals 2470°K [3].

All the curves (Fig. 3 a and b) have a low-temperature section with a low activation energy, which probably corresponds to surface diffusion.

Conversion of U_3O_8 to UO_2 in an atmosphere of hydrogen (Fig. 3, b) at 600°C was accompanied by a sharp increase in the extraction of molybdenum. The further course of the curve is the same as for UO_2 fired in hydrogen. The temperature at the intersection point of these sections is 1270°K.

Depending on the method of preparation, UO_2 samples may absorb oxygen to a greater or lesser degree. At a low temperature, the preparations are oxidized to $UO_{2,3}$ with hardly any change in the crystal lattice [3-5]. U_3O_8 begins to decompose in vacuum when heated to 700°C [3,6] and it decomposes in air at 900°C [3,4]. U_3O_8 may be oxidized to UO_2 when fired in a stream of inert gasses [3]. One may assume that these peculiarities in the behavior of the oxides and also Tammann's temperature of loosening of the lattice were reflected to a certain degree in the curves obtained. However, an exhaustive interpretation of the curves (Fig. 3 a and b) is impossible at the present time.

In 1923, Hahn proposed a method for studying the structural changes in solid bodies by use of the emanation from natural radioactive elements [7,8].

In 1942, Zimens [9] demonstrated the possibility of using nuclear reactions for obtaining inert gases in solid bodies in order to investigate gas diffusion. In subsequent work, Zimens studied the diffusion of inert gases formed during fission in metallic uranium [10-12]. An interesting phenomenon in this work was that the radioactive inert

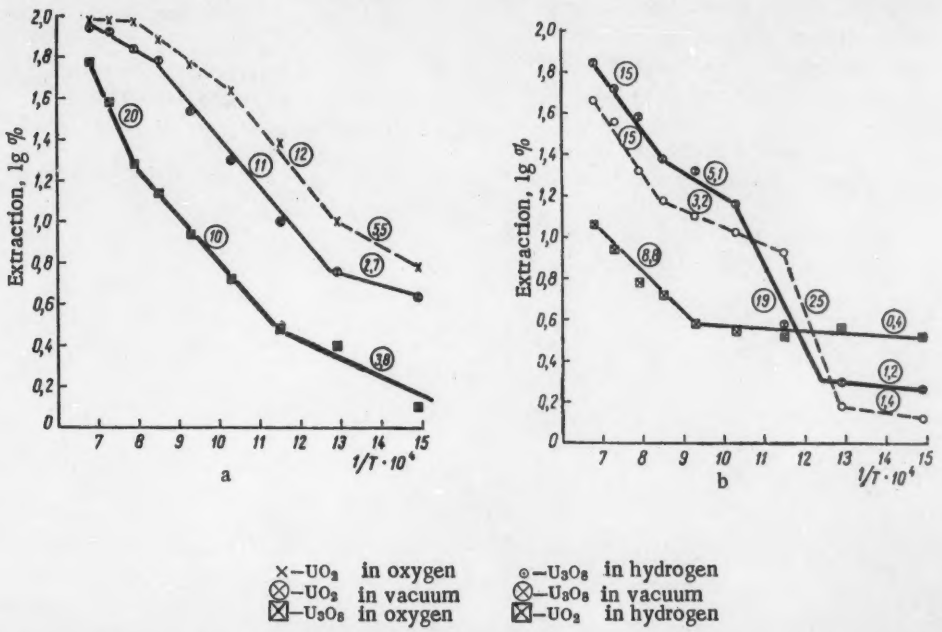

Fig. 3. The relation of the logarithm of the per cent of Mo^{99} extracted from U_3O_8 (a) and UO_2 (b) to the inverse absolute firing temperature:

gas was distributed evenly in the uranium due to its being formed directly within the metal, and, as a result of its chemical inertness, it did not react with the solid body.

Cook and Prout [13] used I^{132} for studying the structural changes in $BaSO_4$. The I^{132} was obtained from Te^{132}, which cocrystallized isomorphically with $BaSO_4$. The authors indicated that this method was less exact since the iodine was chemically active and could react with the components of the system.

In 1957, a short abstract appeared on Lustman's work on the elimination of gaseous fission fragments from irradiated UO_2 [14]. The author proposed that the rate of elimination was determined by gas diffusion in the mother substance. It is stated in the abstract that the rates of the process were determined and the activitation energies calculated and found to be similar to the corresponding values for the diffusion of oxygen in UO_2. Regrettably, no numerical data are given in the abstract. There is also no detailed description of the experimental procedures.

The study of the initial chemical forms of Mo^{99} after its formation, as a result of uranium fission in the systems we studied, was complicated by the following circumstances: 1) the Mo^{99} may be found in different compounds in the irradiated uranium oxides, 2) changes may occur in the composition of the uranium oxides under the effect of the firing and of the chemically active gases (hydrogen and oxygen), and 3) Mo^{99} may react chemically with these gases and uranium oxides to form different Mo^{99} compounds. Other factors are also possible.

CONCLUSIONS

1. Mo^{99} extraction from irradiated U_3O_8 and UO_2 samples increases with an increase in the firing temperature in vacuum, and in a stream of argon, hydrogen, and oxygen. The greatest amount of Mo^{99} was extracted from UO_2 (97%) fired in oxygen in 1200°C, and from U_3O_8 (71%) fired in vacuum at 1200°C.

2. Mo^{99} began to volatilize at 900°C from U_3O_8 and UO_2 fired in a stream of oxygen and in vacuum. The high volatility of Mo^{99} from UO_2 fired in oxygen at temperatures of 1000-1200°C was observed.

3. Extrapolation of the relation obtained for Mo^{99} extraction against firing time showed that 100% of Mo^{99} was volatilized from U_3O_8 in 5 hr of firing in vacuum at 1200°C, and from UO_2 in 7 hr of firing.

4. Graphs were plotted (liter · g per cent extraction against 1/T) from the experimental data and the activation energies of Mo^{99} extraction from uranium oxides calculated.

LITERATURE CITED

1. L. V. Shiryaeva and Yu. M. Tolmachev, Atomnaya Énergiya 3, 318 (1957)*.
2. G. Tammann, Z. anorg. u. allgem. Chem. 149, 67 (1925).
3. D. Katz and B. Rabinovich, Chemistry of Uranium. I [Russian translation] (Moscow, IL, 1954) pp. 205-232, 249-251.
4. W. Biltz and H. Nuller, Z. anorg. u. allegem. Chem. 163, 279 (1927).
5. F. Gronvold and H. Haraldsen, Nature 162, 69 (1948).
6. P. Jolibois, Compt. rend. 224, 1395 (1947).
7. O. Hahn, Applied Radiochemistry [Russian translation] (Leningrad-Moscow, Goskhimizdata 1947).
8. O. Hahn, J. Chem. Soc., Supp. Issue No. 2, 259 (1949).
9. K. Zimens, Z. phys. Chem. A-191, 38 (1942).
10. K. Zimens and P. Schmeling, Z. Electrochem. 58, 599 (1954).
11. K. E. Zimens, Chalmers tekn. hogskol. handl. No. 175, 7 (1956).
12. W. Inthoff and K. Zimens, Chalmers tekn. hogskol. handl. No. 176, 1 (1956).
13. G. Cook and E. Prout, J. Inorg. Nucl. Chem. 3, 255 (1956).
14. B. Lustman, Nuclear Science abstracts 11, No. 14, abstract No. 7384 (1957), WAPD-173.

*See English translation

Received September 4, 1958

DISSOCIATION OF THE UF_6 MOLECULE UNDER THE ACTION OF FRAGMENTS FROM FISSION OF THE URANIUM NUCLEUS

V. A. Dmitrievskii and A. I. Migachev

It was shown that when irradiated with neutrons, uranium hexafluoride decomposed to intermediate uranium fluorides (presumably UF_5 and fluorine). The rate of decomposition was ~G = 0.5 mole /100 ev or 0.21 mole/hr per kw of power liberated in the gas. It was also shown that in addition to dissociation of UF_6 during irradiation there was also recombination of the decomposition products. As a result, equilibrium concentrations of fluorine and UF_6 are set up, and these depend on the strength of the radiation. When mixed with fluorine, uranium hexafluoride is a radiation-stable compound even at room temperature and may be used as a fuel in a nuclear reactor.

The main objection to the design of a reactor operating on the gaseous uranium compound UF_6 consists of the following. It is known that complex molecules of a substance are decomposed under the action of radioactive radiation (see, for example, [1 and 2], etc.). In this process, fission fragments have the greatest destructive effect [3]. It is natural to suppose that UF_6 molecules would decompose to lower uranium fluorides and free fluorine under the action of radioactive radiation from a reactor (mainly under the action of uranium fission fragments). As the lower fluorides of uranium are nonvolatile [4], they would be precipitated and would accumulate on the walls of the reactor.

At the same time it is known that uranium fluorides are comparatively easily fluorinated to uranium hexafluoride by gaseous fluorine [4,5]. Therefore, one might hope that a mixture of uranium hexafluoride with fluorine would be a radiation-stable nuclear fuel under suitable conditions. Goodman [6] had previously put forward a hypothesis on the stabilizing effect of the addition of fluorine. However, due to the absence of experimental data* on the destruction of the UF_6 molecule and the very sparse data on the kinetics of the reverse reactions [4,5], it is impossible to draw any conclusions on the radiation stability of uranium hexafluoride. It was therefore necessary to carry out special experiments.

A steel ampule of 20 mm diameter containing uranium hexafluoride of natural isotope composition was placed in a channel of an RFT reactor [7] with a neutron flux of $0.5 \cdot 10^{13}$ neutrons/cm^2 · sec. The temperature of the ampule walls was maintained constant at 50°C by the cooling circuit of the reactor. The initial gas pressure was 37.5 mm Hg, which corresponded to $1.2 \cdot 10^{-3}$ mole of UF_6. During irradiation, the gas pressure was measured and the composition of the gas mixture analyzed periodically (with the reactor shut down). The pressure of the gas was measured with a remote electric pressure gage. The composition of the gas was analyzed by a "freezing out" method based on the difference in vapor pressure of UF_6 and fluorine. For this purpose, a "finger" of thin-walled German silver with a sealed end was soldered into the ampule. The finger was filled with liquid nitrogen, and uranium hexafluoride condensed onto it. The concentration of fluorine was determined from the total and the residual pressures of the gas mixture.

The uranium hexafluoride was irradiated in the reactor for 33 hours. Figure 1 gives a graph of the relation of the total gas pressure to time and Figs. 2 and 3 give graphs of the changes in the amounts of UF_6 and fluorine formed. A decrease in UF_6 pressure may be induced not only by the effect of radiation, but also by the chemical reaction of the gas with the walls of the apparatus. Therefore, we first obtained the relation of gas pressure to time without irradiation (Fig. 2, upper curve).

As could be expected, the results confirmed the presence of considerable UF_6 dissociation under the effect of irradiation. The character of the given curves is readily explained. UF_6 molecules are decomposed by fission fragments whose range under the experimental conditions was 2-3 times greater than the diameter of the vessel (the average range of a fission fragment in air under normal conditions is 23 mm [8]). As the UF_6 molecules are destroyed, the pressure decreases and the fission fragments lose an increasingly smaller part of their energy in colliding with the gas molecules and thus the destructive effect of the fragments decreases. For this reason, the rate of decrease in the gas pressure falls toward the end of the experiment. Besides that, with the formation of fluorine, reverse recombination processes occur, and UF_6 molecules are again formed. This recombination also leads to a decrease in the "effective" rate of dissociation. The curve in Fig. 3 confirms what has been said. In fact, the initial increase in the partial pressure of fluorine occurs as a result of the decomposition of UF_6 molecules. The rate of increase of fluorine pressure falls with the decrease in the rate of UF_6 molecule destruction. When the rate of uranium hexafluoride destruction becomes quite low, the effect of chemical losses of fluorine as a result of its absorption by the apparatus walls becomes noticeable and the amount of fluorine in the ampule decreases.

*The authors became acquainted with [12] only after this article had been sent to the editor.

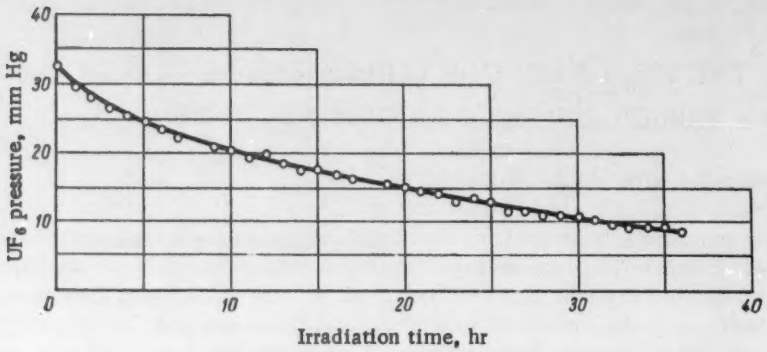

Fig. 1. Relation of total gas pressure to time.

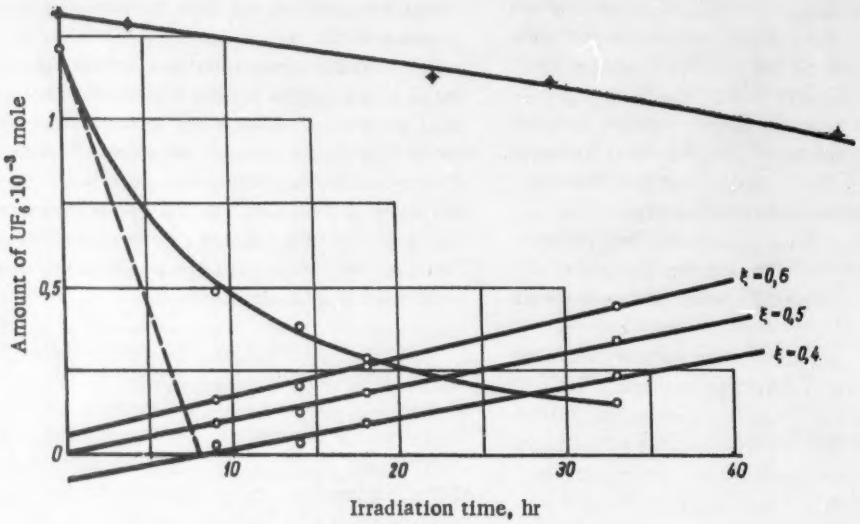

Fig. 2. Changes in the amount of UF_6 with time. Upper curve: control experiment without irradiation.

The reaction of UF_6 dissociation may be written in the following form:

$$UF_6 \rightarrow UF_{6-2\xi} + \xi F_2. \quad (1)$$

To determine the coefficient ξ, let us write the equation for the conservation of the amounts of UF_6 and fluorine. The loss in the number of uranium hexafluoride molecules in unit time dn_1/dt equals:

$$-\frac{dn_1}{dt} = f(w) + c_1. \quad (2)$$

Here $f(w)$ is an unknown function, which depends on the neutron flux, relative concentrations of components in the mixture, etc. The constant c_1 determines the rate of decrease of the amount of UF_6 due to chemical reaction of the gas with the walls of the apparatus. Analogously, taking into account (1), for the change in the number of fluorine molecules with time we have:

$$\frac{dn_2}{dt} = \xi f(w) - c_2. \quad (3)$$

Deducting the unknown function $f(w)$ from (2) and (3) and integrating at the starting conditions $n_1(0) = n_{10}$ and $n_2(0) = 0$, we obtain:

$$\xi(n_{10} - n_1) - n_2 = (\xi c_1 + c_2)t, \quad (4)$$

where $(n_{10} - n_1)$ is the number of dissociated UF_6 molecules. Experimental data on the change in the difference $\xi(n_{10} - n_1) - n_2$ with time at values of $\xi = 0.4$; 0.5 and 0.6 are given in Fig. 2. These graphs show that the line corresponds to (4) (passes through the origin of the coordinates) only at a value of $\xi = 0.5$. It follows from this that dissociation of UF_6 molecules proceeds, with the formation of UF_5, according to the equation:

$$UF_6 \rightarrow UF_5 + \frac{1}{2}F_2.$$

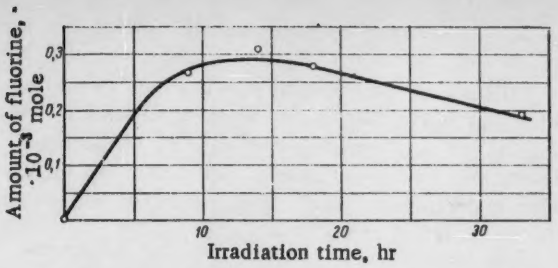

Fig. 3. Change in amount of fluorine with time.

The experiment carried out made it possible to evaluate the rate of UF_6 molecule destruction. Thus, for example, the rate of decrease of the amount of uranium hexafluoride at the initial moment of time (obtained by extrapolation) was approximately $0.14 \cdot 10^{-3}$ mole /hr. This value was less than the true rate of dissociation since the diameter of the experimental vessel was less than the average range of a fragment in the gas, and consequently a large part of the energy of the fission fragments was lost on colliding with the walls. Solid uranium hexafluoride was used in an experiment in order to evaluate the actual rate of destruction of UF_6. In this case, due to high density of UF_6, all the energy of the fission fragments was spent in collisions with uranium hexafluoride molecules.

For this experiment we used an aluminum vessel with a 180 cc capacity, fitted with a cooling coil and a remote pressure gage with a range from 0 to 75 mm Hg for measuring the gas pressure. An amount equaling 388 g of UF_6 with a natural isotope composition was condensed in the ampule. This sample of UF_6 was irradiated in a channel of an F-1 reactor [9] for 16.5 hr. The neutron flux at the ampule was of the order ot $5.8 \cdot 10^9$ neutrons/cm^2·sec. The temperature of the water circulating in the cooling coil was maintained at 8°C during the irradiation. The initial pressure of the gas corresponded to the known value for the pressure of UF_6 vapor over a solid phase at the given temperature, and remained practically the same during the experiment. After irradiation, the uranium hexafluoride was recondensed into another vessel in order to free the fluorine formed within the solid UF_6 crystals. The amount of fluorine formed, calculated from its pressure, was found to be $0.9 \cdot 10^{-3}$ mole. The amount of fluorine found by chemical analysis was found to be $0.71 \cdot 10^{-3}$ mole†. Considering that there was a slight loss of fluorine during the chemical analysis, the agreement may be considered quite satisfactory.

This experiment made it possible to evaluate the rate of dissociation of UF_6 molecules per unit of power liberated in the gas (recombination, which could occur in the preceding experiment, was excluded here since meeting of the dissociation products in the condensed state was improbable). It was found to be 0.21 mole/kw·hr and agreed in order of magnitude with the value of 0.32 mole/kw·hr (0.8 mole/100 ev), which we determined more accurately from other experiments [10].

It was stated above that at a sufficient concentration of elementary fluorine in gaseous uranium hexafluoride, one would expect the reverse reaction (recombination) of fluorine with lower uranium fluorides, formed as a result of UF_6 irradiation. To confirm this, experiments were carried out on the neutron irradiation of uranium hexafluoride, enriched up to a concentration of 75.2% of U^{235}.

† N. N. Balashova carried out the chemical analysis at our request.

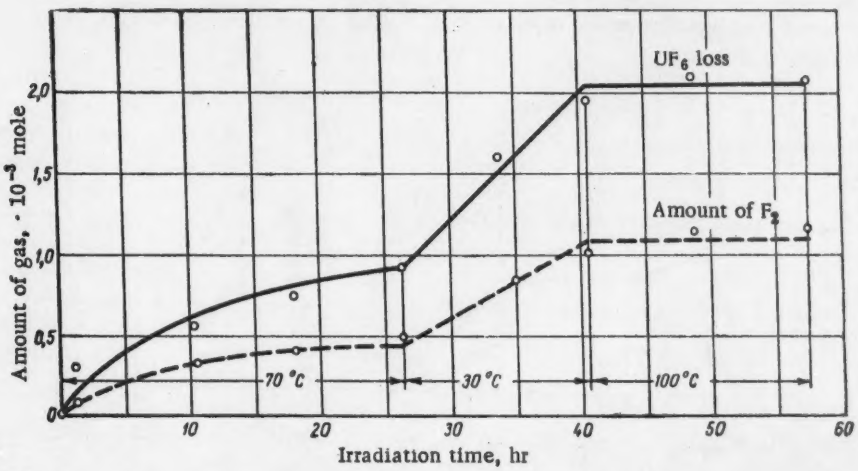

Fig. 4. Loss in the amount of UF_6 and amount of fluorine formed under different irradiation conditions. The middle section of the graph corresponds to irradiation of solid UF_6.

The irradiation was carried out in a channel of an F-1 reactor. The uranium hexafluoride was placed in an aluminum ampule, which was heated by an electric furnace.

The ampule was fitted with a pressure gage with remote reading for measuring gas pressure and with thermocouples for measuring temperature. All the leads and the pressure gage itself were placed in a thermostat to avoid condensation of uranium hexafluoride on cold parts of the apparatus.

The initial gas pressure was 524 mm Hg at a temperature of 70°C ($9.8 \cdot 10^{-3}$ mole). The gas was irradiated for 60 hr in a neutron flux of about 10^{10} neutrons/$cm^2 \cdot sec$. The relation of UF_6 and F_2 pressures to time was investigated. The results obtained are given on the graph in Fig. 4. The experiment was in three stages. At first, the neutron irradiation was carried out under conditions in which all uranium hexafluoride was in the gaseous state and the temperature of the vessel walls was 70°C (left section of the curves in Fig. 4). Over 26 hr of irradiation, the amount of UF_6 dissociated was $0.9 \cdot 10^{-3}$ mole.

In order to ascertain that the fluorine that appeared actually entered the reverse reaction with the lower uranium fluorides, the second stage of the irradiation was carried out under conditions when a considerable part of the UF_6 was condensed. In this case, as has already been mentioned above, due to the low lability of the decomposition products, the measured rate of dissociation should increase noticeably. In fact, the graph in Fig. 4 (middle section) shows that the decomposition rate of uranium hexafluoride increased by a factor of approximately two.

The third stage of the experiment was carried out under conditions when the UF_6 was again gaseous. The graph in Fig. 4 shows that the UF_6 molecules were no longer decomposed. This meant that the fluorine concentration had reached equilibrium.

Thus, this experiment confirmed that under the effect of intense radiation, the lower uranium fluorides were fluorinated even at low temperatures.

A control experiment (without irradiation) showed that the losses of fluorine and UF_6 through interaction with the apparatus walls were negligibly small. Therefore the coefficient ξ in reaction (1) may be calculated as the ratio of moles of UF_6 dissociated to moles of fluorine formed. The average value of ξ, calculated from the experimental data, was equal to 0.52 ± 0.05 and agrees with the value obtained above.

It was interesting to determine whether the dissociation–recombination process of UF_6 molecules was a reversible process (i.e., if the equilibrium concentrations of F_2 and UF_6 could be varied in the required direction by changing the experimental conditions), what relation existed between the equilibrium concentrations and specific power liberated in the gas, and at what gas temperature the usual chemical interaction of fluorine with the lower uranium fluorides started to have an effect. Suitable experiments were carried out on a VVR reactor [11].

An aluminum vessel of 135 mm diameter and 135 mm height was filled with uranium hexafluoride. The vessel was fitted with a tubular aluminum coil to carry water for rapid cooling of the gas. An electric heating coil was placed around the vessel, allowing the gas to be heated to 250°C. A thermoregulator maintained the temperature of the vessel's walls at the required level with an accuracy of ± 1°C.

The pressure gage, valves, and all the leads connecting the working volume of the apparatus were thermostatted. A constant temperature in the thermostat was maintained by means of a contact thermometer and a suitable relay.

The partial pressure of fluorine was determined with the reactor shut down. For this the vessel with the gas was cooled to 8-10°C, and the total pressure of fluorine and UF_6 vapor corresponding to this temperature was measured. The UF_6 vapor pressure was found from a table.

The experiments were carried out with enriched uranium hexafluoride with a $U^{235}F_6$ content of 75.2%. The initial gas pressure was 345 mm Hg at 360°K ($3.1 \cdot 10^{-2}$ mole).

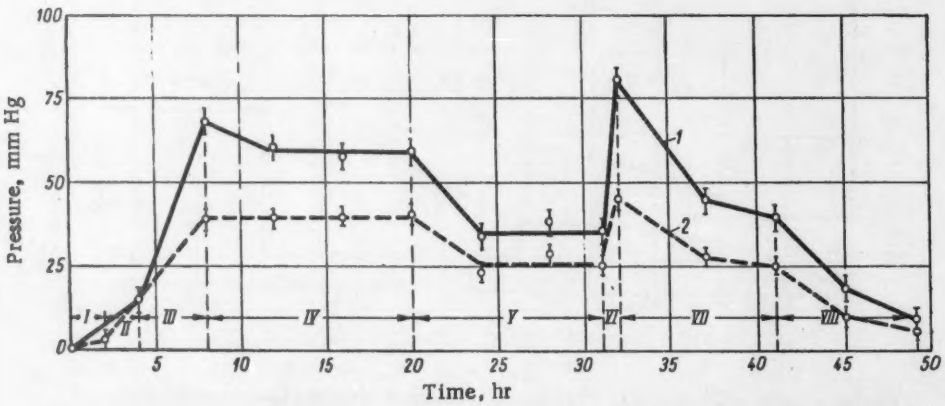

Fig. 5. Decrease in UF_6 pressure (curve 1) and fluorine pressure (curve 2) at different conditions of irradiation with high neutron fluxes.

The experimental results are given by the curves in Fig. 5. The curves are divided into sections corresponding to different experimental conditions. Section I corresponds to gas irradiation at a reactor power of 50 kw (flux of about $0.5 \cdot 10^{11}$ neutrons/$cm^2 \cdot sec$), when all the uranium hexafluoride was in the gaseous state. The time required to establish an equilibrium concentration under these conditions was found to be quite long. Therefore, in order to accelerate the experiments, the uranium hexafluoride was irradiated under conditions when a large part of it was in a condensed state. Section II in the figure corresponds to irradiation of solid uranium hexafluoride at a reactor power of 10 kw and section III, to 50 kw. The figure shows that the amount of fluorine under these conditions increased considerably, while the amount of UF_6 fell correspondingly.

Section IV on the curves again corresponds to irradiation of gaseous uranium hexafluoride. The temperature of the vessel walls was maintained at 100°C, while the power of the reactor was 50 kw. The figure shows that there was no noticeable change in the composition of the gas after 12 hr of irradiation. Therefore, one may conclude that the mixture obtained (12 % fluorine) was in equilibrium under the given experimental conditions.

Section V of the curves corresponds to gas irradiation at a reactor power of 250 kw. The amount of fluorine here fell to 26 mm Hg and then remained constant. The amount of UF_6 rose correspondingly due to "cold" fluorination of its dissociation products. A decrease in the equilibrium concentration of fluorine with an increase in power indicated that the recombination rate increased more than the rate of UF_6 dissociation with an increase in the intensity of the neutron flux.

The next experiment was to elucidate the effect of gas temperature on the value of the equilibrium concentration of fluorine. For additional confirmation of the possibility of uranium hexafluoride in a neutron field, the concentration of fluorine was first increased. For this, the experiment was carried out at a reactor power of 250 kw and under conditions when part of the uranium hexafluorine was in a condensed state (section IV of the curve). After this, the temperature of the vessel was raised to 100°C. Section VII of the curves corresponds to irradiation of the gas at this temperature and a reactor power of 250 kw. The figure shows that the amount of fluorine again fell, while the amount of UF_6 rose correspondingly. Limited time for the work did not allow us to await complete equilibrium, though the course of the curves shows that the equilibrium concentration of fluorine was close to the value of the equilibrium concentration in section V of the curves. This fact indicated that the gas temperature was still insufficient to noticeably affect the rate of chemical flourination of the dissociation products of the UF_6 molecule.

The last section (VIII) of the curves in Fig. 5 corresponds to irradiation of the gas at a reactor power of 250 kw and at a higher temperature (245°C). Here the equilibrium concentration of fluorine fell noticeably (below 2%). Apparently the usual chemical reaction between fluorine and uranium fluorides began to be felt appreciably at this temperature.

In all the experiments described above, the ampules were filled with uranium hexafluoride without the addition of fluorine. The fluorine was formed as a result of dissociation of the UF_6 molecules. It seemed interesting to investigate the stability of UF_6 in the presence of excess fluorine. For this purpose, additional fluorine was introduced into the vessel in such an amount that the fluorine concentration was 25.5% (the fluorine was prepared by electrolysis of potassium bifluoride and contained less than 5% of impurities). The graph plotted from the results of this experiment (Fig. 6) shows that within the limits of experimental error, the amount of uranium hexafluoride did not change. The increase in the partial pressure of UF_6 at the beginning was due to fluorination of the UF_6 decomposition products remaining in the ap-

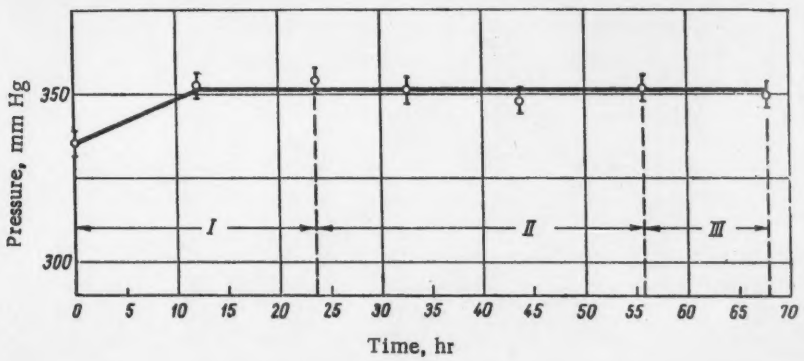

Fig. 6. Changes in the partial pressure of UF_6 in the presence of excess fluorine. Irradiation conditions: section I) 247°C, 250 kw; sections II and III) 50 kw, and 237 and 85°, respectively.

paratus and to products formed from chemical reaction of the UF_6 with the walls of the apparatus when the walls were treated with uranium hexafluoride before starting the experiment.

These experiments show that a reactor could be designed for uranium hexafluoride without fearing its decomposition under the action of neutron irradiation.

Such an experimental reactor was actually designed [10].

In conclusion, the authors consider it their pleasant duty to thank I. K. Kikoin for his interest and valuable advice.

LITERATURE CITED

1. Collection: Chemical Action of High Energy Radiation [Russian translation] (IL, 1948).
2. Collection: Radiation Chemistry [Russian translation] (IL, 1953); Collected Works on Radiation Chemistry [in Russian] (Izd. AN SSSR, 1955).
3. P. I. Dolin and B. V. Ershler, "Investigations in the fields of geology, chemistry and metallurgy," Reports of the Soviet Delegation to the International Conference on the Peaceful Uses of Atomic Energy [in Russian] (Izd. AN SSSR, 1955) p. 293.
4. J. Katz and E. Rabinowitch, Chemistry of Uranium. 1 [Russian translation] (Il, 1957).
5. Nuclear Sci. Abstr. 9, 435 (1955).
6. The Science and Engineering of Nuclear Power (edited by C. Goodman) [Russian translation] (IL, 1948) p. 273.
7. G. I. Kruzhilin, "Reactor construction and reactor theory," Reports of the Soviet Delegation to the International Conference on the Peaceful Uses of Atomic Energy [in Russian] (Izd. AN SSSR, 1955) p. 49.
8. P. Demers, Phys. Rev. 70, 974 (1946); P. Demers, Canad. J. Phys. 31, 78 (1953); M. Rogers and P. Demers, Canad. J. Phys. 31, 97 (1953).
9. V. S. Fursov, Session of the Academy of Sciences on the Peaceful Uses of Atomic Energy (plenary meeting) [in Russian] (Izd. AN SSSR, 1955) p. 15.
10. I. K. Kikoin, V. A. Dmitrievskii, Yu. Yu. Glazkov, I. S. Grigor'ev, B. G. Dubovskii, and S. V. Kersnovskii, "Test reactor with gaseous fissile material (UF_6)," Report No. 2502 presented at the Second International Conference on the Peaceful Uses of Atomic Energy (Geneva, 1958).
11. Yu. G. Nikolaev, "Reactor construction and reactor theory," Reports of the Soviet Delegation to the International Conference on the Peaceful Uses of Atomic Energy [in Russian] (Izd. AN SSSR, 1955) p. 91.
12. H. Bernhardt, W. Davis, and C. Shiflett, "The radiation effect of alpha particles on uranium hexafluoride," Report No. 522, presented by the USA at the Second International Conference on the Peaceful Uses of Atomic Energy (Geneva, 1958).

Received October 23, 1958

RADIATION VULCANIZATION OF FLUORINE COPOLYMERS

F. A. Galil-Ogly, T. S. Nikitina, T. N. Dyumaeva,
A. S. Novikov, and A. S. Kuz'minskii

Irradiation of rubberlike fluorine copolymers gives a rubber with poor physicochemical properties, but with fillers it is possible to obtain rubbers with valuable technical properties. The surface activity of the filler has a strong effect on the properties of the rubbers obtained. The most valuable properties are those of radiation rubbers that contain active channel black. They have a higher resistance to heat aging, are more stable to solvents and static deformation than the usual peroxide rubbers. In contrast to polytetrafluoroethylene and polytrifluorochloroethylene, rubberlike fluorine copolymers of the Kel -F type are cross-linked under the action of ionizing radiation. The degree of cross-linking of the fluorine copolymers is determined by their composition and the irradiation dose and medium. The presence of oxygen promotes a greater degree of cross-linking.

There has been very little study on the effect of ionizing radiation on fluorine-containing polymers up to now. Most attention was directed toward a study of the conversions of the fluorine-containing plastics, polytetrafluoroethylene, andpolytrifluorochloroethylene [1-7].

Ionizing radiation acting on these fluorine polymers caused extensive destruction of the macromolecules, accompanied by the formation of gaseous decomposition products.

In [4] it was established that polytetrafluoroethylene passed from the crystalline to the amorphous state when irradiated with Co^{60} γ rays and on the basis of spectral analysis data and isolation of the volatile substances, a hypothesis was put forward that during irradiation the C-C bond is broken in the main chain to form new structures

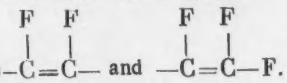

with a double bond of the type and . Similar changes occur in polytrifluorochloroethylene under the action of ionizing radiation.

Radiation vulcanization of a rubberlike substance, "SK Vitron A," which is a copolymerization product of hexafluoropropylene and vinylidene fluoride, was reported in [8]. It was shown that radiation vulcanization gave a rubber with better technical properties than the complicated and technically difficult chemical vulcanization with benzoyl peroxide.

It seemed interesting to study in more detail the radiation chemical changes occurring in fluorine copolymers under the action of ionizing radiation in relation to copolymer composition, the irradiation medium, type of filler and other factors, using some type of fluorine copolymer.

An elastomer of the Kel -F type (copolymer of trifluorochloroethylene and vinylidene fluoride) was chosen for the investigation; Co^{60} sources with activities of 1400 and 21,000 curies were used for irradiating the samples (0.3 - 1.0 mm thick plates). The integral dose of energy absorbed during irradiation was 3-80 · 10^6 r.

The structural changes in the irradiated fluorine copolymer were evaluated by the change in solubility, limiting swelling in acetone, the value of the equilibrium modulus E_∞ and by physicomechanical indices.

Figure 1 gives the relation of the main mechanical properties of the elastomer investigated to radiation dose in the presence of air. During irradiation of the fluorine copolymer, gaseous products were evolved, but their composition was not investigated. The amount of volatile substances evolved could be decreased by introducing into the copolymer additives such as lead and calcium oxides, various blacks, etc.

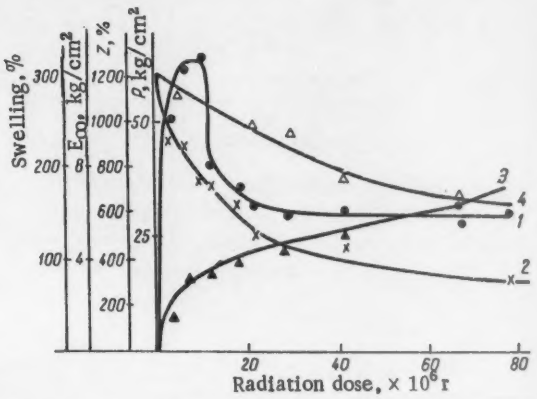

Fig. 1. The relation of the properties of the fluorine copolymer to radiation dose. 1) Tensile strength; 2) specific elongation; 3) equilibrium modulus; 4) limiting swelling.

In contrast to polytrifluorochloroethylene, in the irradiation of Kel -F type of fluorine copolymer containing about 66 % of vinylidene fluoride and 33% of trifluorochloroethylene, the process of structurization (i.e., cross-linking) predominated and this led to the formation of a

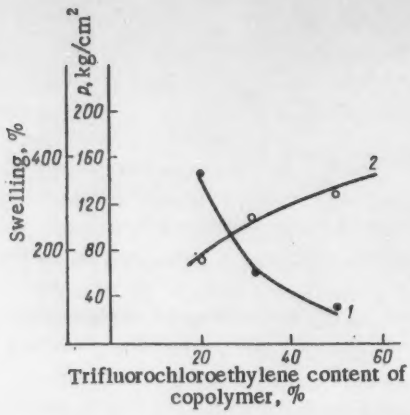

Fig. 2. Effect of trifluorochloroethylene content of the copolymer on the properties of radiation vulcanizates (integral radiation dose $10 \cdot 10^6$ r). 1) Tensile strength, 2) limiting swelling

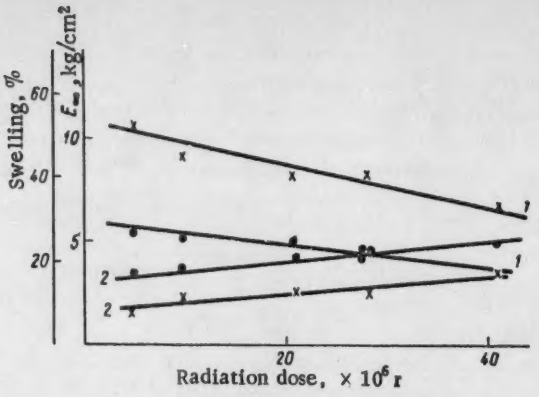

Fig. 3. Effect of medium on the character of structural changes in a fluorine copolymer during irradiation. 1) Swelling; 2) equilibrium modulus; ●) air; ×) vacuum

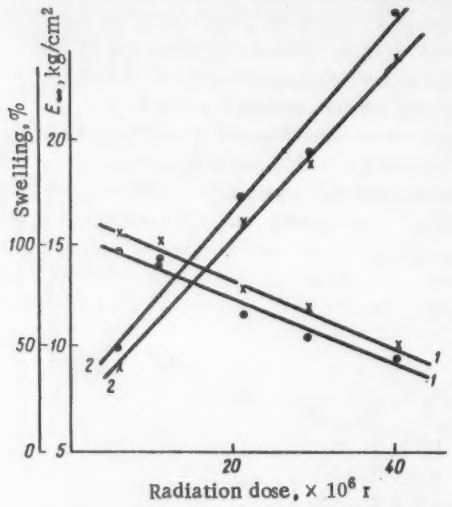

Fig. 4. Effect of medium on the character of the structural changes in the fluorine copolymer with channel black during irradiation. 1) Limiting swelling; 2) equilibrium modulus; ●) air; ×) vacuum.

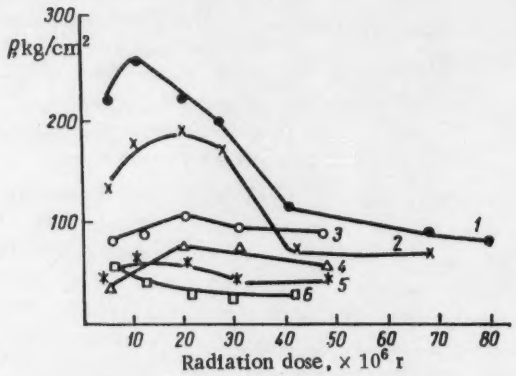

Fig. 5. Relation of properties of radiation vulcanizates of fluorine copolymer to type of filler. 1) 30 parts by weight of channel black; 2) 30 parts by weight of powdered silica gel; 3) 30 parts by weight of chimney soot; 4) 30 parts by weight of thermatomic black; 5) 30 parts by weight of zinc oxide; 6) without filler.

solid space lattice (vulcanization). This was outwardly shown as a loss in solubility and a sharp change in the mechanical properties. One could assume that the sharp decrease (after reaching a maximum) in the strength of the irradiated fluorine copolymer with an increase in radiation dose was connected with the loss of the copolymer's molecular chain's capacity for orientation during stretching. The reason for this phenomenon could have been destruction of the regular order of the chains, the rather high density of the space lattice, or some other factors which hindered orientation.

An increase in the vinylidene fluoride content of the copolymer resulted in an increase in the rate of its structurization during irradiation and this was accompanied by a fall in the swelling maximum of the copolymer in a solvent and an increase in tensile strength.

Figure 2 shows graphically the effect of vinylidene fluoride content of the Kel -F type copolymer on the character of the changer in its properties during irradiation. It should be noted that the rate of structurization of fluorine copolymers during irradiation in air was considerably higher than in the absence of oxygen (Fig. 3). Apparently, due

to the oxygen, additional structurization occurred as a result of peroxide bonds, ether bridges, and other oxygen-containing cross-links being formed.

The effect of oxygen fell considerably when a mixture of copolymer and channel black was irradiated since the latter already contained a large amount of oxygen-containing compounds (Fig. 4) on its surface in the form of phenol, peroxide, ether, and other groups; this confirmed the hypothesis put forward above.

In order to determine whether it was possible to obtain materials with valuable technical properties by radiation vulcanization, the fluorine copolymer was irradiated with various fillers: channel black, chimney soot, thermatomic black, powdered silica gel, and zinc oxide. For comparing the effect of various fillers during irradiation of the fluorine copolymer, equal amounts by weight of fillers were used in the mixtures (30 parts by weight to 100 parts by weight of copolymer).

Figure 5 shows the changes in strength indices and Fig. 6 the equilibrium modulus of the fluorine copolymer during irradiation in the presence of the given fillers.

These figures show that according to the degree that they affect the strength indices of the rubbers obtained by irradiation, the fillers may be arranged in the following order: channel black, powdered silica gel, chimney soot, thermatomic black, and zinc oxide.

In the presence of channel black and powdered silica gel, the strength of the fluorine copolymer rubbers changed very sharply with an increase in radiation dose, whereas this change was not observed for rubbers with chimney soot, thermatomic black, and zinc oxide within the limits of radiation dose investigated. The optimal radiation dose for a mixture with channel black was $10\text{-}20 \cdot 10^6$ r and with powdered silica gel was $20\text{-}30 \cdot 10^6$ r. After reaching a maximum, a further increase in the radiation dose resulted in a sharp decrease in strength. This phenomenon was apparently due to a further increase in the density of the space lattice, which hindered the orientation of the copolymer chains during stretching.

The activity of all the fillers during radiation vulcanization was probably explained by the formation of a considerable number of chemical bonds between the copolymer molecules and the surface of the filler particles. The sharp increase in the equilibrium modulus observed in the presence of such fillers confirmed the hypothesis put forward (Fig. 6). An analogous phenomenon was observed in the radiation vulcanization of a series of other rubbers with different fillers [9,10].

The density of the space lattice formed per unit of energy absorbed depended on the type of filler used for fluorine copolymers, as was the case in the examples given above.

It is known that the activity of fillers for "chemical" (peroxide and sulfur) vulcanization is determined by the nature of their surface. It was therefore interesting to elucidate the effect of the nature of the filler's surface on radiation vulcanization of fluorine copolymers. For this purpose, fluorine copolymers were irradiated in the presence of various fillers, introduced in amounts corresponding to a specific surface of 1860 m^2 per 100 parts by weight of polymer.

Figure 7 gives data on the changes in limiting swelling in acetone at room temperature of radiation vulcanizates of the fluorine copolymer in relation to the type of filler introduced into them. The equal slope of the lines (after a definite minimal dose) for all the rubber-filler vulcanizates investigated indicated an equal rate of formation of the space lattice in the presence of different types of fillers, taken with an equivalent surface. This indicated that in the case of radiation vulcanization of fluorine copolymers,

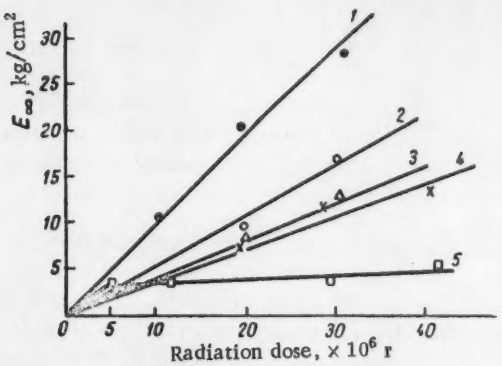

Fig. 6. Relation of density of formation of space lattice in radiation vulcanizated of fluorine copolymer to type of filler. 1) 30 parts by weight of channel black; 2) 30 parts by weight of chimney soot; 3) 30 parts by weight of thermatomic black; 4) 30 parts by weight of powdered silica gel; 5) without filler.

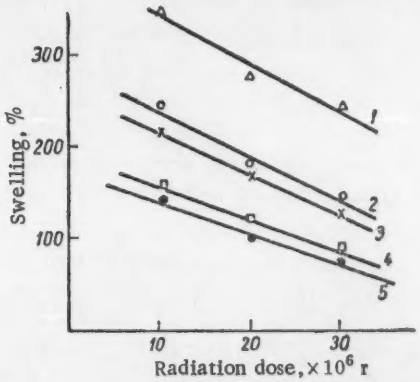

Fig. 7. Effect of filler on the density of the rubber space lattice formed during irradiation of fluorine copolymer. 1) Without filler; 2) 40 parts by weight of powdered silica gel; 3) 169 parts by weight of thermatomic black; 4) 52 parts by weight of chimney soot; 5) 20 parts by weight of channel black.

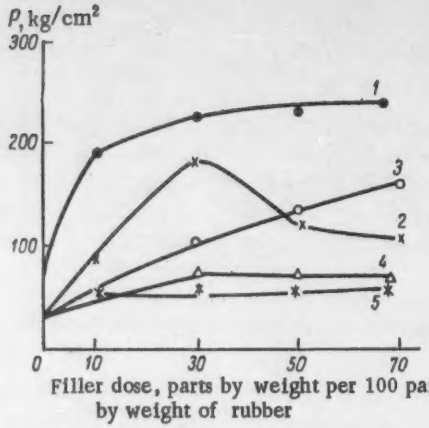

Fig. 8. Relation of the strength of fluorine copolymer rubbers to amount of filler (radiation dose $20 \cdot 10^6$ r). 1) Channel black; 2) powdered silica gel; 3) chimney soot; 4) thermatomic black; 5) zinc oxide.

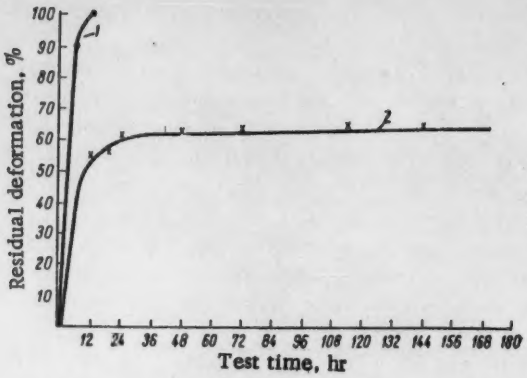

Fig. 9 Kinetics of accumulation of residual deformation in rubbers from fluorine copolymer with 20% compression and t = 150°C. 1) Peroxide rubber; 2) radiation vulcanizate with 30 parts by weight of channel black.

Form of vulcanization	Type of filler (30 parts by weight per 100 parts by weight of polymer)	Radiation dose, 10^6 r	Tensile strength, kg/cm²	Specific elongation, %	Residual elongation, %	Swelling in acetone in 24 hours, %	Coefficient of frost resistance, −15°C	Residual deformation after compression by 20% (150°, 6 hr), %	Rupture at 150°C		Aging at 250°C				After 1 day in aggressive media			
											3 days		10 days					
									tensile strength, kg/cm²	specific elongation, %	tensile strength kg/cm²	specific elongation, %	tensile strength, kg/cm²	specific elongation, %	swelling, %	tensile strength, kg/cm²	specific elongation, %	residual elongation, %
Radiation	Channel black	20	255	300	22	82	0,10	38	47	230	88	300	87	100	13	190	350	15
	Pow. silica gel	20	180	500	15	166	0,19	51	24	225	48	100	—	—	8,5	114	400	10
	Chimney soot	30	93	300	7	68	0,12	45	19	100	24	100	—	—	—	—	—	—
	Thermatomic black	30	66	350	7	110	—	—	12	100	38	100	—	—	—	—	—	—
	Zinc oxide . . .	30	45	320	5	162	—	—	10	50	104	100	—	—	—	—	—	—
Peroxide	Pow. silica gel	—	261	270	2	240	0,11	93	17	270	Burns		—	—	10,5	160	350	30
	Channel black	—	200	500	0	—	—	100	—	—	»		—	—	—	—	—	—

as for other rubbers, the nature of the surface did not have a substantial effect on the vulcanization rate.

The density of the space lattice of vulcanizates formed in the presence of the above fillers, taken with an equivalent surface, was different with equal radiation doses. The rubbers including channel black, which contained up to 3.2% of oxygen and 1.07% of hydrogen according to elementary analysis data, had the greatest density of space lattice. Chimney soot was second in this respect; its oxygen content was 0.72%, its hydrogen 0.57%. Thermatomic black was least active of the three carbon blacks tested and it did not contain oxygen.

Thus, the data given indicated that the number of cross-links formed during radiation vulcanization depends on the surface activity of the filler. In this case, the more oxidized the surface of the filler, the greater the density of the space lattice of the vulcanizate.

Figure 8 gives the relation of the amount of filler in the mixture to the strength of the fluorine copolymer rubber after irradiation. The graph shows that the strength of the rubbers from fluorine copolymers increases with an increase in the content of channel black and chimney soot. An increase in the content of thermatomic black and zinc oxide from 10 to 70 parts by weight per 100 parts of rubber had practically no effect on the strength of the rubber. The changes in the strength of rubber from the fluorine copolymer with powdered silica gel is described by a curve with a maximum. The reason for such behavior of a rub-

ber with powdered silica gel in relation to its content is unknown and requires further investigation.

The table gives characteristics of rubbers from the fluorine copolymer with different fillers; it also shows that radiation vulcanization of the fluorine copolymers in the presence of channel black and powdered silica gel gave rubbers with quite high physicomechanical indices. Rubbers obtained by radiation vulcanization were superior to the corresponding rubbers obtained by benzoyl peroxide vulcanization in frost resistance and resistance to the action of solvents and static deformations. Considerably less change was observed in the properties of radiation rubbers under the action of some aggressive media than in the case of peroxide rubbers.

Figure 9 gives the kinetics of accumulation of residual deformation with 20% compression (t = 150°C) for rubbers obtained by peroxide and radiation vulcanization.

The graph shows that accumulation of residual deformation in rubbers with channel black obtained by radiation vulcanization was much less than in rubbers with benzoyl peroxide.

This difference seems to indicate that these rubbers may contain different types of chemical bonds in their structure.

The better properties of radiation rubbers in comparison with those of the usual type, indicate the possibility of using radiation vulcanization in the future for preparing objects from saturated polymers instead of using the technically complicated vulcanization with benzoyl peroxide. This method reveals the possibility of vulcanization of such high polymers to give rubbers with various valuable technical properties.

LITERATURE CITED

1. J. Byrne, T. Costikyan, C. Hanford, D. Jonhson, and W. Mann, Ind. Eng. Chem. 45, 2549 (1953).
2. A. Charlesby, Plastics 18, 142 (1953).
3. A. Charlesby, Nucleonics 12, 18 (1954).
4. J. Ryan, Mod. Plastics 32, 152 (1953).
5. J. Bresse, J. Flanary, J. Goode, C. Watson, and J. Watson, Nucleonics 14, 75 (1956).
6. W. Griffin, Rubber World 136, 687 (1957).
7. N. Slovokhotova, Material of the Tenth All-Union Conference on Spectroscopy [in Russian] (Lvov University Press, 1957) p. 430.
8. S. Dixon, D. Rexford, and J. Rugg, Chem. Eng. News 34, 4881 (1956).
9. A. S. Kuz'minskii, T. S. Nikitina, and V. B. Karpov, Atomnaya Énergiya 1, 137 (1956) *
10. W. W. Jackson and D. Hale, Rubber Age 77, 865 (1955).

Received February 15, 1958

*See English translation.

ON AN APPROXIMATE METHOD FOR THE HOMOGENIZATION OF A HETEROGENEOUS REACTOR

V. V. Smelov

In most cases of calculations on heterogeneous reactors use has been made of a method of homogenization based on the replacement of the heterogeneous reactor by a homogeneous one (with effective values of the parameters). Whereas the calculation of the effective cross sections for capture and fission is a simple problem [1-3], the determination of the effective diffusion coefficient involves great difficulties, and until very recently there has been no adequately grounded method for its calculation. In this connection an important advance has been achieved in a paper by Shevelev [4].

In the present paper it is shown that the problem of homogenization is basically associated with a specific functional, which depends on the statement of the problem. A general principle of homogenization is discussed, which uses as this functional the quantity k_{eff}. It is shown that in calculations on heterogeneous reactors, the use of effective capture and fission cross sections obtained by averaging over the spatial neutron spectrum in an infinite lattice gives an error in k_{eff} that is proportional to the Laplacian κ^2 of the reactor. Attempts to increase the degree of precision lead to a situation in which the effective parameters lose their "universality," that is, come to depend on the geometry of the reactor. It is shown that the use of universal parameters, in principle, excludes the possibility of a unique determination of the effective diffusion coefficient, even if one considers the diffusion of the neutrons in a definite direction. Nevertheless, formulas are obtained that give the most correct determination of the diffusion coefficient that is possible. The diffusion coefficient so obtained depends on the direction in the lattice. The method of homogenization is considered for plane, cylindrical, and spherical geometries of the cells.

INTRODUCTION

Many problems connected with calculations of the diffusion of neutrons in a periodic lattice require the effective homogenization of the heterogeneous medium. It turns out that the parameters of the equivalent homogenized reactor are not uniquely determined;* in particular, they depend on the requirements imposed on the effective homogeneous medium. Let us make this clear by an example. Suppose the neutrons diffused perpendicular to the layers of a plane-parallel lattice that consists of alternate layers of two substances. We require that the neutron flux produced in the homogenized medium by a plane source located at infinity should be weakened in the path $\delta_1 + \delta_2$ (δ_1 and δ_2 are the thicknesses of the layers of the heterogeneous lattice) by the same factor as that by which the flux is actually weakened in each pair of layers of the heterogeneous medium. As the result we get the effective diffusion length $L_\perp$ [1]. If, however, the given plane-parallel arrangement is the core of a reactor, then it can be homogenized by a calculation made so that the multiplication factor of the reactor shall be unchanged. The diffusion length $L_\perp$ obtained under these conditions may be considerably different from that determined by the former procedure (see below). It is obvious that in the theory of reactors, in which the multiplication coefficient is the most important quantity, the method of homogenization must be based on the second requirement.

Assuming for simplicity that the initiation, diffusion, and absorption of the neutrons all occur at the same energy, in the P_1 approximation we can use the diffusion equation

$$\nabla D \nabla \Phi - \Sigma_c \Phi + \nu \Sigma_f \Phi = 0. \qquad (1)$$

At the boundaries of the layers, Φ and $D\nabla\Phi$ are continuous; at the outer boundary of the reactor $\Phi = 0$; ν is the eigenvalue of the problem, inversely proportional to the effective multiplication factor of the reactor. In (1) the quantitites D, Σ_c and Σ_f are periodic functions with period equal to the lattice constant.

If in (1) we replace the quantities D, Σ_c, and Σ_f by D', Σ'_c, and Σ'_f, we get a new eigenfunction Φ' and a new eigenvalue ν'. Furthermore, the variation of the eigenvalue $\Delta\nu = \nu - \nu'$ is given by the formula

$$\Delta\nu = \frac{1}{\int\limits_{(V)} \Sigma'_f \Phi\Phi' dV} \left\{ \int\limits_{(V)} (D - D') \nabla\Phi\nabla\Phi' \, dV + \right.$$
$$+ \int\limits_{(V)} (\Sigma_c - \Sigma'_c) \Phi\Phi' \, dV -$$
$$\left. - \nu \int\limits_{(V)} (\Sigma_f - \Sigma'_f) \Phi\Phi' \, dV \right\}, \qquad (2)$$

* We are not concerned here with the ambiguity that is due to the direction of diffusion of the neutrons in the lattice [1].

where the integration extends over the entire volume of the reactor. If we choose D', Σ'_c, and Σ'_f in such a way that (2) gives $\Delta\nu = 0$, then the primed quantities will characterize a reactor with new parameters but with the same multiplication coefficient as the original reactor. We shall call two such reactors equivalent. The problem of the homogenization of a reactor will be solved if the parameters D', Σ'_c, and Σ'_f of the equivalent reactor are constants.

In order for $\Delta\nu$ to be equal to zero it is sufficient that each term in the brackets in (2) be zero :

$$\sum_n \int_{V_n} \Delta\Sigma_c \Phi\Phi' \, dV = 0, \quad \sum_n \int_{V_n} \Delta\Sigma_f \Phi\Phi' \, dV = 0,$$

$$\sum_n \int_{V_n} \Delta D \nabla\Phi \nabla\Phi' \, dV = 0, \tag{3}$$

where $\Delta\Sigma_c = \Sigma_c - \Sigma'_c$, $\Delta\Sigma_f = \Sigma_f - \Sigma'_f$, $\Delta D = D - D'$. In the formulas (3) the summations are taken over the elementary cells of the lattice. Denoting by φ_0 the flux of neutrons in the infinite lattice, each of the cells considered let us represent the functions Φ and Φ' in the form

$$\Phi(x, y, z) = \varphi_0(x, y, z)[\mu_n + \varepsilon_n(x, y, z)],$$
$$\Phi'(x, y, z) = \mu'_n + \varepsilon'_n(x, y, z), \tag{4}$$

where μ_n and μ'_n are constants, and the functions ϵ_n and ϵ'_n are zero at the center of the cell. Substituting the expressions (4) in the terms (3), and omitting for simplicity the index n from μ, μ', ϵ, and ϵ', we get

$$\sum_n \left\{ \mu\mu' \int_{V_n} \Delta\Sigma_c \varphi_0 \, dV + \mu' \int_{V_n} \Delta\Sigma_c \varphi_0 \varepsilon \, dV + \right.$$
$$\left. + \mu \int_{V_n} \Delta\Sigma_c \varphi_0 \varepsilon' \, dV + \int_{V_n} \Delta\Sigma_c \varphi_0 \varepsilon\varepsilon' \, dV \right\} = 0, \tag{5}$$

$$\sum_n \left\{ \mu\mu' \int_{V_n} \Delta\Sigma_f \varphi_0 \, dV + \mu' \int_{V_n} \Delta\Sigma_f \varphi_0 \varepsilon \, dV + \right.$$
$$\left. + \mu \int_{V_n} \Delta\Sigma_f \varphi_0 \varepsilon' \, dV + \int_{V_n} \Delta\Sigma_f \varphi_0 \varepsilon\varepsilon' \, dV \right\} = 0, \tag{6}$$

$$\sum_n \left\{ \mu \int_{V_n} \Delta D \nabla\varphi_0 \nabla\varepsilon' \, dV + \int_{V_n} \Delta D \varepsilon \nabla\varphi_0 \nabla\varepsilon' dV + \right.$$
$$\left. + \int_{V_n} \Delta D \varphi_0 \nabla\varepsilon \nabla\varepsilon' \, dV \right\} = 0. \tag{7}$$

The conclusions from (5), (6), (7) that are presented below have been obtained for reactors without reflectors, but clearly these results are valid for the various reactors with reflectors.

The Plane Lattice

Let the medium containing the fissionable substance be a plane lattice of successsive layers of two materials with the thicknesses $2\delta_1$ and $2\delta_2$. We consider a parallelepiped in the medium (Fig. 1) of thickness $2\delta = 2(\delta_1 + \delta_2)$ in the direction perpendicular to the layers, and arbitrary dimensions in the other two directions.

Let us first examine the case in which the reactor is infinite in the directions of the x and z axes and finite in the y direction. We denote the width of the reactor in the y direction by H. Assuming for simplicity that fission occurs only in the first zone of the cell, we write the solution of Eq. (1) in the form

$$\Phi(x, y) = \varphi(x) \cos \frac{\pi}{H} y, \tag{8}$$

where

$$\varphi(x) = \begin{cases} \cos \alpha_1 x & \text{for} \quad 0 \leqslant x \leqslant \delta_1, \\ B \operatorname{ch}[\alpha_2(\delta - x)] & \text{for} \quad \delta_1 \leqslant x \leqslant \delta. \end{cases} \tag{9}$$

Here, α_1 and α_2 refer, respectively, to zones 1 and 2 of Fig. 1, and can be written in the form

$$\alpha^2 = \left| \frac{\pi^2}{H^2} + \frac{\Sigma_c - \nu\Sigma_f}{D} \right|. \tag{10}$$

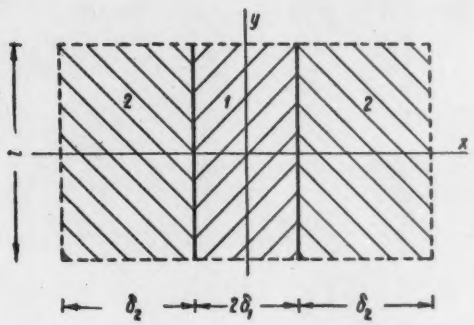

Fig. 1. Elementary cell reactor (l is arbitrary).

The eigenvalue ν is determined from the transcendental equation

$$\alpha_1 D_1 \operatorname{tg} \alpha_1\delta_1 - \alpha_2 D_2 \operatorname{th} \alpha_2\delta_2 = 0, \tag{11}$$

and the coefficient B is given by the formula

$$B = \frac{\cos \alpha_1\delta_1}{\operatorname{ch} \alpha_2\delta_2}. \tag{12}$$

The quantities $\varphi(x)$, α, ν, and B depend on the parameter $\varkappa^2 = \frac{\pi^2}{H^2}$. (For $\varkappa^2 = 0$ we shall attach the index 0 to these quantities.) By using (10) and (11), one can readily verify that the difference $\varkappa^2 - \frac{(\nu - \nu_0)\Sigma_f}{D} \equiv \lambda$ is of the same order of small quantities as $\varkappa^2$:

$$\lambda = O(\varkappa^2). \tag{13}$$

In what follows, we shall distinguish the following two cases :

1) $\alpha_0^2 \gg |\lambda|$, (14)

2) α_0^2 comparable with $|\lambda|$ or $\alpha_0^2 \ll |\lambda|$. (15)

In the first case we get from the expression (10) the approximate result $\alpha = \alpha_0 \pm \frac{\lambda}{2\alpha_0}$. In the second case we can convince ourselves that $\alpha = O(\kappa)$. Let the dimensions of the reactor be such that either the condition

$$\frac{\delta_i \lambda_i}{2\alpha_{0i}} \ll 1 \tag{16}$$

is satisfied (in the case in which (14) holds), or else the following condition is satisfied:

$$\delta_i \alpha_i \ll 1 \tag{17}$$

(in the case of either of the conditions (15)). Using (16) and (17), in which the index i is the number of the zone, we easily get †

$$\varphi(x) = \begin{cases} \left(1 + \frac{x\lambda}{2\alpha_{01}} \operatorname{tg} \alpha_{01} x\right) \cos \alpha_{01} x, \\ \left| 1 - \frac{\alpha_1^2 x^2}{2} \right|, \\ B\left[1 + \frac{\lambda_2 (\delta - x)}{2\alpha_{02}} \operatorname{th} \alpha_{02} (\delta - x)\right] \times \\ \times \operatorname{ch} \alpha_{02} (\delta - x), \\ \left| B_0 \left[1 + \frac{\alpha_2^2 (\delta - x)^2}{2}\right]\right|. \end{cases} \tag{18}$$

Let us similarly express B in terms of B_0:

$$B = B_0 \left[1 + \frac{\delta_1 \lambda_1}{2\alpha_{01}} \operatorname{tg} \alpha_{01} \delta_1 - \frac{\delta_2 \lambda_2}{2\alpha_{02}} \operatorname{th} \alpha_{02} \delta_2\right], \quad \left| B_0 \left[1 - \frac{\alpha_1^2 \delta_1^2 + \alpha_2^2 \delta_2^2}{2}\right]\right|. \tag{19}$$

Shifting the origin to the center of an arbitrary cell and using (18) and (19) inside the cell under consideration, we can write (8) in the approximate form

$$\Phi(x, y) = \varphi_0(x) \left[\mu - \kappa \sqrt{1 - \mu^2} \cdot y + O(\kappa^2)\right], \tag{20}$$

where μ is the value of $\cos \kappa y$ at the center of the cell. Comparing (20) with (4), we find the expression for the function ϵ:

$$\varepsilon = -\kappa \sqrt{1 - \mu^2}\, y + O(\kappa^2). \tag{21}$$

Noting that $\Phi' = \cos \kappa y$, we get for ϵ' the expression (21) with $O(\kappa^2) = \kappa^2 y^2 (-\mu/2 + \ldots)$.

Using the arbitrariness of the dimension l of the cell along the y axis, we can convince ourselves that for $l \to 0$ the first and second terms in (5) and (6) go to zero as l, and the third and fourth as l^2. If we further take into account (21), we can rewrite (5) in the form ‡

$$\sum_n \mu \left\{ \mu \int_{V_n} \Delta \Sigma_c \varphi_0 \, dV + \int_{V_n} \Delta \Sigma_c \varphi_0 \cdot O(\kappa^2) \, dV \right\} = 0. \tag{22}$$

If the reactor is large enough, the second term in the brackets can be neglected ** and we get the well-known formula:

$$\Sigma_c' = \frac{\int_0^\delta \Sigma_c \varphi_0 \, dx}{\int_0^\delta \varphi_0 \, dx}. \tag{23}$$

The error thus incurred is proportional to the value of the Laplacian of the reactor, κ^2.

Since ϵ' depends only on y, (7) takes the form

$$\sum_n \int_{V_n} \Delta D \varphi_0 \frac{\partial \varepsilon}{\partial y} \frac{d\varepsilon'}{dy} \, dV = 0. \tag{24}$$

According to (21), the left member of this equation is of order κ^2; i.e., it is comparable with the error made in averaging the absorption and fission cross sections. This means that in principle it is not possible to find the effective diffusion coefficient unambiguously from (24) if the order of precision is less than κ^2. †† These arguments do not mean, however, that the diffusion coefficient of the homogenized arrangement can be chosen arbitrarily. (It is obvious that D' must first of all satisfy the condition $D_{min} \leq D' \leq D_{max}$.) It is necessary to choose D' so as to satisfy (24) as accurately as possible, since the errors in the averaged absorption and fission cross sections do not depend on the choice of D' [(Cf. (5) and (6)] and can compensate each other to a considerable extent, as can be seen from (2).

It has already been remarked that ϵ', and consequently also $d\epsilon'/dy$, do not depend on x. For fixed y the function $\partial \epsilon / \partial y$ is a quantity with only a weak dependence on x, since it gives the slope of the general neutron "background" at a given distance from the boundary of the reactor. This fact also follows directly from (21). Thus, when we take into account the aribitrariness of the dimension l, the product $(\partial \epsilon / \partial y)(\partial \epsilon' / \partial y)$ can be regarded as approcimately constant over a cell. From this we get the following expression for the effective diffusion coefficient in the y direction:

$$D' = \frac{\int_0^\delta D \varphi_0 \, dx}{\int_0^\delta \varphi_0 \, dx}. \tag{25}$$

† The expressions between the strokes | . . . | in (18) and (19) are for case 2.

‡ All conclusions obtained from (5) are also valid for (6), because of their identity of form.

** For small μ this assertion is not true. But in this case the "weight" of both terms is small because of the factor μ that occurs as the coefficient of the curly brackets.

†† An increase of the order of accuracy in the homogenization inevitably has the consequence that the effective parameters lose their "universality", i.e., will then depend on the shape and dimensions of the reactor.

If the thicknesses of the layers are small and the absorption is small, then $\varphi_0 \approx$ const, and (25) takes the form

$$D' = \frac{D^{(1)}\delta_1 + D^{(2)}\delta_2}{\delta_1 + \delta_2},$$

which is in full agreement with Eq. (10.2) obtained in [1].

Now let the reactor be infinite in the directions of the y and z axes, but finite in the x direction; that is, the neutrons diffuse perpendicular to the layers. It can be verified without difficulty that in this case the function $\epsilon(x)$ can be written in the form

$$\varepsilon(x) = \varkappa\varepsilon_1(x) + \varkappa^2\varepsilon_2(x), \tag{26}$$

where the function $\epsilon_1(x)$ is an odd function relative to the center of the cell. Substituting (26) in (5) and dropping terms of the order of magnitude κ^2, we again arrive at (23).

In the case of transverse diffusion, as in that of longitudinal diffusion, the left member of (7) is of the order of magnitude κ^2. Neglecting the terms of higher orders in this equation and using (26), we get

$$\sum_n \left\{ \mu \left(\frac{d^2\varepsilon'}{dx^2}\right)_0 \int_{V_n} \Delta D x \frac{d\varphi_0}{dx}\, dx + \right.$$
$$\left. + \left(\frac{d\varepsilon'}{dx}\right)_0 \varkappa \int_{V_n} \Delta D \varepsilon_1(x) \frac{d\varphi_0}{dx}\, dx \right\} +$$
$$+ \sum_n \left(\frac{d\varepsilon'}{dx}\right)_0 \varkappa \int_{V_n} \Delta D \varphi_0 \frac{d\varepsilon_1}{dx}\, dx = 0, \tag{27}$$

where $(d\epsilon'/dx^2)_0$ and $(d^2\epsilon'/dx^2)_0$ are taken at the center of the cell. In this expression let us first examine the second sum. The function $\epsilon_1(x)$ shows a "break" at the boundaries of the layers, but can be regarded as approximately a linear function within the limits of each of the layers. Its derivative $d\epsilon_1/dx$ will then be a piecewise continuous function; taking account of the boundary conditions, we can write it in the form

$$\frac{d\varepsilon_1}{dx} = \begin{cases} C & \text{for} \quad -\delta_1 \leqslant x \leqslant \delta_1, \\ C\dfrac{D^{(1)}}{D^{(2)}} & \text{for} \quad -\delta \leqslant x \leqslant -\delta_1,\ \delta_1 \leqslant x \leqslant \delta. \end{cases} \tag{28}$$

It will be shown below that the terms of the first sum in (27) cancel each other to a considerable extent. By using (28) we get from the second sum

$$\Sigma'_{tr} = \frac{\int_0^{\delta} \Sigma_{tr}\varphi_0\, dx}{\int_0^{\delta} \varphi_0\, dx}, \tag{29}$$

where $\Sigma'_{tr} = \dfrac{1}{3D'}$, $\Sigma_{tr} = \dfrac{1}{3D}$.

Before going on to the transformation of the first sum in (27), let us compare the functions $\kappa\,\epsilon_1(x)$ and $\epsilon'(x)$. These two functions are both continuous and monotonically decreasing (as x varies from the center of the reactor to its boundary), and they are equal at the points $x = 0$ and $x = \delta$: $\varkappa\varepsilon_1(0) = \varepsilon'(0) = 0$, $\varkappa\varepsilon_1(\delta) \approx \varepsilon'(\delta)$. For these reasons we may regard them as nearly equal in the range $0 \leq x \leq \delta$. It follows from this that $\epsilon_1(x)$ is nearly equal to $-\sqrt{1-\mu'^2}\,x$, since $\varepsilon'(x) \approx -x\varkappa\sqrt{1-\mu'^2}$.

Recalling that

$$\left(\frac{d^2\varepsilon'}{dx^2}\right)_0 = -\varkappa^2\mu', \left(\frac{d\varepsilon'}{dx}\right)_0 = -\varkappa\sqrt{1-\mu'^2}, \text{and } \mu \approx \mu',$$

we can see that the first term in the curly brackets in (27) is equal to $-\mu^2\varkappa^2 \int_{V_n} \Delta D x \frac{d\varphi_0}{dx}\, dx$, and the second term is close to the value $(1-\mu^2)\varkappa^2 \cdot \int_{V_n} \Delta D x \frac{d\varphi_0}{dx}\, dx$. Thus the first sum in (27) takes the form

$$\varkappa^2 \int_{V_n} \Delta D x \frac{d\varphi_0}{dx}\, dx \cdot \sum_n (1 - 2\mu_n^2). \tag{30}$$

Since $\mu_n = \cos\dfrac{2\pi\delta}{H}n$, , the sum here goes to zero, as was asserted earlier.

If the absorption is small and the thicknesses of the layers are not large, $\varphi_0 \approx$ const, and (29) takes the form

$$\Sigma'_{tr} = \frac{\Sigma^{(1)}_{tr}\delta_1 + \Sigma^{(2)}_{tr}\delta_2}{\delta_1 + \delta_2},$$

which is in complete agreement with the result obtained in [1].

The Cylindrical Lattice

Let us now consider a periodic lattice of cells with a cylindrical geometry. The method for obtaining the effective adsorption and fission cross sections, and also the longitudinal diffusion coefficient, does not differ in any way from that explained in the preceding section. Therefore we have the formulas:

$$\left.\begin{aligned} \Sigma'_c &= \frac{\int_{V_n} \Sigma_c\varphi_0\, dV}{\int_{V_n} \varphi_0\, dV}, \quad \Sigma'_f = \frac{\int_{V_n} \Sigma_f\varphi_0\, dV}{\int_{V_n} \varphi_0\, dV}, \\ D'_{||} &= \frac{\int_{V_n} D\varphi_0\, dV}{\int_{V_n} \varphi_0\, dV}. \end{aligned}\right\} \tag{31}$$

Now suppose the neutrons diffuse perpendicular to the axes of the cells in any direction. Let us take the x axis in the direction of motion of the neutrons. We take first the case

$$\varphi_0 \approx \text{const}. \tag{32}$$

Substituting this value in (7), we get

$$\sum_n \int_{V_n} \Delta D \nabla \varepsilon \nabla \varepsilon' \, dV = 0. \qquad (33)$$

We shall determine the effective diffusion coefficient in two stages. In the first stage we "construct" an auxiliary reactor, equivalent to the original reactor, in which the absorption and fission cross sections are constant throughout a cell and are given by (31) (with $\varphi_0 = 1$), and the diffusion coefficient is a function of the variable y only.‡‡ We denote by D^* and ϵ^* the quantities belonging to the auxiliary reactor. In the reactors under consideration the flow of neutrons occurs along the x axis, and consequently, we can assume that

$$\frac{\partial \varepsilon}{\partial y} \ll \frac{\partial \varepsilon}{\partial x}, \quad \frac{\partial \varepsilon^*}{\partial y} \ll \frac{\partial \varepsilon^*}{\partial x}. \qquad (34)$$

By the use of these conditions we can write Eq. (33) in the form

$$\sum_n \int \underbrace{dy \int_{V_n}} (D - D^*) \frac{\partial \varepsilon}{\partial x} \frac{\partial \varepsilon^*}{\partial x} \, dx = 0. \qquad (35)$$

We shall determine the function $D^*(y)$ in accordance with the requirement that in each term of (35) the inside integral must vanish for arbitrary y:

$$\int (D - D^*) \frac{\partial \varepsilon}{\partial x} \frac{\partial \varepsilon^*}{\partial x} \, dx = 0. \qquad (36)$$

Along the path of integration in (36) the derivative $\frac{\partial \varepsilon^*}{\partial x}$ is continuous, and $\frac{\partial \varepsilon}{\partial x}$ is a piecewise continuous function. The latter assertion is a consequence of the fact that at the zone boundaries the normal derivative of the function ϵ has a discontinuity determined by the condition

$$D^{(1)} \left[\frac{\partial \varepsilon^{(1)}}{\partial x} \cos \alpha + \frac{\partial \varepsilon^{(1)}}{\partial y} \sin \alpha \right] = D^{(2)} \left[\frac{\partial \varepsilon^{(2)}}{\partial x} \cos \alpha + \frac{\partial \varepsilon^{(2)}}{\partial y} \sin \alpha \right],$$

where α is the angle between the normal to the separating boundary and the x axis. When we take into account (34), for almost the entire range of variation of α we can neglect the second term in the square brackets in comparison with the first; that is,

$$D^{(1)} \frac{\partial \varepsilon'}{\partial x} = D^{(2)} \frac{\partial \varepsilon^{(2)}}{\partial x}. \qquad (37)$$

Let us now rewrite (36) in the following way:

$$D^*(y) \int \left(\frac{1}{D^*} - \frac{1}{D} \right) \left(D \frac{\partial \varepsilon}{\partial x} \right) \frac{\partial \varepsilon^*}{\partial x} \, dx = 0 \qquad (38)$$

In view of (37), the function $D \frac{\partial \varepsilon}{\partial x}$ in (38) is continuous. As in the preceding section (case of trasverse diffusion), we shall regard the functions $\frac{\partial \varepsilon^*}{\partial x}$ and $D \frac{\partial \varepsilon}{\partial x}$ as approximately constant over the interior of a cell. Therefore we get

$$\frac{1}{D^*(y)} = \frac{\sum_i \frac{1}{D_i} \delta_i(y)}{\sum_i \delta_i(y)}. \qquad (39)$$

Here, $\delta_i(y)$ is the optical path length in the ith zone traversed by a ray parallel to the x axis and having the coordinate y, and the summation extends over the zones in a cell.

The second stage is the passage from the auxiliary reactor to the homogeneous reactor. Here, obviously,

$$\Sigma_c' \equiv \Sigma_c^*, \quad \Sigma_f' \equiv \Sigma_f^*.$$

To obtain the diffusion coefficient D' we again use (7), which in the present case can be written in the form

$$\sum_n \int_{V_n} (D' - D^*) \frac{\partial \varepsilon^*}{\partial x} \frac{d\varepsilon'}{dx} \, dV = 0. \qquad (40)$$

In the equation that has been obtained (unlike (36)) the derivatives $\partial \epsilon^* / \partial x$ and $\partial \epsilon' / \partial x$ are continuous in both variables and can be regarded as approximately constant within a cell. Using (39), we have as the result

$$D' \int_{V_n} dV = \int_{V_n} D^*(y) \, dV = \int dy D^*(y) \int dx = \int dy \frac{\sum_i \delta_i(y)}{\sum_i \frac{1}{D_i} \delta_i(y)} \int dx.$$

Introducing the notation $\delta(y) = \sum_i \delta_i(y)$ and noting the fact that $\int dx = \delta(y)$, we finally get

$$D' = \frac{1}{V_n} \int \frac{[\delta(y)]^2}{\sum_i \frac{1}{D_i} \delta_i(y)} \, dy, \qquad (41)$$

where V_n is the volume of a cell.

We note that (25), (29), and (31) show an essential dependence on the neutron spectrum φ_0 in the infinite lattice. In the case analyzed above, the transition to the consideration of the auxiliary reactor does not distort this spectrum, since $\varphi_0 = \varphi_0^* = \text{const}$. But in the case $\varphi_0 \neq \text{const}$ the neutron spectrum φ_0 is not conserved. Therefore it is more suitable to our purpose to "construct" on the basis of (41) the following formula for D':

$$D' = \frac{1}{\int_{V_n} \varphi_0 \, dV} \int \frac{\left(\int_{\delta(y)} \varphi_0 \, dx \right)^2}{\int_{\delta(y)} \frac{1}{D} \varphi_0 \, dx} \, dy. \qquad (42)$$

‡‡ In the original reactor, D depends on two variables.

For $\varphi_0 = \text{const}$, (42) goes over into (41). If, as is shown in Fig. 1, we separate out a cell from the plane lattice considered in the preceding section, then for longitudinal diffusion (42) becomes identical with (25), and for transverse diffusion, with (29).

Finally, we can propose the following universal formula:

$$D' = \frac{1}{\int\limits_{V_n} \varphi_0\, dV} \iint \frac{\left(\int\limits_{\delta(y,\,z)} \varphi_0\, dx \right)^2}{\int\limits_{\delta(y,\,z)} \frac{1}{D}\, \varphi_0\, dx}\, dy\, dz. \qquad (43)$$

Here the x axis is taken along the direction of diffusion of the neutrons, and $\delta(y, z)$ has a meaning analogous to that of $\delta(y)$ in (42). Expressions (25), (29), (31), (41), and (42) are automatically obtained from (43); that is, this last equation enables us to calculate the longitudinal and transverse diffusion coefficients for both the plane and cylindrical geometries of the cells (and also for the spherical).

Homogenization Formulas For Spatial-Energetic Problems

As is well known, in calculations on reactors, use is often made of the age-diffusion equation:

$$\frac{\partial}{\partial u}\left[\xi\Sigma_s \Phi\right] = \nabla D \nabla \Phi - \Sigma_c \Phi + \\ + \nu \int\limits_{-\infty}^{\infty} \chi(\vec{r};\ u,\ u')\, \Phi(\vec{r},\ u')\, du'. \qquad (44)$$

Here $\xi\Sigma_s$ is the moderating power of the substance [3], and $\chi(\vec{r}; u, u')$ is a function satisfying the following normalization condition:

$$\int\limits_{-\infty}^{\infty} \chi(\vec{r};\ u,\ u')\, du = \nu_f(\vec{r},\ u')\, \Sigma_f(\vec{r},\ u'),$$

where $\nu_f(\vec{r}, u')$ is the yield of secondary neutrons for one absorbed neutron of lethargy u'.

If we write the formula for the variation of the eigenvalue and require that $\Delta\nu$ vanish, a sufficient condition for this will be for the following equations to hold:

$$\int\limits_{-\infty}^{\infty} du \int\limits_{V} \left[\xi\Sigma_s - (\xi\Sigma_s)'\right] \Phi(\vec{r}, u) \times \\ \times \frac{\partial \Phi^*(\vec{r}, u)}{\partial u}\, dV = 0,$$

$$\int\limits_{-\infty}^{\infty} du \int\limits_{V} (\Sigma_c - \Sigma_c')\, \Phi(\vec{r},\ u)\, \Phi^* \times \\ \times \chi(\vec{r},\ u)\, dV = 0, \qquad (45)$$

$$\int\limits_{-\infty}^{\infty} du \int\limits_{V} (D - D')\, \nabla\Phi\, \nabla\Phi^*\, dV = 0,$$

$$\int\limits_{-\infty}^{\infty} du \int\limits_{-\infty}^{\infty} du' \int\limits_{V} \left[\chi(\vec{r};\ u,\ u') - \right. \qquad (45)\ \text{(cont.)}$$

$$\left. - \chi'(u, u')\right] \Phi(\vec{r},\ u')\, \Phi^*(\vec{r},\ u')\, dV = 0.$$

In (45), $\Phi^*(\vec{r}, u)$ is the solution of the following adjoint equation with the homogenized (perturbed) parameters $(\xi\Sigma_s)'$, D', Σ_c', χ' [4]:

$$-(\xi\Sigma_s)' \frac{\partial \Phi^*}{\partial u} = \nabla D' \nabla \Phi^* - \Sigma_c' \Phi^* + \\ + \nu \int\limits_{-\infty}^{\infty} \chi'(u',\ u)\, \Phi^*(\vec{r},\ u')\, du'.$$

Equating to zero the inside integrals in (45), which are integrals over the volume of the reactor, we get the following formulas:

$$(\xi\Sigma_s)' = \frac{\int\limits_{V_n} \xi\Sigma_s \varphi_0(\vec{r},\ u)\, dV}{\int\limits_{V_n} \varphi_0\, dV},$$

$$\Sigma_c'(u) = \frac{\int\limits_{V_n} \Sigma_c(\vec{r},\ u)\, \varphi_0(\vec{r},\ u)\, dV}{\int\limits_{V_n} \varphi_0\, dV},$$

$$\chi'(u,\ u') = \frac{\int\limits_{V_n} \chi(\vec{r};\ u,\ u')\, \varphi_0(\vec{r},\ u')\, dV}{\int\limits_{V_n} \varphi_0(\vec{r},\ u')\, dV}.$$

where $\varphi_0(\vec{r}, u)$ is the neutron flux in the infinite lattice, and the integration is taken over the volume of a cell.

The previously obtained formulas (25), (29), (42), and (43) remain valid for the averaging of the diffusion coefficient $D'(u)$.

In the region of thermalization, where the thermal motions of the nuclei of the moderator are of importance, and also the crystalline and molecular bonds, we can describe the spatial-energetic distribution of the neutron flux in the diffusion approximation by the following system of equations [4]:

$$\left.\begin{aligned} \nabla\vec{\Phi}_1(\vec{r},\ v) &= \int\limits_0^{\infty} K_0(\vec{r}; v, v')\, \Phi_0(\vec{r},\ v')\, dv' + \\ &+ \nu \int\limits_0^{\infty} \chi(\vec{r};\ v,\ v')\, \Phi_0(\vec{r},\ v')\, dv', \\ \nabla\Phi_0(\vec{r},\ v) &= \int\limits_0^{\infty} K_1(\vec{r}; v, v')\, \vec{\Phi}_1(\vec{r},\ v')\, dv', \end{aligned}\right\} \qquad (46)$$

where

$$K_0(\vec{r};\ v,\ v') = \frac{1}{v'}\{G_0(\vec{r};\ v,\ v') - [w_a(\vec{r},\ v') + w_s(\vec{r},\ v')]\,\delta(v - v')\},$$

$$K_1(\vec{r};\ v,\ v') = \frac{1}{v'}\{G_1(\vec{r};\ v,\ v') - [w_a(\vec{r},\ v) + w_s(\vec{r},\ v)]\,\delta(v - v')\}^{***}.$$

If a solution $\{\varphi_0(\vec{r},\ v),\ \vec{\varphi}_1(\vec{r},\ v)\}$, of the system (46) in the infinite lattice has been found, then, applying the methods explained above, we get the following homogenization formulas:

$$K_0'(v,\ v') = \frac{\int\limits_{V_n} K_0(\vec{r};\ v,\ v')\,\varphi_0(\vec{r},\ v')\,dV}{\int\limits_{V_n} \varphi_0(\vec{r},\ v')\,dV},$$

$$\chi(v,\ v') = \frac{\int\limits_{V_n} \chi(\vec{r};\ v,\ v')\,\varphi_0(\vec{r},\ v')\,dV}{\int\limits_{n} \varphi_0(\vec{r},\ v')\,dV}.$$

The averaging of the function $K_1(\vec{r};\ v,\ v')$ is carried out by formulas that are given below for the various cases.

Plane Lattice. For diffusion of neutrons along the layers

$$K_1'(v,\ v') = \frac{\int\limits_0^{\delta} K_1(x;\ v,\ v')\,\frac{\varphi_0(x,\ v')}{\Sigma_{tr}^{\text{eff}}(x,\ v')}\,dx}{\int\limits_0^{\delta} \frac{\varphi_0(x,\ v')}{\Sigma_{tr}^{\text{eff}}(x,\ v')}\,dx}, \quad (47)$$

where 2δ is the thickness of the cell in the x direction, and

$$\Sigma_{tr}^{\text{eff}}(x,\ v) = -\frac{1}{\varphi_0(x,\ v)}\int\limits_0^{\infty} K_1(x;\ v,\ v')\,\varphi_0(x,\ v')\,dv'.$$

For diffusion of neutrons perpendicular to the layers,

$$K_1'(v,\ v') = \frac{\int\limits_0^{\delta} K_1(x;\ v,\ v')\,\varphi_0(x,\ v')\,dx}{\int\limits_0^{\delta} \varphi_0(x,\ v')\,dx}. \quad (48)$$

Cylindrical Lattice. For diffusion of neutrons along the layers,

$$K_1'(v,\ v') = \frac{\int\limits_{V_n} K_1(\vec{r};\ v,\ v')\,\frac{\varphi_0(r,\ v')}{\Sigma_{tr}^{\text{eff}}(\vec{r},\ v')}\,dV}{\int\limits_{V_n} \frac{\varphi_0(\vec{r},\ v')}{\Sigma_{tr}^{\text{eff}}(\vec{r},\ v')}\,dV}, \quad (49)$$

where

$$\Sigma_{tr}^{\text{eff}}(\vec{r},\ v) = -\frac{1}{\varphi_0(\vec{r},\ v)}\int\limits_0^{\infty} K_1(\vec{r};\ v,\ v')\,\varphi_0(\vec{r},\ v')\,dv'.$$

For diffusion of neutrons perpendicular to the axes of the cells (in the direction of the x axis),

$$K_1'(v,\ v') = \frac{\int dy K_1(y;\ v,\ v')\,\frac{\varphi_0(y,\ v')}{\Sigma_{tr}^{\text{eff}}(y,\ v')}}{\int dy\,\frac{\varphi_0(y,\ v')}{\Sigma_{tr}^{\text{eff}}(y,\ v')}},$$

where

$$K_1(y;\ v,\ v') = \frac{\int\limits_{\delta(y)} K_1(x,\ y;\ v,\ v')\,\varphi_0(x,\ y;\ v')\,dx}{\int\limits_{\delta(y)} \varphi_0(x,\ y;\ v')\,dx},$$

$$\varphi_0(y,\ v) = \int\limits_{\delta(y)} \varphi_0(x,\ y;\ v)\,dx,$$

$$\Sigma_{tr}^{\text{eff}}(y,\ v) = -\frac{1}{\varphi_0(y,\ v)}\int\limits_0^{\infty} K_1(y;\ v,\ v')\,\varphi_0(y,\ v')\,dv'.$$

Finally, we can write a universal formula that makes it possible to calculate $K'_1(v, v')$ in the longitudinal and transverse directions for the plane, and also the cylindrical geometry of the cells (and for the spherical geometry)†††

$$K_1'(v,\ v') = \frac{\iint K_1(y,\ z;\ v,\ v')\,\frac{\varphi_0(y,\ z;\ v')}{\Sigma_{tr}^{\text{eff}}(y,\ z;\ v')}\,dy\,dz}{\iint \frac{\varphi_0(y,\ z;\ v')}{\Sigma_{tr}^{\text{eff}}(y,\ z;\ v')}\,dy\,dz},$$

where

$$K_1(y,\ z;\ v,\ v') = \frac{\int\limits_{\delta(y,\ z)} K_1(x,\ y,\ z;\ v,\ v')\,\varphi_0(x,\ y,\ z;\ v')\,dx}{\int\limits_{\delta(y,\ z)} \varphi_0(x,\ y,\ z;\ v')\,dx},$$

$$\varphi_0(y,\ z;\ v) = \int\limits_{\delta(y,\ z)} \varphi_0(x,\ y,\ z;\ v)\,dx,$$

$$\Sigma_{tr}^{\text{eff}}(y,\ z;\ v) = -\frac{1}{\varphi_0(y,\ z;\ v)}\int\limits_0^{\infty} K_1(y,\ z;\ v,\ v')\,\varphi_0(y,\ z;\ v')\,dv'.$$

*** The remaining notations are the same as in [4]. This reference also contains a detailed exposition of the method of solution of the system (46).

††† It is assumed that the x axis is along the direction of diffusion of the neutrons.

Equation (51) automatically goes over into (47), (48), (49), and (50).

An Illustration of the Ambiguity in the Parameters of the Homogenized Medium

We shall illustrate by a concrete example the fact that the method of Shevelev [1] and the method based on the conservation of the multiplication coefficient lead to different values of the diffusion lengths (cf. Introduction).

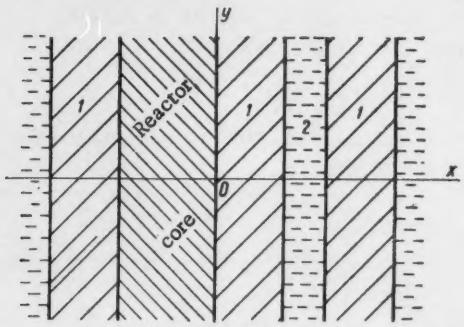

Fig. 2. A plane-parallel reactor.

Let the core of a plane-parallel reactor be surrounded by an infinite reflector consisting of successive layers of two substances 1 and 2 (Fig. 2), for which the values of the parameters are as follows:

Substance 1	Substance 2
$\delta_1 = 10$ cm	$\delta_2 = 20$ cm
$\Sigma_c = 0.25$ cm^{-1}	$\Sigma_c = 0.022$ cm^{-1}
$\Sigma_{tr} = 0.635$ cm^{-1}	$\Sigma_{tr} = 2.08$ cm^{-1}
$L_1 = 1.45$ cm	$L_2 = 2.7$ cm

Homogenizing the reflector by using (5.1) of [1], we find that $L_\perp = 1.99$. On the other hand, we can get a value of $L_\perp$ by using the equations:

$$\left.\begin{aligned} \sum_n \int_{\delta_1+\delta_2} (\Sigma_c - \Sigma_c')\,\Phi\Phi'\,dx = 0, \\ \sum_n \int_{\delta_1+\delta_2} (D - D')\,\nabla\Phi\,\nabla\Phi'\,dx = 0, \end{aligned}\right\} \qquad (52)$$

where the summation is taken over all pairs of layers in the reflector. In the system of equations (52) the function $\Phi(x)$ is known and is given by (2.1) of [1]. The function $\Phi'(x)$ is of the form

$$\Phi'(x) = \text{const} \cdot e^{-(x/L_\perp')}, \qquad (53)$$

where $L'_\perp$ is an as yet unknown parameter, which is connected with Σ'_c and D' by the relation

$$L_\perp'^2 = \frac{D'}{\Sigma_c'}. \qquad (54)$$

By the use of (53) and (54), the system (52) can be solved easily by an iteration method [2]; this gives

$$L_\perp' = 1{,}45.$$

This value $L'_\perp$ is the same as the diffusion length for the first zone, which directly adjoins the core (Fig. 2). This fact is obvious and has a physical meaning. In fact, the thickness of the first zone is almost seven times the diffusion length in it for the neutrons; i.e., zone 1 is practically equivalent to an infinite reflector [3]; consequently, replacement of substance 2 by substance 1 does not affect the reactivity of the reactor.

In this example it is seen that $L_\perp$ and $L'_\perp$ differ by almost 40 per cent.

The writer thanks G. I. Marchuk and V. V. Orlov for valuable advice in the working out of this topic.

LITERATURE CITED

1. Ya. V. Shevelev, Atomnaya Énergiya 2, 224 (1957).‡‡‡
2. W. E. Milne, Numerical Calculus [Russian translation] (IL, 1951).
3. S. Glasstone and M. Edlund, Foundations of the Theory of Nuclear Reactors [Russian translation] (IL, 1954).
4. G. I. Marchuk, Numerical Methods for Calculations on Nuclear Reactors [in Russian] (Atomizdat, Moscow, 1958).

Received August, 1958

‡‡‡ See English Translation.

COMPLETE SYMMETRY AND ISOTOPIC SPIN CONSERVATION IN THE NONLEPTONIC DECAY OF HYPERONS

Professor Gyo Takeda (Institute of Nuclear Studies, University of Tokyo)

and M. Kato (Department of Physics, University of Tokyo)

The possibility is considered that there exists a universal V-A interaction and complete symmetry in the nonleptonic decay of hyperons. The departure from the expected symmetry that is observed in actual decays is explained by effects caused by the mesonic structure of hyperons. In close connection with the idea of complete symmetry, a new isotopic spin is defined, which is equal to $\frac{1}{2}$ for all baryons and to 0 or 1 for K mesons. The law of conservation of this isotopic spin holds in nonleptonic decays.

1. Introduction

Many conservation laws have been established in the physics of elementary particles; these include the laws of conservation of the number of baryons, the charge, the strangeness, and the isotopic spin. Some of these laws hold only approximately, and the causes for their violations are either the electromagnetic or the weak interactions. It is quite possible that there exist further, less exact laws of conservation or symmetry, which are still unknown because they are violated to a considerable degree on account of the strong interaction of π or K mesons. Such a principle is the complete symmetry of baryons, which has been considered by Gell-Mann [1] and Schwinger [2], who assume that the interaction with K mesons destroys this symmetry and prevents its experimental observation.

In the study of the problem of the isotopic spin change ΔI in the nonleptonic decay of hyperons it has been found that the selection rule $\Delta I = 1/2$ is satisfied approximately [3]. Prentki and others [4] and one of the authors [5] have made an attempt to interpret the rule $\Delta I = 1/2$ as a conservation law $\Delta(I + I') = 0$, which holds strictly for interactions leading to nonleptonic decay, if we exclude the K-mesonic and electromagnetic interactions. Small departures from this law can occur on account of electromagnetic interactions or interactions with K mesons.*

The purpose of our further investigation of nonleptonic decay of hyperons is to try to find hitherto unknown symmetry or conservation laws that may hold for the interactions leading to the decay of bare baryons. Departures from the expected conservation laws must be due either to the π meson cloud or to the K meson cloud surrounding the bare particle. Studies of these departures can throw some light on the properties of the meson clouds of hyperons.

2. Experimental Data on the Nonleptonic Decays of Hyperons

Before going on with our program, let us examine the available experimental data on nonleptonic decays. The decay amplitudes A and asymmetry coefficients α for the decays of the various hyperons are shown in Table 1.†,‡

TABLE 1 Values of the Decay Amplitude and the Asymmetry Coefficient

Decay	$\lvert A\rvert^2$	$\lvert\alpha\rvert$	
$\Lambda \to p + \pi^-$	$0{,}78 \cdot 10^{-14}$	≈ 1	$(A_{\Lambda^-}$
$\to n + \pi^0$	$0{,}41 \cdot 10^{-14}$	not measured	(A_{Λ^0})
$\Sigma^+ \to p + \pi^0$	$1{,}04 \cdot 10^{-14}$	$\lvert\alpha_0\rvert \approx 1$	(A_0)
$\to n + \pi^+$	$1{,}24 \cdot 10^{-14}$	$\lvert\alpha_+\rvert \approx 0$	(A_+)
$\Sigma^- \to n + \pi^-$	$1{,}06 \cdot 10^{-14}$	$\lvert\alpha_-\rvert \approx 0$	(A_-)

Since parity may not be conserved in these decays, the amplitudes consist of two parts, A^S and A^P; the first corresponds to π mesons in the s state, and the second, in the p state. Gell-Mann and Rosenfeld [6] have treated A as an amplitude in the complex plane; that is, $A = A^S + iA^P$. The branching ratio for the Λ-decay reaction agrees with the selection rule $\Delta I = 1/2$. The large asymmetry coefficient in the Λ decay ($|\alpha| \approx 1$) means that $|A^S| = |A^P|$ for the decay $\Lambda \to p + \pi^-$, and is an

*In one way of describing these departures they are regarded as electromagnetic corrections to the selection rule $\Delta I = 1/2$. In another approach, it is assumed that decays with $\Delta I \neq 1/2$ exist also for the interaction of bare particles. It is then assumed that owing to the complete symmetry of the interaction of the π mesons, decays in which $\Delta I \neq 3/2$ (sic) do not occur in real processes, but the K-mesonic interactions destroy this symmetry and make these decays possible (cf. [5] pp. 641 and 642).

†The decay amplitude A is defined by the expression $|A|^2 = \hbar\Gamma/2pc$, where Γ is the corresponding decay probability and p is the momentum of the π meson emitted in the decay (cf. [6] p. 447).

‡Measurements have been made of the product of the asymmetry coefficient α and the hyperon polarization P. According to the data from the most recent experiments, made in Berkeley, the product αP is large for the decay $\Sigma^{\pm} \to p + \pi^0$ and very small for the decay $\Sigma^{\pm} \to n + \pi^{\pm}$ [7]. The values of the coefficient α shown in the table agrees with the measured values of αP, although this does not show that they are reliable.

indication that the decay is produced by an interaction of the type $V \mp A$.

When applied to the Σ decay, the rule $\Delta I = 1/2$ imposes the following condition on the amplitudes:

$$-A_+ + \sqrt{2}A_0 = A_-. \tag{1}$$

From (1) and the observed ratio of amplitudes

$$|A_+|^2 \approx |A_0|^2 \approx |A_-|^2, \tag{2}$$

it follows that A_+, A_- and $\sqrt{2}A_0$ must form a triangle in the complex A plane with angles close to 45°, 45°, and 90°. This means that the ratio A^S/A^P, or the asymmetry coefficient, is different for the three types of Σ decays. In fact, the results of recent measurements of the coefficients $\alpha(\alpha_\pm \approx 0, |\alpha_0| \approx 1)$ agree with this prediction and show that the two sides A_+ and A_- of the triangle must approximately coincide with the two axes of the complex A plane.

3. Universality and Complete Symmetry of the Decay of Bare Hyperons

Our working hypothesis is that in the interactions causing decay of the bare particles the largest possible number of conservation or symmetry laws holds, and the problem reduces to finding out whether the observed departures from these laws can be explained as effects due to the meson clouds of the particles. If we know very little even about the π-mesonic structure of the nucleon, on which there is a comparatively large amount of experimental data, then we really know nothing at all about the mesonic structure of hyperons. In what follows we wish only to indicate a possible mesonic structure and the decay scheme associated with it, which can give a qualitative explanation of the observed deviations from the proposed conservation laws.

The observed large asymmetry ($|\alpha| \approx 1$) of the Λ decay indicates that the decay is mainly caused by an interaction of the type $V \mp A$. If the actual Λ particle coincides for a large part of the time with the bare Λ particle so that the influence of the meson cloud on the decay is negligibly small, then the decay of the bare Λ particle is also due to an interaction of the type $V \mp A$. This interaction and its possible universality for the decay of bare fermions has been considered earlier [8] and may be of very great importance. Therefore we assume that the decay of bare hyperons ($\Sigma \to N + \pi$ and $\Lambda \to N + \pi$) is a decay of the type $V \mp A$.

The observed branching ratio of the Λ decay, $(\Lambda \to n + \pi^0)/(\Lambda \to p + \pi^-) \approx 1/2$, agrees with the selection rule $\Delta I = 1/2$. This rule will also be valid for the decay of the bare Λ particle, since it is assumed that the interactions with the π and K mesons do not depend on the charge and do not change ΔI. Although the validity of the rule $\Delta I = 1/2$ is not inescapably indicated for the Σ decay, the experimental data are in agreement with it. Moreover, if this rule did not hold, there would be a probability for the Λ particle to decay with a ΔI not equal to 1/2, since the decay of the Λ particle can go not only directly, but also by way of a virtual Σ decay. In order to preserve the maximum possible symmetry between the Λ and Σ decays we assume that the rule $\Delta I = 1/2$ holds for all nonleptonic decays of hyperons.

As was noted in Section 2, the rule $\Delta I = 1/2$ does not in itself completely determine the Σ decay, but gives only (1). In accordance with our working hypothesis we assume that in the decay of bare hyperons there appears a symmetry that is essentially equivalent to Gell-Mann's complete symmetry, as applied to the interaction causing the decay [1].

The idea is as follows:

$$\Sigma^+ \text{ and } Y^0 \left(= (\Lambda^0 - \Sigma^0)/\sqrt{2}\right) \text{ or}$$
$$Z^0 \left(= (\Lambda^0 + \Sigma^0)/\sqrt{2}\right) \text{ and } \Sigma^-$$

form a pair of baryons just like p and n or Ξ^0 and Ξ^-:

$$\Psi_Y = \begin{pmatrix} \Sigma^+ \\ Y^0 \end{pmatrix}, \quad \Psi_Z = \begin{pmatrix} Z^0 \\ \Sigma^- \end{pmatrix},$$
$$\Psi_N = \begin{pmatrix} p \\ n \end{pmatrix} \text{ and } \Psi_\Xi = \begin{pmatrix} \Xi^0 \\ \Xi^- \end{pmatrix}. \tag{3}$$

The four fields Ψ_s are isospinors with isotopic spin 1/2, in an isotopic space that is different from the usual one. Gell-Mann's complete symmetry requires that the interaction of π mesons with each of the four fields must be the same:

$$H_\pi = f\{\overline{\Psi}_N \gamma_5 \vec{\tau} \Psi_N \vec{\Phi}_\pi + \overline{\Psi}_\Xi \gamma_5 \vec{\tau} \Psi_\Xi \vec{\Phi}_\pi + \overline{\Psi}_Y \gamma_5 \vec{\tau} \Psi_Y \vec{\Phi}_\pi + \overline{\Psi}_Z \gamma_5 \vec{\tau} \Psi_Z \vec{\Phi}_\pi\}. \tag{4}$$

If there is interaction only with the π mesons, then the masses of all baryons must be the same, and the actual differences of the masses must be caused by the interaction with the K mesons. Here we assume that complete symmetry holds even in the decays of bare hyperons, and will suppose that the decay corresponds to the following interaction:

$$g\{\overline{\Psi}_Y \vec{\tau} \gamma_\mu (1 \pm \gamma_5) \Psi_N \partial_\mu \vec{\Phi}_\pi + \overline{\Psi}_Z \vec{\tau} \gamma_\mu (1 \pm \gamma_5) \Psi_\Xi \partial_\mu \vec{\Phi}_\pi\} + \text{Hermitian adjoint expression.} \tag{5}$$

This complete symmetry of the interactions contains within itself the law of conservation of the quantum number of the new isotopic spin, which is equal to 1/2 for each of the baryons and 1 for the π meson.

The rule $\Delta I = 1/2$, where I is the ordinary isotopic spin, and the universality of the $V \mp A$ interaction are also valid.

If the interaction (5) is subject to no corrections associated with the π meson and K meson interactions, the universal interaction $V \mp A$ gives an asymmetry coefficient α equal to ± 1 for all Σ and Λ decays. Furthermore, owing to the complete symmetry,

$$|A_0|^2 : |A_+|^2 : |A_-|^2 = 1 : 2 : 0. \tag{6}$$

Since it is assumed that the strong π-meson interaction has complete symmetry and does not lead to a difference of the baryon masses, the relation (6) must hold

even in the presence of π-meson interactions. The asymmetry coefficient will, however, differ from the value ± 1, since the π-meson interaction can have different effects in increasing or decreasing Σ and V. Nevertheless the coefficient α must be the same for all the nonleptonic decays of hyperons. Only the K-mesonic interactions can lead to the observed difference in the values of α for the various decays. In the following section we shall consider the problem of the changes of the decay amplitude A that are caused by the π-mesonic and K-mesonic structures of the hyperons, and shall show that the observed values of A can be obtained if we take these effects into account.

4. Effects of the Mesonic Structure of Hyperons on the Amplitudes for Nonleptonic Decays

Since the magnitude and phase of the amplitude A in the complex plane can be strongly affected by the presence of the meson clouds around the particle, we shall first try to get a somewhat clearer idea of the structure of these clouds. Actual Λ and Σ particles are regarded as complex states of the system, including the state of the bare particle, the state of the bare particle plus one π-meson, and so on:

$$\begin{aligned} \Lambda &: \tilde{\Lambda},\ \tilde{\Sigma}^{\pm,0}+\pi^{\mp,0},\ \ldots \\ \Sigma^{\pm} &: \tilde{\Sigma}^{\pm},\ \tilde{\Lambda}+\pi^{\pm},\ \tilde{\Sigma}+\pi,\ \ldots \end{aligned} \qquad (7)$$

We shall consider here only the π-meson cloud, since it is more important for our further work than the K-meson cloud, and is probably more intense. Thus the bare particles $\tilde{\Lambda}$ or $\tilde{\Sigma}$ in (7) are to be regarded as particles that already include the K-meson cloud. Therefore the $\tilde{\Sigma}$ particle is heavier than the Λ particle, if the actual difference of the masses of the Σ and Λ particles is due to the K-meson interaction. Then the energy difference between the states $\tilde{\Sigma}$ and $\tilde{\Lambda}+\tilde{\pi}$ is small, and the state $\tilde{\Lambda}+\pi$ can have a large amplitude. At the same time, for both the cases of the Λ particle and the Σ particle the configurations $\Sigma+\pi$ are energetically less favorable, and may be relatively unimportant.

We now adopt an extreme point of view, assuming that the Λ particle is practically the same as the $\tilde{\Lambda}$ particle, and that the Σ particle is a superposition of the states $\tilde{\Sigma}$ and $\tilde{\Lambda}+\pi$. The deviations from this assumed structure may be sizable, but we shall hope that the qualitative aspects of the following discussion will, nevertheless, retain some validity. It is proper to make here one more remark about the importance of the K-mesonic interactions. It is assumed that the K-mesonic interaction causes a splitting of the mass level of the baryons, and we have included this effect as a mass difference between $\tilde{\Sigma}$ and $\tilde{\Lambda}$. Otherwise, in the actual states of the Λ and Σ particles the configurations $\tilde{\Sigma}+\pi$ would have to have the same importance as the configurations $\tilde{\Lambda}+\pi$ have in the Σ particle, and our further arguments about the asymmetry coefficient α would be incorrect.

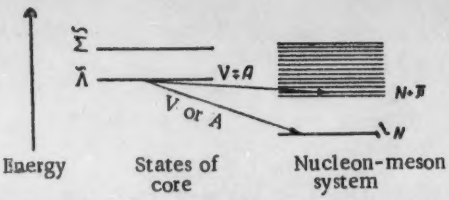

Scheme of possible transitions caused by the interaction that leads to the decay of bare particles [5]

The interaction (5) for the decay of bare hyperons is expressed in terms of the bare-particle fields** Ψ_Y, Ψ_Σ, Ψ_N, Ψ_Ξ and Φ_π. Since the bare nucleon Ψ_N and the bare π meson can form a real nucleon, the interaction (5) can of itself lead, for example, to the virtual decay of a $\tilde{\Lambda}$ particle with the formation of a real neutron. This transition leaves unchanged the momentum, the spin, and other conserved quantities, except for the energy of the system, and, therefore, the transition can only be regarded as a virtual process. The possible transitions caused by the interaction (5) are shown schematically in the diagram. The hyperon core $\tilde{\Sigma}$ and $\tilde{\Lambda}$ can dissociate into states of the continuous spectrum with one nucleon and one π meson, or into the state of the real nucleon ($\tilde{\Lambda}\to n$ or $\tilde{\Sigma}^{+}\to p$). It is important to note that only the V- or A-interaction can lead to the transition $\tilde{\Lambda}\to n$ or ($\tilde{\Sigma}\to p$), since the relative parity of $\tilde{\Lambda}$ (or $\tilde{\Sigma}$) and N has a definite value. Therefore parity is always conserved, if the relative parity is positive, or is always nonconserved, if the relative parity if negative. In the continuous-spectrum states the π meson can be in an s or a p orbit relative to the nucleon. Therefore both A^s and A^p can be different from zero for the transitions to states of the continuous spectrum.

The existence of transitions in which the core of the particle becomes a nucleon has an important manifestation in the reduction of the magnitude of the asymmetry coefficient $|\alpha|$ from 1 to 0 for the decays $\Sigma^{+}\to n+\pi^{+}$ and $\Sigma^{-}\to n+\pi^{-}$. The first-order perturbation by the interaction (5) does not contain this transition, which appears only when we take into account the strong interaction between the bare nucleon and the π meson. We assume that this transition is greatly enhanced owing to the π-meson interaction.

The interaction (5) and our model of hyperon structure, $\Lambda\approx\tilde{\Lambda}$ and $\Sigma^{\pm}\approx\tilde{\Sigma}^{\pm}$ plus $\tilde{\Lambda}+\pi^{\pm}$, lead to the following decays:

	Decay scheme	Decay amplitude
Σ decay	$\tilde{\Sigma}^{+}\xrightarrow[V\mp A]{} p+\pi^{0}$	(a_s+ia_p)
	$\tilde{\Sigma}^{+}\xrightarrow[V\mp A]{} n+\pi^{+}$	$\sqrt{2}(a_s+ia_p)$
	$\tilde{\Lambda}+\pi^{\pm}\xrightarrow[V\text{ or }A]{} n+\pi^{\pm}$	ib_p

**Since we are going to consider the modification of the interaction (5) associated with the π-meson cloud only, the interaction that we should really use in (5) would be expressed not in terms of bare-particle fields, but in terms of fields including the K-meson clouds. We shall, however, neglect this distinction here.

	Decay scheme	Decay amplitude
Λ decay	$\tilde{\Lambda} \xrightarrow[V \mp A]{} p + \pi^-$	$(a_s' + ia_p')$
	$\xrightarrow[V \mp A]{} n + \pi^0$	$\sqrt{\frac{1}{2}}(a_s' + ia_p')$.

The decay amplitude $a_s + ia_p$ is the amplitude corresponding to the transitions of $\tilde{\Sigma}$ to states of the continuous spectrum $N + \pi$, multiplied by the probability amplitude for formation of the bare $\tilde{\Sigma}$ particle in the real Σ particle. Since the $V \mp A$ interaction holds, $|a_s| \approx |a_p|$. The amplitude ib_p is the amplitude for transition of the $\tilde{\Lambda}$ particle to a neutron, multiplied by the probability amplitude for formation of the configuration $\tilde{\Lambda} + \pi$ in the real Σ particle. We assume that the relative parity of Λ and N is positive, and therefore consider only the amplitude of the p wave. From our point of view this choice is the more desirable, for the preservation of the greatest possible symmetry, although it is not essential for the present treatment. The resulting amplitudes for the three types of Σ decay are:

$$A_+ = \sqrt{2}(a_s + ia_p) + ib_p,$$
$$A_- = ib_p \qquad (8)$$

and

$$A_0 = a_s + ia_p,$$

where

$$|a_s| \approx |a_p|. \qquad (9)$$

The influence of the mesonic structure of hyperons on their decay amplitudes appears only in the ratio b_p/a_p, and a nonvanishing value of this parameter changes the simple predictions obtained on the basis of the law of the universality of the $V \mp A$ interaction and complete symmetry with respect to the Σ decay. Let us now see whether it is possible by a suitable choice of this ratio to get the observed calues of the asymmetry coefficients and the relative values of the quantities A shown in Table 1.

From (8) it follows that $|\alpha_0| \approx 1$ and $|\alpha_-| \approx 0$, which is in agreement with the experimental results. The value of b_p/a_p is determined from the requirement $|\alpha_+| \approx 0$, which gives

$$\sqrt{2}\,a_p + b_p = 0. \qquad (10)$$

Therefore A_+ and A_- contain only s and p amplitudes, respectively. It follows from (10), (8), and (9) that the decay probabilities are

$$|A_+|^2 \approx |A_-|^2 \approx |A_0|^2 \approx 2a^2, \qquad (11)$$

which agree with the observed ratio of the three decay amplitudes.

For the Λ decay, the observed branching ratio of the reaction is easily explained as a consequence of the interaction (5), which contains the selection rule $\Delta I = 1/2$.

As for the decay amplitude, the assumption about the complete symmetry of the interaction causing the decay leads to the approximate equality of the decay probabilities for $\Lambda \to p + \pi^-$ and $\Sigma^+ \to p + \pi^0$, which agrees with the experimental results. If we follow on with our model, the ratio $|A_{\Lambda^-}|^2/|A_0|^2 (= |a'/a|^2)$ will be equal to unity divided by the probability of formation of a bare $\tilde{\Sigma}$ particle in the real Σ particle. Theoretically, this ratio must be > 1 and it then disagrees with the experimental value, which is somewhat smaller than 1. No serious meaning should be attached to this contradiction, in view of our extremely special choice of the mesonic structure of the hyperons.

5. Discussion

We have succeeded in showing that it is possible to secure agreement of the observed hyperon decays with the proposed laws, namely with the universal $V \mp A$ interaction and with complete symmetry in the decays of the bare particles. An important part has been played by the configurations $\tilde{\Lambda} + \pi$ in the Σ particle and the transition of $\tilde{\Lambda}$ to a neutron with conservation of parity. Although we have as yet no quantitative ideas about the mesonic structure of the hyperon, our results can be regarded as some justification for the proposed laws, and also for the importance given to the $\tilde{\Lambda} + \pi$ configuration in the Σ particle.

The difficulty of observing the symmetries and conservation laws that hold in the interactions causing the decay of the bare particles is due to the fact that they are to a considerable degree destroyed by the stronger interactions. Several authors have stated that in the stronger interactions greater symmetry is manifested, or a larger number of conservation laws hold, than in the weak interactions. The original idea of complete symmetry was indeed developed in this direction. If such an argument is indeed correct, then it will be easier to find these symmetry laws than to find others. We believe that this assertion is not always correct, and that there can be cases in which a weaker interaction has greater symmetry than a strong interaction. In fact, our proposed complete symmetry holds both for the π-mesonic interactions and for the interactions that cause the decays, and does not hold for the K-mesonic interactions.

The decays of baryons occur not through separation of the π-meson or K-meson clouds from the baryon core, but rather through a change of the core itself, which is accompanied by a change of the isotopic spin, the strangeness, and so on. Therefore we can say that the most important stage of the decay occurs in a definite region of the core, although the size of this region cannot be stated on the present level of our knowledge. If there is a certain symmetry, or if a certain conservation law holds, in the interaction causing the decay, this will be of great significance for the future study of the laws of nature that act in the small region of the core.

The interaction (5) with complete symmetry provides the possibility of ascribing to each elementary particle an isotopic spin, with values different from the usual ones. We

list here the new values of the isotopic spin, together with the old values:

	N	Λ	Σ	Ξ	K	π
New value	1/2	1/2	1/2	1/2	0,1	1
Old value	1/2	0	1	1/2	1/2	1.

We have given only the values of the izotopic spin. In the new classification there must be four isotopic-spin doublets, as shown in (3). The new isotopic spin is conserved in π-mesonic interactions and in the weak interactions that cause decays, but is not conserved in the K-mesonic interactions. Since the new isotopic spin is not conserved in K-mesonic interactions, the value of the isotopic spin of the K meson itself is not determined by the strong interactions. We require, however, that the new isotopic spin be conserved not only in the decay of the bare hyperon, but also in the decay of the bare K meson into a π meson. From the rule $\Delta I = 1/2$, interpreted as the law of conservation of the new isotopic spin, it follows that the isotopic spin is 0 for the K_1^0 meson and 1 for the K^+, K_2^0, and K^- mesons.

TABLE 2 Conservation or Nonconservation of Isotopic Spin for Various Types of Interactions

	Type of interaction			Decay
	π mesonic	K mesonic	electro magnetic	
New isotopic spin . . .	0	×	×	0
Old isotopic spin. . . .	0	0 (?)	×	×

Let us examine the question: which classification in terms of isotopic spin is more convenient for the description of the elementary particles? Since, in the old classification, the strong π-mesonic and K-mesonic interactions conserve the isotopic spin, it is of course easier to use the terms of the old classification in the study of the production of elementary particles, their scattering, and other processes associated with the strong interactions. The new classification can be more convenient than the old for the study of the weak interactions, in which the new isotopic spin of the bare particles is conserved (cf. Table 2). Moreover, up to the present there has been no experimental decision of the question as to whether the usual isotopic spin is conserved in K-mesonic interactions. We think that these two isotopic spins complement each other. For example, the existence of the K-meson charge doublets (K^+, K^0) and ($\bar{K}^0$, K^-) and the problem of the K_1^0 and K_2^0 mesons is more easily understood by ascribing to the K meson the usual value 1/2 of the isotopic spin. On the other hand, the $\Delta I = 1/2$ rule for nonleptonic K decay is more easily understood by using the new isotopic spin, which is 0 or 1 for the K mesons.

In Section 3 the assumption was made that the interaction (5) that causes the decays is a Yukawa-type interaction. We can also assume that this interaction is a Fermi-type interaction, which is biquadratic in the bare-baryon fields. In this case we can preserve the universal interaction law $V \mp A$ and the complete symmetry if, for example, we write the interaction in the following form:

$$g\{\bar{\Psi}_Y \vec{\tau}\gamma_\mu (1 \pm \gamma_5)\Psi_N (\bar{\Psi}_N \vec{\tau}\gamma_\mu\gamma_5 \Psi_N + \bar{\Psi}_Y \vec{\tau}\gamma_\mu\gamma_5 \Psi_Y) + \\ + \bar{\Psi}_Z \vec{\tau}\gamma_\mu (1 \pm \gamma_5)\Psi_\Xi (\bar{\Psi}_\Xi \vec{\tau}\gamma_\mu\gamma_5 \Psi_\Xi + \bar{\Psi}_Z \vec{\tau}\gamma_\mu\gamma_5 \Psi_Z)\} + \\ + \text{Hermitian adjoint expression.} \qquad (12)$$

In (12), the conservation of the new isotopic spin is obvious; it also gives the $\Delta I = 1/2$ rule. We cannot distinguish here which of the interactions (Yukawa type or Fermi type) is the fundamental one. If the Fermi-type interaction is the fundamental one, it must be remembered that the interaction (12) is only one example from among the interactions of this type that give the universal $V \mp A$ law, complete symmetry, and conservation of the new isotopic spin.

In conclusion, we make a remark about the observed departure from the $\Delta I = 1/2$ rule. The existence of nonleptonic decays of K^+ mesons into two π mesons shows clearly that this rule holds only approximately. The electromagnetic interaction is definitely a cause of violations of this rule, although the results of a preliminary study evidently show that the observed probability of K^+ decay cannot be explained by this effect alone. We shall deal with this problem at another time. If the electromagnetic correction is too small, we must assume that the decay of the bare particle comes from an interaction that causes not only transitions with $\Delta I = 1/2$, but also some with values of ΔI different from 1/2. It is easy to show that the conservation of the new isotopic spin is inconsistent with the existence of such transitions. Therefore we must either renounce the complete symmetry that we have introduced and the conservation of the new isotopic spin in the decays of bare baryons, or else renounce the charge independence of the K-mesonic interactions, which has so far not been proved experimentally to good accuracy. The cause of the decay of the K^+ meson into two π mesons remains unclear.

LITERATURE CITED

1. M. Gell-Mann, Phys. Rev. 106, 1296 (1957).
2. J. Schwinger, Proceedings of the Seventh Rochester Conference (Interscience Publishers, N. Y., 1957).
3. R. Dalitz, Proc. Roy. Soc. A69, 527 (1956); G. Takeda, Phys. Rev. 101, 1547 (1956); M. Kawaguchi, Phys. Rev. 107, 573 (1957).

4. B. d'Espagnat, J. Prentki, and A. Salam, Nuclear Phys. No. 5, 447 (1958).

5. G. Takeda, Progr. Theoret. Phys. 19, 631 (1958).

6. M. Gell-Mann and A. Rosenfeld, Annual Rev. Nucl. Sci. 7, 407 (1957).

7. R. L. Cool, B. Cork, J. W. Cronin, and W. A. Wenzel, UCRL-8539, 1958, to be published; Drell, Proceedings of the Eighth Annual High-Energy Physics Conference at CERN (Geneva) (Interscience Publishers, N. Y., 1958).

8. R. Feynman and M. Gell-Mann, Phys. Rev. 109, 193 (1958).

Received December 18, 1958

THE PROBLEM OF THE USE OF ORGANIC COMPOUNDS AS MODERATORS IN NUCLEAR REACTORS

B. G. Dubovskii and M. N. Lantsov

Experiments for studying the properties of organic compounds used as moderators were carried out in a small, water-water physical reactor. Fuel elements of highly enriched uranium were arranged in a triangular lattice, whose parameters are given in the table. The critical state was reached by gradually raising the level of the moderator in the reactor tank. The radius of the active zone was the same in all experiments. At the sides and bottom, the active zone was surrounded by a reflector made of iron and a mixture of iron and moderator. The ends of the fuel elements acted as the top reflector, and the height of the elements was approximately twice that of the active zone of the critical assembly.

The critical masses, rates of increase in reactivity $d\rho/dh$ on raising the level of the moderator above critical, and the values of the Laplacian of the distribution of thermal neutrons κ^2 were determined experimentally. In determining the value of $d\rho/dh$ (from the value of the reactor period) in relation to the level of the moderator, a correction was introduced for the difference in value of prompt and delayed neutrons. The correction was calculated from formulas for a two-group approximation, which gave reasonable agreement with experiment for normal water. For the critical assemblies described, the correction for the value of delayed neutrons reached 20-30%. Although this correction is considerable, the error associated with allowing for it in the determination of τ was small (of the order of 1%).

The value of the Laplacian κ^2 was found from the distribution of thermal neutrons. The experimental points obtained were treated by the method of least squares for all the critical assemblies studied. Due to the limited number of points obtained in measuring the neutron distribution (9 points along the diameter and 20 along the height), it was impossible to show accurately the change in the efficiency of the reflector on replacing one moderator by another. The value of the economy of the reflector for different liquids was measured within 1 cm limits, which was within the limits of error of the measurement.

The most careful measurements of κ^2 were carried out for normal water. The value thus obtained for the economy of the reflector was taken for all the moderators.

Comparative Data of Experiments with Various Organic Liquids and Normal Water*

Characteristics of critical assembly and moderator / Moderator	Ratio of nuclear concentrations of hydrogen and U^{235} C_H/C_5	Critical mass in 1 kg of U^{235}	Ratio of critical volumes of active zones	Ratio of multiplication factors, K_∞**	Neutron age in pure moderator τ, cm^2	Ratio of numbers of hydrogen nuclei in 1 cc	Ratio of numbers of moderating nuclei in 1 cc	Liquid density, g/cc	Boiling point, °C
Water	251	7,07	1	1	31,4	1,00	1,000	1,00	100
Isoamyl alcohol $(CH_3)_2CHCH_2CH_2OH$	250,5	7,07	1	0,95	25,5±2	0,996	0,999	0,813	132
Cyclohexanone $CH_2(CH_2)_4CO$	218	7,16	1,013	1,012	33,5±2,7	0,871	0,988	0,947	155
Benzyl alcohol $C_6H_5CH_2OH$	174	7,84	1,104	1,005	36±2,9	0,694	0,915	1,043	205
Toluene $CH_3C_6H_5$	169	8,49	1,19	1,018	41±3,2	0,678	0,848	0,866	111
Formic acid (87%) HCOOH	—	—	—	—	49,5±2,6***	0,533	0,81	1,19	—
Mixture of organic compounds	~137	8,37	1,184	1,029	52,5±4,2	~0,55	~0,75	—	—

*84% of the lattice volume was occupied by moderator, 6% by uranium, 5% by steel, and 5% by air pores.

**Due to the large error in the measurement, the values of the ratio of K_∞ should be considered as qualitative.

***Direct measurement up to indium resonance energy (measurements carried out by L. A. Geraseva and V. V. Vavilov).

The results of the measurements made it possible to solve the following equations* with respect to K_∞ (multiplication factor) and τ (neutron age in the lattice studied):

$$\left.\begin{aligned}(1+\chi^2\tau)(1+\chi^2L^2)&=K_\infty,\\ \frac{d\rho}{dh}&=\frac{2\pi^2L^2+2\pi^2\tau+4\pi^2\chi^2L^2\tau}{K_\infty H^3},\end{aligned}\right\}\qquad(1)$$

where L^2 is the square of the diffusion length of neutrons in the lattice and $H = h_{cr} + \delta_{end}$ is the effective height of the active zone, equal to the sum of the geometric height of the active zone and the end economy of the reflector.

From these equations, we determined with great accuracy not the values of K_∞ and τ themselves, but the ratio of these values for reactors with the given organic liquid and with normal water.

The neutron age for the organic liquid studied was determined from the expression

$$\tau_{org}=\tau_{H_2O}\eta,\qquad(2)$$

where η is the ratio of the values of τ obtained from relation (1) for reactors with organic liquid and normal water. Here it was assumed that the values of neutron moderation in uranium and the constructional materials were small and similar to each other.

The results of the experiments are presented in the table.

Summary

1. Replacement of water by organic liquids in water-water reactors did not lead to an essential increase in the critical volume of the reactor. A slight increase in the volume of the active zone occurred due to the escape of neutrons from the reactor.

2. The neutron age in organic liquids increased more slowly than the concentration of hydrogen nuclei in them fell.

3. Due to the presence of carbon in the organic liquids, the value of the neutron age τ in them was much less than in water (at the same concentration of hydrogen nuclei). This property of organic liquids of the isoamyl alcohol type offers prospects of their use in biological shields of small nuclear reactors.

4. To obtain more accurate results, comparative experiments on reactors with organic moderators are best carried out on less enriched uranium.

In addition to the authors, E. A. Plaksin and V. M. Fedorov participated in the experiments.

The authors would like to thank Prof. A. K. Krasin for setting the problem and for valuable advice in discussion of the work and also E. I. Inyutin, P. A. Palibin, and V. P. Shelud'ko for help in preparing for the measurements.

Recieved January 6, 1959

*S. Krasik and A. Radkovskii, "Atomic power," Reports of the Soviet Delegation at the International Conference on the Peaceful Use of Atomic Energy (Geneva, 1955) (Gosénergoizdat, 1956) p. 375.

CALCULATION OF HEAT GENERATED IN A SHUTDOWN REACTOR

T. N. Zubarev and A. K. Sokolov

The solution of the nonsteady state neutron diffusion equation* must be used to calculate the residual heat yield in thermal reactors, associated with the presence of delayed neutrons. Suppose that prior to shutdown, the neutron flux was Φ_0 and the shutdown took place as a result of an instantaneous reduction in reactivity to a value $-\rho$, where we have $\rho / k_{eff} \approx \rho$, $\lambda_i \ll 1/T$ (k_{eff} is the criticality factor or effective multiplication factor of the neutrons in the shutdown reactor, λ_i is the decay constant of fragment nuclei of the ith group, and T is the neutron lifetime in the reactor).

Then, by solving the nonsteady state neutron diffusion equation, we obtain the following relation for the thermal neutron flux Φ in the shutdown reactor, starting from a time t:

$$\frac{\Phi(t)}{\Phi_0} = \sum_{j=0}^{m} A_j \exp(\omega_j t), \qquad \sum_{j=0}^{m} A_j = 1, \qquad \sum_{j=0}^{m} \frac{\lambda_i A_j}{\omega_j + \lambda_i} = 1, \quad i = 1, 2, \ldots, m. \tag{1}$$

here m is the number of delayed-neutron groups, and ω_j are the roots of the equation

$$\frac{\rho}{k_{eff}} = \frac{\omega T}{1+\omega T} + \frac{1}{1+\omega T} \sum_{i=1}^{m} \frac{\omega \beta_i}{\lambda_i + \omega},$$

in which β_i is the fraction of delayed neutrons of the eff group out of the total number of neutrons produced by fission of the uranium nucleus.

The complicated form of (1) hinders its use in calculations. To simplify calculations, we may use an approximate formula obtained in the analysis of a series of calculations based on (1):

$$\frac{\Phi(t)}{\Phi_0} \approx \frac{\rho}{\rho+\beta} \exp\left(-\frac{\rho+\beta}{T} t\right) + \sum_{i=1}^{m} \frac{\beta_i}{\rho+\beta} \exp\left(-\frac{\rho}{\rho+\beta} \lambda_i t\right), \qquad \beta = \sum_{i=1}^{m} \beta_i. \tag{2}$$

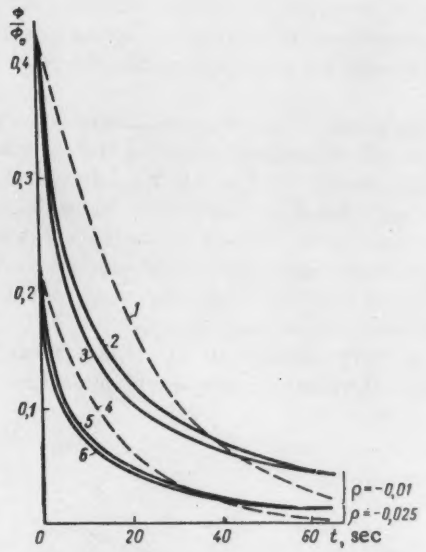

Time dependence of thermal neutron flux in a reactor after shutdown. Curves 1, 2, 4, 5 are based on (1), curves 3 and 6 are based on (2); for curves 1 and 4, m = 1, and for curves 2, 3, 5, and 6, m = 6.

The results of the calculations based on (1) and (2) are shown in the diagram. Calculations based on (2) are distinguished by their simplicity and allow excellent accuracy for the entire range of negative reactivity values which are of practical interest. For values of negative reactivity $|\rho| > 0.03$; the results of calculations based on (1) and (2) display good agreement in practice.

Received December 19. 1958

*S. Glasstone, and G. Edlund, The Elements of Nuclear Reactor Theory (New York, 1952).

DILATOMETRIC STUDIES OF ROLLED URANIUM RODS

I. V. Batenin, A. N. Rudenko, and B. V. Sharov

It is well known that in the thermal cycling of textured uranium rods an irreversible lengthening takes place, reflected in the corresponding dilatometric curves [1].

In studies made using a vacuum dilatometer on technically pure uranium samples hot-rolled at high reduction at approximately 300°C to a 4 mm diameter, an anomalous departure of the dilatometric curves during the first thermal cycle was observed. In heating above 525°C (Fig. 1a), and in subsequent cooling, the dilatometric curve 0-1-7-8 corresponds to the well-known curve for rods with saturated axial texture [010].

The anomalous behavior of the curves was observed upon cooling if the heating temperature in the first cycle fell within the range 200-500°C. When the uranium was heated to approximately 180°C, the cooling curve coincided with the heating curve, but failed to coincide on heating above 180°C; thus, when the sample was heated to 215°C, cooling proceeded according to curves 2-a-0; when heated to 300°C, according to curves 3-9; when heated to 450°C, according to curves 4-10; when heated to 485°C, according to curves 5-11; and when heated to 520°C, according to curves 6-c-0. In cases 3-9, 4-10, and 5-11, corresponding to heating to temperatures of 250-520°C, shortening of rod length ensued.

For a rod compressed in the first thermal cycle (0ab, Fig. 1b), subsequent heating led to an appreciable shift of the inversion point (up to about 400°C) on the heating

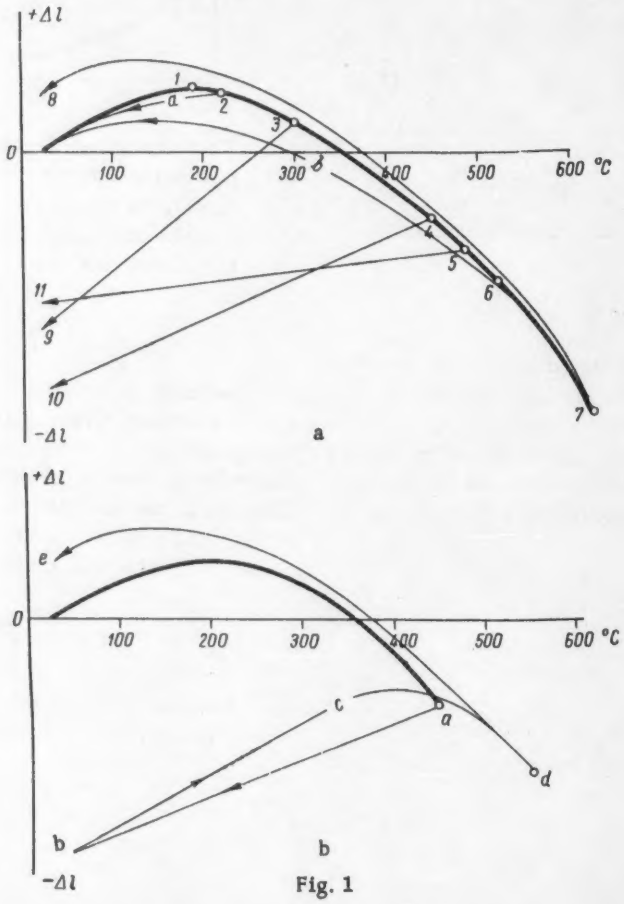

Fig. 1

Dilatometric curves. a) 8 cycles; b) 2 cycles.

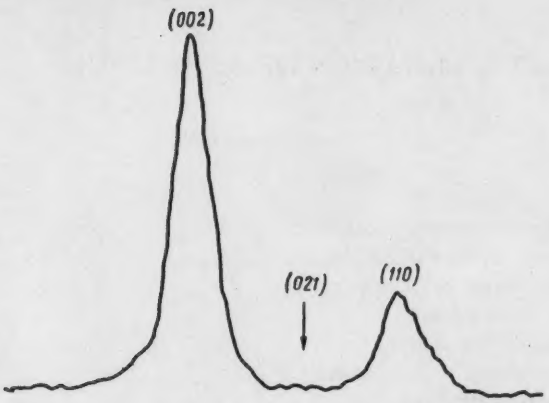

Fig. 2. X-ray diagram of initial uranium sample.

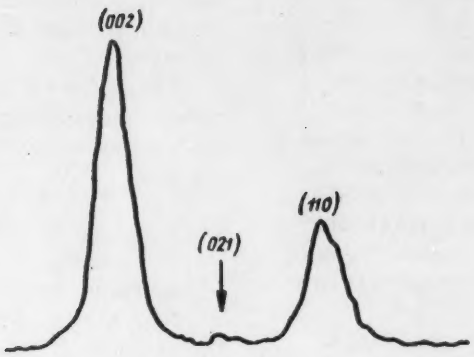

Fig. 3. X-ray diagram of uranium sample preheated to 300°C.

curve bcd. On cooling from a temperature of about 600°C, the inversion point is again shifted to the temperature approximating 200°C. If, during the second thermal cycle, the temperature corresponding to the heating-curve inversion point is not exceeded, the cooling curve will then coincide in practice with the heating curve.

A slight textural change corresponds to the anomalous dialometric curves, as we see from an analysis of the intensities of diffraction pattern lines on X-ray pictures of a polished slide passing through the rod axis, taken on CuK_α radiations (Figs. 2 and 3). It is clear from inspection of the diagrams that the ratio of line intensities $\frac{I_{(002)}}{I_{(110)}}$ is reduced by about 27 % after heating, while the (021) line is absent on both X-ray diagrams. Simultaneously with the variation in texture on heating to 300°C, we note a decrease in the width of the diffraction lines: the reduction in width for the (002) line is about 20%.

It is possible that the anomalous behavior of the dilatometric curve during the first heating of a strained uranium rod is associated with the diffusion of impurities present in technically pure uranium. On heating to comparatively low temperatures, secondary segregation of impurity atoms may occur as the result of "upward" diffusion [2]. The dilatometric curve for high purity uranium possibly lacks the anomalous behavior discussed here.

LITERATURE CITED

1. F. Foote, "Metallurgy in nuclear energy and radiation effects on materials," Reports of Foreign Scientists to the International Conference on the Peaceful Uses of Atomic Energy (Geneva 1955) [Russian translation] (Metallurgizdat, 1956) p. 89.
2. S. T. Konobeevskii, Zhur. Éksptl. i Teor. Fiz. 13, 200 (1943).

Received December 19, 1958

RADIOACTIVATION DETERMINATION OF BERYLLIUM

Kh. B. Mezhiborskaya

The use of the (γ, n) reaction for a radioactivation determination of beryllium has been described in the literature [1-3]. Our experience over a period of five years has confirmed the lasting value of this method.

Sb^{124} was used as the γ source. Two analysis procedures were employed: direct counting of the neutrons generated, and activation of an indium detector.

The first variation was accomplished by means of an SCh-3 apparatus, which had a proportional neutron counter, type SNM, filled with BF_3 enriched in B^{10}. With a γ source of 200-300 mC activity and analysis samples of about 200 g, the sensitivity of the method was about 0.001 % Be; the length of determination was 10-20 min.

For the second variation of the analysis we used a source with an activity of about 2 curies, which was placed in a lead container holding a paraffin block. The weight of the analysis sample was 5-100 g and the weight of the indium detector (in the form of a disc) was 25 g. The sample and the indium detector were exposed for 45 min and then the activity produced in the detector was measured with a scintillation γ counter. The sensitivity of the determination for a 5-g sample was about 0.015 % BeO.

In laboratory practice it was more convenient to count the neutrons directly.

In the apparatus designed for this variation, the source, sample, and paraffin moderator layer were arranged coaxially.

Elements with high capture cross sections for slow neutrons caused errors in the measurement results. To avoid these, a sample and standard were measured successively at layer thickness of 3, 8, and 15 mm and then the results obtained were extrapolated to zero layer thickness.

Limits of BeO concentration, %	Mean square error of separate determination, rel. %	Deviation from data of chemical analysis, rel. %
0,001—0,01	10—20	0—50
0,01—0,10	2—8	0—16
Above 0,10	1—4	1—8

The accuracy of the radioactivation method for the direct neutron counting variation may be assessed from the data presented in the table.

LITERATURE CITED

1. B. S. Aidarkin, G. V. Gorshkov, A. G. Grammakov, V. S. Zhadin, and A. G. Kolchina, Translations of the Radium Institute, 5 [in Russian] (Izd. AN SSSR, 1957) p. 89.
2. A. Gaudin, J. Dasher, J. Pannel, and W. Freyberger, Mining Engng. 187, 495 (1950).
3. A. Gaudin and J. Pannel, Analyt. Chem. 23, 1261 (1951).

Received December 12, 1958

RADIATION CHANGES OF SOME PHYSICAL PROPERTIES OF GRAPHITES WITH DIFFERENT DEGREES OF GRAPHITIZATION

Yu. N. Aleksenko and L. E. Kakushadze

On the basis of data from the work of V. I. Klimenkov and Yu. N. Aleksenko*, the authors of the present work arrived at the conclusion that the increase in volume observed during the neutron irradiation of graphite could be due to a reduction in size of the crystallites, i.e., degraphitization. To test this hypothesis, we irradiated six samples of graphite with different degrees of graphitization. Sample No. 1 was prepared from normal reactor graphite, graphitized at a temperature of about 2500°C, and sample No. 6 from sintered oil coke, which had been annealed but not graphitized. Each sample was a square-section block measuring 5 x 5 x 70 mm. Holes 0.3 mm in diameter were drilled through the blocks in the center and at distances of 5 and 10 mm from each end. These holes were used for the insertion of thermocouples and also current-carrying and potential leads for determining the electroresistance and the thermal conductivity of the samples. All six samples, inside a hermetically sealed aluminum container, were placed in the experimental channel of an RFT reactor.

The integral neutron flux was $6.2 \cdot 10^{20}$ neutrons/cm^2 at a flux rate of $(1.5 - 2) \cdot 10^{13}$ neutrons/cm^2 · sec. During the irradiation, the temperature of the samples was kept within the limits of 350 – 450°C so that after irradiation, the samples retained only the quite stable structural de-

*V. I. Klimenkov and Yu. N. Aleksenko, Session of the Academy of Sciences, USSR on the Peaceful Use of Atomic Energy (Meeting of the Div. Phys.-Mat. Sciences)(Izd. AN SSSR, 1955) p. 322.

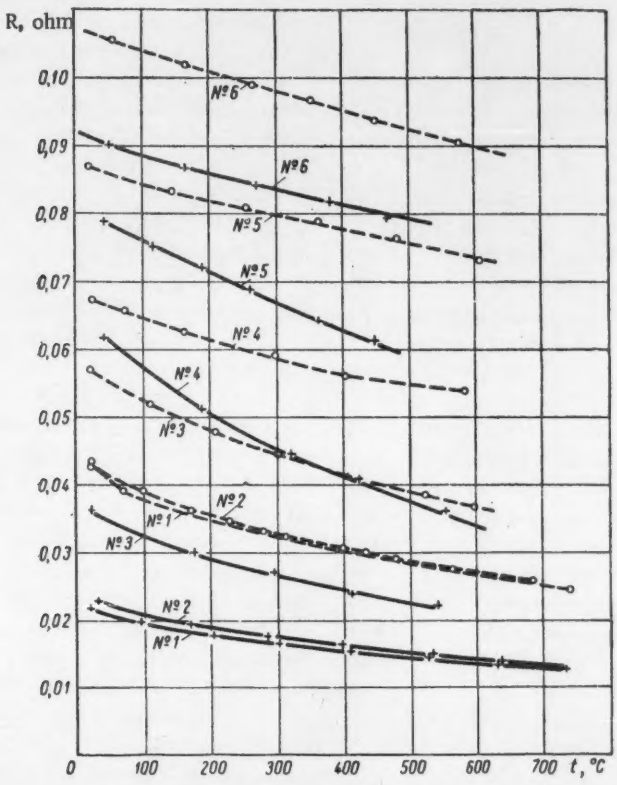

Fig. 1. Temperature dependence of electroresistance of graphite samples. Solid curves) before irradiation; dotted curves) after irradiation.

fects which interested us and whose annealing began at temperatures of not less than 500°C.

Before and after irradiation, the linear dimensions, electroresistance, and thermal conductivity of all six samples were determined. The linear dimensions were measured with a normal micrometer and the electrical resistance with a potentiometer. To prevent oxidation of the sample during determination of the temperature dependence of the electroconductivity, the sample was heated in a quartz ampule evacuated with a forevacuum pump. The temperature of the sample was measured with a Chromel-Alumel thermocouple and a PP-6 potentiometer. A PPTV-1 potentiometer was used to measure the potential drop across the sample. The thermal conductivity of the sample was determined by the temperature wave method. It was assumed that the thermal capacity of the graphite did not change during irradiation.

The results of measuring the linear dimensions of the samples are presented below:

Sample No.	Dimension, mm	
	before irradiation	after irradiation
1	70.21	70.22
2	70.07	70.06
3	69.43	69.56
4	69.74	69.75
5	70.60	70.60
6	70.05	70.04

These results show that an irradiation temperature of about 400°C, the volume of the graphite hardly changed (the specific elongation of the samples did not exceed 0.02 %).

Figure 1 shows the temperature dependence curves for the electroresistance of the samples before and after irradiation. From this figure it follows that absolute value of the extra resistance produced during irradiation was approximately the same for all six samples and that as was proposed, annealing of the additional resistance was not observed experimentally over the whole temperature range of the sample.

The changes in the slope of the curves shown on the graph cannot be explained as yet. It is shown that as regards electroconductance, graphite behaves as a semiconductor. This determines the strong dependence of the electroconductance on the presence of various impurities in the graphite. Graphites of different degrees of graphitization differ from each other not only in the dimensions of the crystallites but also in the content of foreign bodies, as refinement of the graphite proceeds simultaneously with its graphitization.

Figure 2 shows the temperature dependence curves of the thermal conductivity of samples No. 1, 3, 4, and 6 before and after irradiation.

Changes in the temperature dependence of the thermal conductivity of samples caused by irradiation appeared as a decrease in the sizes of regions with a homogeneous structure, and it was as if each sample had been displaced into a region of lower graphitization. (The curve for sample No. 1 after irradiation almost coincided with the curve for sample No. 3 before irradiation, and the same may be said of the curves for samples Nos. 3 and 4.) Here the relative change in the value of the thermal conductivity of less graphitized samples was less (for samples No. 1 and 3 at 100°C it was about 50%, whereas for sample No. 6 it was almost absent). The absolute change in the value of the thermal resistance ($1/\gamma$ in technical units) for samples No. 1, 3, and 4 was 0.009, 0.0137, and 0.010, respectively (for 100°C). The absolute change in the thermal resistance of sample No. 6 was difficult to assess since the accuracy of the thermal conductivity measurements was 10 % and the relative change in the thermal conductivity of sample No. 6 lay within these limits.

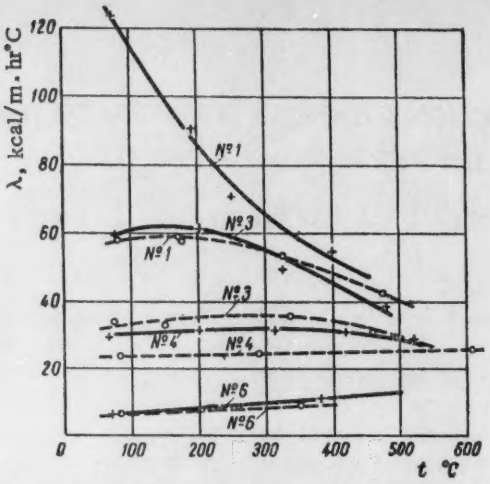

Fig. 2. Temperature dependence of thermal conductivity of graphite samples. Solid curves) before irradiation; dotted curves) after irradiation.

The results obtained make it possible to draw the following conclusions:

1. Within the limits of accuracy of the measurements, the absolute value of the change in electrical and thermal resistances of the samples caused by radiation destruction does not depend on the degree of graphitization. The relative change in the electroresistance and thermal conductivity is lower the less the graphitization of the samples.

2. Curves of the temperature dependence of the thermal conductivity show that radiation dislocations of the graphite crystal lattice act on the propagation of its thermal oscillations as constant scatterers like crystallite boundaries or foreign inclusions.

3. The mechanism of action of radiation dislocations on the electroconductivity of graphite is apparently determined by the appearance of additional electrical charge-carrier "traps" in the semiconductor (this idea is confirmed by the change in the Hall coefficient of irradiated graphite, which we observed previously).

4. The fact that in our experiment there was hardly any "swelling" of the samples gives grounds for surmising that this effect is caused by less stable radiation dislocations of the structure, which cannot be fixed in the irradiated graphite under the given temperature conditions.

The following should be noted. In the irradiation of graphite at room temperature, the "swelling" effect was found to be extremely stable and removed only by annealing at temperatures of about 2000°C. This indicates that in the experiment described, so-called radiation annealing was observed, this also leads to the fact that some dislocations of the crystal lattice by the simultaneous action of temperature and radiation are considerably less stable than those by the action of temperature alone.

Received December 12, 1958

TOTAL CROSS SECTION OF Np^{237} IN THE 2-10,000 ev ENERGY REGION

Yu. V. Adamchuk, S. S. Moskalev, and M. I. Pevzner

Data available in the literature on the behavior of the total cross section of Np^{237} are limited to the 0.01-5 ev energy region [1,2].

In 1956, the authors measured the total neutron cross section of Np^{237} in the 2.5-10,000 ev energy region. The measurements were carried out using two samples of NpO_2, 5.31 g/cm² and 0.702 g/cm² in thickness, containing 11.6 % Pu^{239}.

A mechanical selector was used in the work, in conjunction with the 80-channel time analyzer employed with the RPT reactor [3]. The mechanical shutter of the selector consists of two coaxial steel cylinders (l = 40 cm, R = 5 cm), each of which features six narrow radial slits distributed uniformly over the perimeter of the cylinders. The first cylinder, which functions as collimator, was fixed while the second cylinder, the rotor, was rotated by the action of compressed air. The radially diverging slits of the selector had a maximum width of 0.25 mm in the collimator and 0.5 mm in the rotor.

The flight path was 24.97 m, the critical speed of rotation of the rotor part was 25,000 rpm, and the maximum resolution achieved was 0.12 μ sec/m.

A train of seven BF_3 proportional counters (BF_3 enriched with B^{10}) 49.5 cm in length served as neutron detector (at operating pressure of 600 mm Hg). The efficiency of the detector, in recording neutrons with energies of 100 ev, was about 5 %.

NpO_2 powder (about 500 mg) was packed into special molds of aluminum foil, which were mounted in the slots between detachable plates of the container. The container had four slots, three of them with a thick and a thin sample of Np^{237} and a boron sample as a control. It was placed between the collimator and rotor parts of the selector during operation.

The neutron energy dependence of the total cross section of Np^{237} in the region of energies ranging from 2.7 ev to 10,000 ev may be seen in Fig. 1. In computing the cross sections, Pu^{239} impurity was neglected, and it was assumed that the chemical composition of the samples corresponded to the formula for $Np^{237}O_2$.

Resonance levels are manifested, in the energy dependence of the total cross section, at the following energies (ev):

3,86±0,02,	4,22±0,002,	4,90±0,02,	5,81±0,03,
6,43±0,04,	7,74±0,05,	8,43±0,06,	9,33±0,06,
11,06±0,08,	12,50±0,10,	14,63±0,12,	16,03±0,14.
17,1±0,2,	17,9±0,2,	18,9±0,2,	

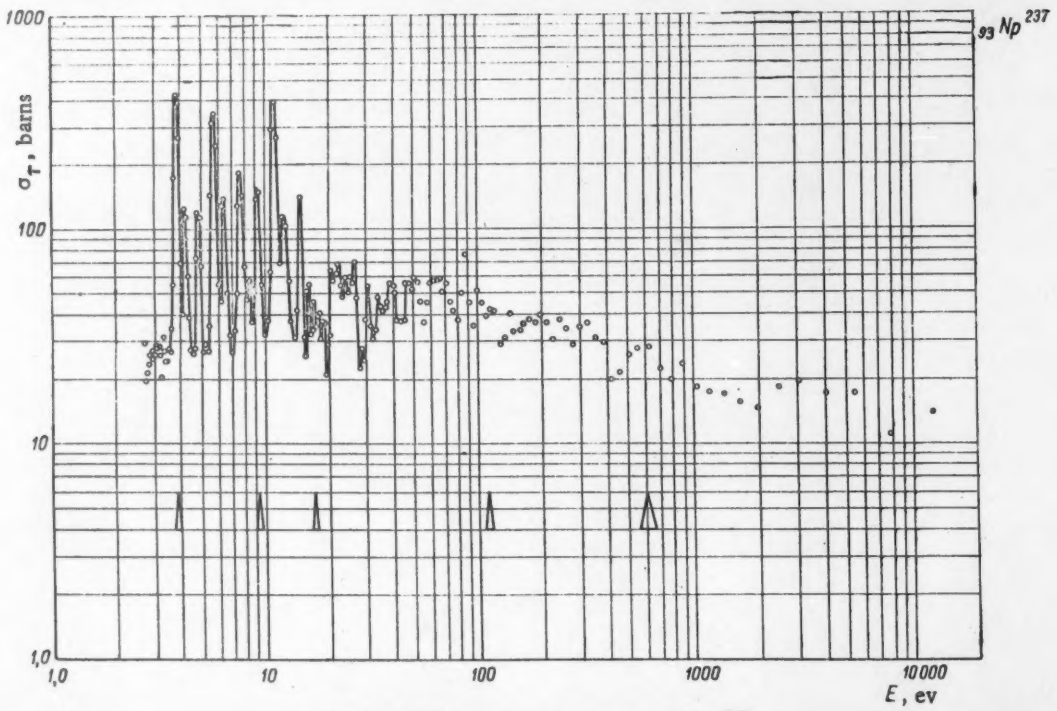

Fig. 1. Total neutron cross section of Np^{237}

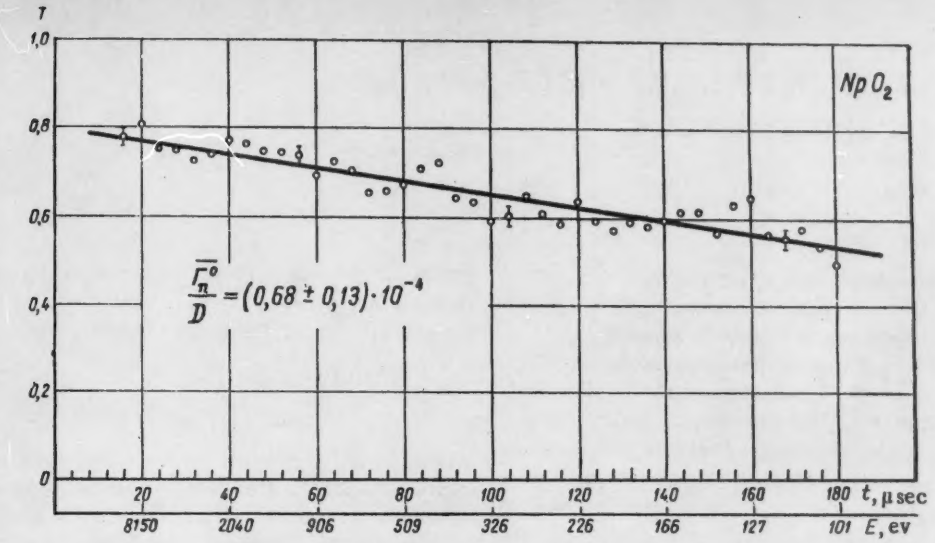

Fig. 2. Transmission curve for neptunium oxide.

The levels for energies of 7.74 and 11.06 ev may be explained by the presence of Pu^{239} impurity.

At high energies, groups of resonance levels appear on the scene. The average spacing between levels $\overline{D}$, obtained from our data in taking into account contributions [1,2], is 0.7 ev for both spin states.

Figure 2 shows the dependence of the transmission T in the region of poor resolution (100-12,000 ev) on the time of flight t. In that energy region, the resolution of the selector does not permit observation of discrete levels, and cross sections averaged over many resonances are therefore obtained from the experiment. The strength function $\overline{\Gamma_n^0}/D$, where $\overline{\Gamma_n^0}$ is the average spacing od neutron width, reduced to 1 ev, may be determined along the slope of the transmission curve [4,5]. The value of $\overline{\Gamma_n^0}/D$ obtained by this method for Np^{237} is

$$(0{,}68 \pm 0{,}13) \cdot 10^{-4}.$$

The value obtained for the total resonance integral of Np^{237}, $I = \int_{E_1}^{E_2} \sigma_t(E') \frac{dE'}{E'}$ over the range of 2.7-12,000 ev, obtained from the data on total cross section, is 360 barns.

LITERATURE CITED

1. Yu. V. Adamchuk, V. F. Gerasimov, B. V. Efimov, V. S. Zenkovich, V. I. Mostovoi, M. I. Pevzner, and A. A. Chernyshov, Materials of the International Conference on the Peaceful Uses of Atomic Energy (Geneva, 1955) 4, p. 1645.
2. M. Smith, R. Smith, E. Joki, and J. Evans, Phys. Rev. 99, 611 (1955).
3. V. I. Mostovoi, M. I. Pevzner, and A. P. Tsitovich, Materials of the International Conference on the Peaceful Uses of Atomic Energy (Geneva, 1955) 4, p. 1640.
4. D. Gayther and K. Nicholson, Proc. Phys. Soc. 70A, 51 (1957).
5. P. E. Nemirovskii, Dissertation [in Russian] (1956).

Received January 6, 1959

ON THE EXISTENCE OF LIGHT NUCLEI WITH LARGE NEUTRON OR PROTON EXCESS

A. I. Baz'

One of the consequences of charge independence is the existence of similar levels in isobaric nuclei (e.g., the levels of mirror-image nuclei or isobaric triplets). Such levels, observed in nuclei of like mass number A, but with different N and Z, exhibit identical properties (momentum, parity, isotopic spin, etc.), and the energies of two similar states of isobaric nuclei are distinguished solely by the Coulomb energies of the nuclei and the neutron and proton masses:

$$\Delta E(Z_1, Z_2) = [E_{coul}(Z_1) - E_{coul}(Z_2) + (Z_2 - Z_1)\cdot 0{,}78] \text{ Mev.} \quad (1)$$

Here $\Delta E(Z_1, Z_2)$ is the difference in energies of the two isobaric nuclei with charges Z_1 and Z_2 found in similar states, $E_{coul}(Z)$ is the Coulomb energy of a nucleus of charge Z, and 0.78 is the difference between the mass of the neutron and proton. Equation (1) usually serves to determine the Coulomb energies of different nuclei. It is possible, however, to reverse the problem in terms of the known energy of a single nucleus by using (1) to determine the energy of a second isobar existing in a similar state. This approach was used by the author to compute the ground state energies of several light-element isotopes exhibiting proton or neutron excess. The outsome was that in the region $A \leq 40$ there must exist a large number of still undiscovered β-active nuclei which are stable with respect to emission of nucleons. The findings are reported below. The reviews of Ajzenberg and Lauritsen, and of Endt and Kluyver, [1,2], were utilized in the calculations. In determining the difference between the Coulomb energies of two nuclei of charges Z and Z + 1, we used the formula

$$E_{coul}(Z+1) - E_{coul}(Z) = 1{,}214\,\frac{Z}{A^{1/3}} \text{ Mev} \quad (2)$$

based on data dealing with mirror-image nuclei.

Nuclei with Z − N = 2. In the region $A \leq 40$, it is found that there must exist the following not yet discovered β^+-active nuclei:

Nucleus	Maximum energy of positron decay, E_{max}	Half life τ, sec
Ne^{18}*	3.2	3
Mg^{22}	4.2	5
Si^{26}	3.7	10
S^{30}	4.2	5
A^{34}	4.5	0.5
K^{36}	10.7	3
Ca^{38}	4.8	1

Let us analyze, the case of isobars with A = 18. There are two nuclei known with A = 18: the F^{18} and O^{18} nuclei. In the first, we find that N = Z and the ground state has isotopic spin T = 0, in the second, N = Z + 2 and the ground state has T = 1. The difference in energies is

$$E(O^{18}) - E(F^{18}) = (E_{T=1} - E_{T=0}) + \\ + (E_{coul}(8) - E_{coul}(9)) + 0{,}78,$$

where $(E_{T=1} - E_{T=0})$ is the excitation energy of the first level with T = 1 in the F^{18} nucleus (this level is similar to the ground state of O^{18}), whereas the second and third terms take into account the difference in the Coulomb energies of those nuclei and the difference in neutron and proton mass. Utilizing (2) and the mass difference $E(O^{18}) - E(F^{18})$ known from empirical evidence to be about 1.67 Mev, we arrive at $E_{T=1} - E_{T=0} = 1$ Mev. At the same time, if there exists a nucleus Ne^{18}, in which Z = N+2 and the ground state of which must have T = 1, then the energy of that nucleus will be

$$E(Ne^{18}) - E(F^{18}) = (E_{T=1} - E_{T=0}) + \\ + (E_{coul}(10) - E_{coul}(9)) - 0{,}78.$$

Substituting into the above the value of $(E_{T=1} - E_{T=0})$ obtained earlier and utilizing (2), we arrive at $E(Ne^{18}) - E(F^{18}) = 4{,}2$ Mev. We must now verify whether this nucleus is stable with respect to disintegration into heavy particles. With the viewpoint of energy gain, it would appear most likely to favor proton emission, i.e., the decay mode $Ne^{18} \rightarrow F^{17} + p$, but this process is however impossible from an energetic standpoint. We thereupon conclude that the sole mode of decay of Ne^{18} is β^+ decay in the form $Ne^{18} \rightarrow F^{18} + \beta^+$. The maximum energy of positron decay is readily determined from the mass difference of Ne^{18} and F^{18}. The half life may also be estimated. Decay will proceed for the most part with the formation of the first excited state F^{18} with T = 1, since log ft for that transitio.. (a superallowed transition) must equal 3.5. Using this value of ft and the known energy of decay, the half life $\tau \approx 3$ sec. The remaining data were obtained analogously.

Nuclei with Z − N = 3. The existence of the following β^+-active nuclei, with Z − N = 3, is possible:

Nucleus	E_{max}	Nucleus	E_{max}
Ne^{17} ?	13.6	S^{29}	12.4
Na^{19} ?	10	Cl^{31} ?	10.5
Mg^{21}	8.3	A^{33}	9.8
Al^{23} ?	11.1	K^{35} ?	10.4
Si^{25}	11.1	Ca^{37}	9.8
P^{27} ?	11.5	Sc^{39} ?	11.5

*This isotope was discovered rather recently.

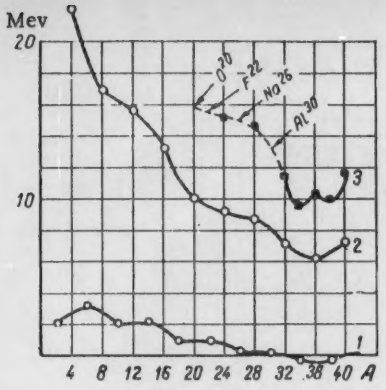

a

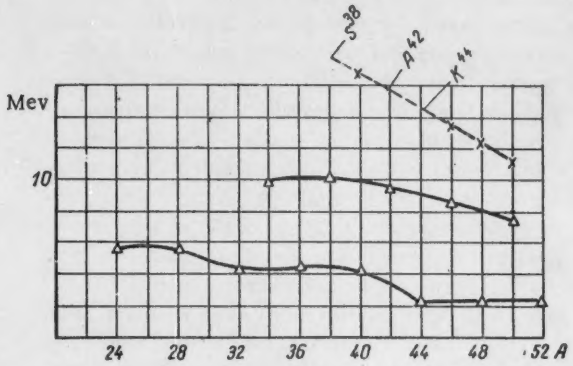

b

Fig. 1. Differences in energy levels with different isotopic spin. a: O) differences in energies of first states with T = 1 and T = 0; □) differences in energies of first states with T = 2 and T = 0, b: ×) differences in energies of first states with T = 3 and T = 1; Δ) differencies in energies of first states with T = 2 and T = 1.

The half lives of all of those nuclei $\tau \approx 0{,}1$ sec. The question of the decay of those nuclei to heavy particles is more complex than was the preceding case, since the binding energy of the proton in most of the nuclei (marked by a question mark) is very small (0.5 – 1.5 Mev), which is about equal to the precision with which the energies of those nuclei are known. It may turn out, therefore, that some of the nuclei, marked by the question marks, are actually unstable to decay with proton emission.

Nuclei with N – Z = 4 and with N – Z = 6. In addition to nuclei with proton excess, there exist several still unknown isotopes of light elements with large neutron excess. It is possible to establish their energy values on the basis of the following considerations.

By making use of data presently known on the binding energy of light nuclei, we may construct curves on which the differencesin energies of lower-lying levels with isotopic spins T = 0, 1, 2, 3... for nuclei with even mass numbers A are plotted (see Figure) [3]. The smooth slope of the curves obtained in that manner (solid lines) allows extrapolation of the curves to regions where experimental data are as yet not available (the extrapolated sections of the curves are drawn in the form of a dashed line). This extrapolation serves to predict the binding energies of several isotopes not yet discovered. Curve 3 (Figure a), for example, makes it clear that in nuclei with mass number A = 30, the first state with T = 2 must lie approximately at 13.7 Mev above the first state with T= 1; to the first level with13.2 Mev T = 0 in a system of 30 nucleons, there corresponds the ground state of the nucleus P^{30}(N= Z), to the first level with T= 1, there corresponds the ground state of the nucleus Si^{30} (N – Z = 2), and, finally, we have corresponding to the first level with T = 2, the ground state of the nucleus Al^{30}(N – Z = 4). This requires, in order to find the actual difference in the energies of the Al^{30} and Si^{30} nuclei, taking the difference in Coulomb energies and the difference in neutron and proton mass into account.

It is then found that the total energy of Al^{30} is greater than the energy of Si^{30} by approximately 9 Mev. It is readily appreciated that the Al^{30} nucleus is stable to decay into heavy particles and that Al^{30} must consequently be a β emitter. The energies of decay of several other isotopes were evaluated in similar fashion, and are presented below:

Nucleus	E_{max}	τ, sec	Nucleus	E_{max}	τ
O^{20}	4.3	5	S^{38}	3	1 min-1 day
F^{22}	12	0.1	A^{42}	0.5	–
Na^{26}	11.3	0.1	K^{44}	6.3	–
Al^{30}	9	1			

It is known that some of these isotopes exist (e.g., A^{42}, K^{44}). The curves in Figure a permit determination of the energy of their ground states.

Concluding remarks. The energies of the nuclei are probably determined to an accuracy not inferior to ± 1.5 Mev, since it would be difficult to fall into a larger error in the evaluation of the Coulomb energies and in the extrapolation of the curves plotted. The esimate of the half lives was made arbitrarily, and errors of up to 10 times in either direction are possible here.

Isotopes with proton excess are apparently obtained with greater ease by (p,n) reactions or (He^3,n) reactions. The threshold of the former is of the order ot 10 Mev, while the threshold of the latter is appreciably higher. The most convenient reaction for producing isotopes with neutron excess is the reaction (t,p). The threshold of this reaction is, as a rule,very low. In addition, all isotopes referred to in this discussion must be formed by bombarding the corresponding nuclei with higher-energy particles: such reactions as (p,3p), (p,2n), (α,2p), etc.

LITERATURE CITED

1. F. Ajzenberg and T. Lauritsen, Rev. Mod. Phys. 27, 77 (1955).
2. P. Endt and J. Kluyver, Rev. Mod. Phys. 26, 95 (1954).
3. A. Baz' and Ya. Smorodinskii, Uspekhi Fiz. Nauk. 55, 236 (1958).

Received January 6, 1959

DETECTION OF SLOW NEUTRONS BY THE CAPTURE γ-RAYS OF CADMIUM DURING MEASUREMENTS OF THE MOISTURE CONTENT OF ORGANIC AND INORGANIC SOILS BY THE NEUTRON METHOD

V. A. Emel'yanov and V. E. Nesterov

The neutron method of measurement of the moisture content of organic and inorganic soils is the only method which provides an absolute measurement in situ, since the main moderator of fast neutrons in these soils is hydrogen, the content of which is almost entirely accounted for by moisture. Therefore, this method attracted the attention of many investigators as soon as sources of fast neutrons suitable for work under field conditions became available.

In choosing the means of detection of slow neutrons for investigations under field conditions, it is necessary that the radiometer be compact and work from a battery supply, and the neutron source should be of the least possible intensity. The method used in previous experiments for detecting slow neutrons was that of activating foils (silver, rhodium, and indium) and measuring the induced activity with Geiger-Muller counters [1-3]. However, it became necessary to use neutron sources of fairly large activity, because of the ineffective neutron counting of the activiation method. Because of this, and also due to the poor operation of the moisture measurements with respect to slow neutron detection by the foil activation method, a preference began to be shown in later work for the use of proportional boron counters [4]. Nevertheless, the awkward size of the radiometers with such counters (an amplifier with a gain of the order of 10,000, a discriminator, and a counter supply voltage of about 1500 v are required) makes their application under field conditions quite difficult.

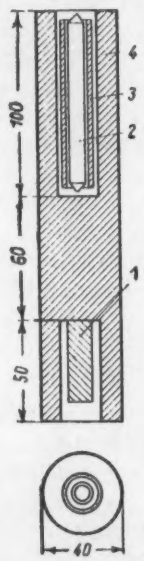

Fig. 1. Diagram of the Apparatus. 1) Source; 2) counter; 3) cadmium shield; 4) lead (dimensions in millimeters).

In order to use radiometers with Geiger-Muller counters, a means of slow neutron detection which involves the γ rays formed in the (n, γ) reaction in cadmium is incorporated in the present work.

The device involved an STS-1 or STS-5 halogen counter with a detachable shield made of sheet cadmium 0.5 mm thick, and a Po-Be fast neutron source of about 106 neutr/sec which was distributed in a cylindrical lead shield (Fig. 1) and which shielded the counter from the effect of the direct and scattered γ rays emanating from the Po-Be source. By measuring the γ-ray intensity with the cadmium shield and without it, it is possible to distinguish the contribution of the capture γ radiation from the cadmium shield (the "cadmium difference"). The value of the cadmium difference is proportional to the slow neutron density at the point of measurement.

Tests of the apparatus were made under both laboratory and field conditions. The pulses from the counter were recorded by an ordinary compact battery radiometer with a cold-cathode thyratron conversion circuit. The laboratory measurements were made in cylindrical containers of ϕ 30 cm and depth 30 cm loaded with inorganic argillaceous soil. The device was introduced into a vertical hole. Since the container with the soil was not infinite (with regard to the slowing of the neutrons), the counting rate in the laboratory experiments was less than in the field tests. The field tests employed inorganic argillaceous bank soils and residual organic sandy soils. The diameter of the sampling holes was 5 cm. As a control, an SNM-5 proportional boron counter was used with a specially constructed field radiometer using 1K2 P tubes (cathode follower, amplifier, and discriminator) and MTKh-90 thyratrons (conversion decade circuit). The source was fastened to the end of the aluminum counter tube.

In order to determine the intensity which is recorded by the device of the direct and scattered γ-radiation from the Po-Be source, this source was replaced by Cs^{137} with the same γ activity.

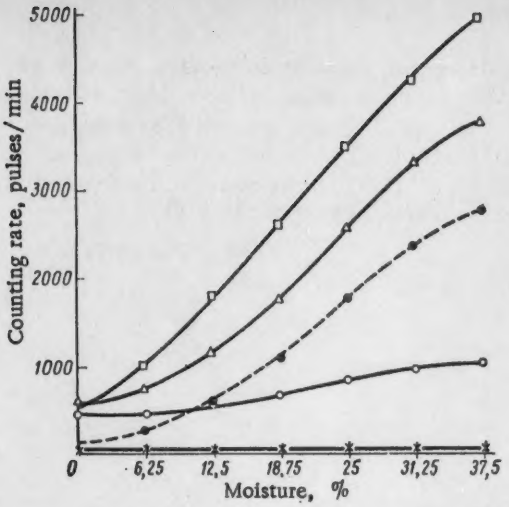

Fig. 2. Counting rate as a function of organic soil moisture (laboratory test). ▭ -SNM-5 boron counter; Δ-STS-5 with cadmium shield; O-STS-5 without shield; O "cadmium difference"; ✳ -background + γ rays from Cs^{137}

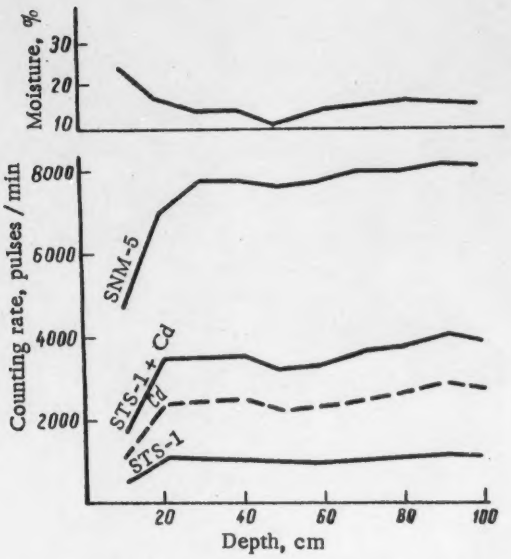

Fig. 3. Results of the field test of the apparatus (inorganic sandy argillaceous soil).

The results of the several experiments displayed in Figs. 2 and 3 show that the regularity of the changes in the counting rate as a function of the moisture in the detection of neutrons for both cadmium difference and proportional boron counter is the same. The sensitivity to moisture changes, i.e., the ratio of the counting rate for a moist medium to that for a dry medium, is higher in the first case. The intensity of the recorded direct and scattered γ radiation is low from the Po-Be source (no higher than background) in which the scattered radiation intensity depends only slightly on changes in the natural density and moisture of sandy and argillaceous organic and inorganic soils.

In the parallel tests in which three STS-5 counters were used in the apparatus, the effective counting of slow neutrons by the cadmium difference and the proportional boron counter were comparable, although the package of these counters was considerably smaller than the SNM-5 boron counter (the diameter and length of the package were 2.5 and 11 cm, while the corresponding dimensions of the boron counter were 3.5 and 30 cm). The nearness of the neutron source to the detector due to the decrease in the thickness of the lead between them increases the counting rate and the sensitivity to moisture changes.

The apparatus described was intended for the testing of a still simpler and more effective means of measuring moisture content in soils, in which it is sufficient to determine only the counting rate for a shielded cadmium counter. Such a detector records the capture γ radiation from the cadmium shield, hydrogen, and other elements in the inorganic soils, and from the lead shield combination of n-n and n-γ processes). The direct and scattered radiation from the Po-Be source, as was already indicated, has no effective value for the present apparatus. For inorganic soils whose moisture content is greater than ~ 5% (a smaller moisture content under natural conditions occurs only in sand), the main portion of this capture radiation is due to the cadmium shield; a smaller (and, moreover, always constant) share is due to the lead shield, whereas a still smaller part (for small moisture contents of the soils) comes from the hydrogen which is contained in them. Under conditions of high moisture, the intensity of the capture γ radiation from the hydrogen is greater than that from the lead shield. The portion of the capture γ radiation emitted by the other elements in the soil is small and depends only slightly on the density according to the data of the experiments carried out and an analysis of the chemical composition of the inorganic soil.

The results of the preliminary investigation of the method of simultaneous n-n and n-γ samplings show that it can be recommended for field testing on sandy, argillaceous, clayey organic and inorganic soils, and moist sands.

The authors express their gratitude to E. G. Petrov for a discussion of the results obtained, and to V. P. Izmailov for his assistantance in making the measurements.

LITERATURE CITED

1. J. Spinks, D. Zane, and B. Torchinsky, Canad. J. Technol. 29, 371 (1951).

2. D. Zane, B. Torchinsky, and J. Spinks, Engng. J. 36, 1 (1953).

3. P. Mortier and M. DeBoodt, Netherlands J. Agr. Sci. 4, 111 (1956).
4. W. Gardner and D. Kirkham, Soil Sci. 73, 391 (1952), J. Stone, D. Kirkham, and A. Read, Soil Sci. Soc. America Proc. 19, 419 (1955), J. Sharpe, Brit. J. Appl. Phys. 4, 93 (1935), C. Van Bavel, E. Hood, and N. Underwood, Trans. Amer. Geophys. Union 35, 595 (1954), J. Holmes, Austral. J. Appl. Sci. 7, 45 (1956), C. Van Bavel, N. Underwood, and R. Swanson, Soil Sci. 82, 29 (1956), G. Stewart and S. Taylor, Soil Sci. 83, 151 (1957), L. Stolzy and G. Cahoon, Soil Sci. Soc. America Proc, 21, 571 (1957).

Received January 8, 1959

MEASUREMENT OF THE HARD PORTION OF THE NEUTRON SPECTRUM IN A BR-5 REACTOR BY USE OF AN IONIZATION CHAMBER CONTAINING He^3

A. I. Abramov and M. G. Yutkin

A small-sized spherical ionization chamber filled with a mixture of He^3 and A* was used to measure neutron spectra in a BR-5 reactor with an active zone of plutonium oxide and a nickel shield [1]. As is known, a considerable part of the fast neutron spectrum of reactors belongs in the interval of energies from 100 to 1000 kev, in which the measurement of neutron energies by proton recoil yields low accuracy. The use of a time-of-flight method in this case is quite complicated due to the difficulty of gaining access to the inside of the reactor; in addition, such experiments as the investigation of the distribution of the various groups of neutrons along the length of a certain channel cannot generally be carried out by this method.

The use of He^3 for spectrometric investigations of fast neutrons has been described in a manner of articles [2-6]. Provided there is no amplitude distortion of the pulses from the chamber or the counter containing the He^3, the energies of the incident neutrons are completely determined. However, because of the influence of wall, induction, and other effects, the well-defined connection between the pulse amplitudes and neutron energies is broken, which leads to considerable difficulty in analyzing the experimental results. In addition, if the investigated spectrum contains neutrons with energies higher than 1 Mev, then it is necessary to consider the pulses from the recoils of helium atoms in deciphering the curves which are derived.

In the present work, an ionization chamber together with the cascade of a preliminary amplification were placed in one of the reactor channels. The spectrum of the pulses from the chamber was measured with a single-channel analyzer. The channel width of the analyzer corresponded in most cases to an energy interval of 200 kev for the neutrons being counted. In order to make a more accurate analysis of the experimental data, spectra were taken of the pulses from monochromatic neutrons with energies which corresponded to the mean of the selected energy intervals. The curves which were obtained with the basic measurements were graphically decomposed into these spectra. All distortions of the spectrum originating in the ionization chamber were thus automatically taken into account.

Distributions of different groups of neutrons were recorded (starting at 125 kev and higher) along the length of the loop channel and passing through the active zone of the reactor, and also along the length of the oscillator channel passing at a distance of 430 mm from the center through the nickel shield. The lower boundary of the energy region being investigated is determined by the finite resolving power of the chamber. The data obtained enable one to obtain neutron spectra for every point of these channels. As an example, the figure shows

*A description of the chamber will be published in "Pribory i Tekhnika Éksperimenta".

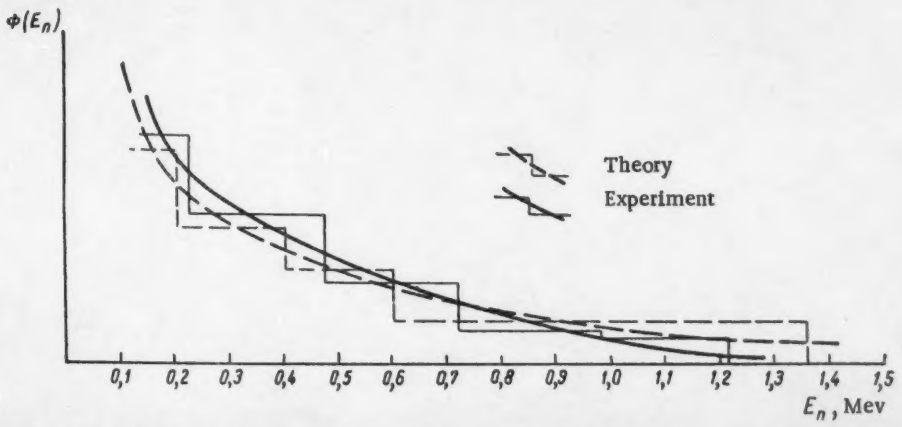

Comparison of experimental and calculated neutron spectra in the shield of a BR-5 reactor. On the vertical axis: neutron flux per unit energy interval, arbitrary units; on the horizontal axis: neutron energy, Mev.

a histogram (the fine unbroken line) of the neutron spectrum taken in the oscillator channel opposite the center of the active zone. The dashed line in the same figure shows the result of a 9-group calculation. The smooth curves (continuous and dashed, respectively), which were constructed according to the histogram, show that the spectrum in the reactor shield turned out to be much softer than expected. As is evident from the figure, the number of neutrons in the oscillator channel with energies above 1 Mev is relatively small; it was, therefore, possible in this case to neglect the distortions introduced by the recoiling helium atoms.

The recoiling helium atoms introduce an essential contribution to the pulse spectrum. In the present investigation, their role was taken into account theoretically with the aid of data on the cross sections for He^3 from [7]; however, due to lack of time during the period of the physical operation of the BR-5 reactor, these measurements could not be carried out with sufficient statistical accuracy, and they will, therefore, be repeated after the end of the servicing period.

The authors thank O. D. Kazachkovskii and Yu. Ya. Stavisskii for a number of valuable opinions and hints, and also V. N. Andreev for help in the analysis of the experimental results.

LITERATURE CITED

1. A. I. Leipunskii et al., "Fast neutron experimental reactors in the Soviet Union," Report No. 2129, presented at the Second International Conference for the Peaceful Uses of Atomic Energy (Geneva, 1958).
2. J. Coon, Phys. Rev. 80, 488 (1950).
3. R. Batchelor, Proc. Phys. Soc. A65, 674 (1952); A68, 452 (1955).
4. R. Batchelor, R. Aves, and T. Skyrme, Rev. Sci. Instr. 26, 1037 (1955).
5. R. Batchelor and H. Hyder, J. Nuclear Energy 3, 7 (1956).
6. N. P. Glazkov, Pribory and Tekh. Éksp. No. 4, 96 (1957).
7. D. Hughes and R. Schwartz, Neutron Cross Sections (McGraw-Hill, N. Y., 1958).

Received January 8, 1959

YIELDS OF Ru^{103} AND Ru^{106} ON FISSION OF U^{235} AND Pu^{239} BY FAST NEUTRONS

M. A. Bak, S. S. Bugorkov, T. A. Il'inskaya, Yu. G. Petrov, K. A. Petrzhak, V. M. Solntsev, A. V. Sorokina, and V. N. Ushatskii

This paper describes radiochemical methods used to determine the yields of isotopes Ru^{103} and Ru^{106} on fission of U^{235} and Pu^{239} by fast neutrons.

The yields of Ru^{103} and Ru^{106} were found by comparing the yield of Mo^{99} found earlier*. Uranium oxide with 90% U^{235} content and plutonium oxide were compacted separately into aluminum cartridges. The cartridges were wrapped in 1 mm thick cadmium foil and were placed in aluminum cups filled with boron carbide. The density of the charge was 1.4 g/cm^3. The layer of boron carbide surrounding the cartridge on all sides, and 2 cm thick, brought about practically complete absorption of neutrons of energies up to 10 ev. Two uranium samples and four plutonium samples were prepared.

The samples were bombarded in the central channel of the heavy water reactor of the Academy of Sciences of the USSR for 52.2 hr. The reactor power was held constant during the irradiation. The irradiated channel was filled with water. Under those conditions, the neutron spectrum was softer then the neutron fission spectrum. Though the ratio of the number of neutrons with energies $E_n > 1.5$ Mev to the number of neutrons with energies $E_n > 2.5$ Mev is 1.8 for the fission spectrum, this ratio became 4 ± 1.5 under the conditions of the experiment.

The bombarded samples of uranium and plutonium were dissolved, and the ruthenium and molybdenum produced were isolated chemically.

Molybdenum was isolated with high yield (about 80 mg) of inactive carrier by the α-benzoinoxime method. Ruthenium was isolated with a small amount of carrier (about 8 mg) by multiple distillation.

In fissioning uranium and plutonium, the two ruthenium isotopes Ru^{103} and Ru^{106} were produced, with the daughter products Rh^{103} and Rh^{106}, respectively, being found in equilibrium with them.

Drops of a solution of known weight, containing the four isotopes mentioned, were placed on a thin organic film (about 3 μg/cm^2) and left to dry. The thickness of the sources so prepared did not exceed 20 μg /cm^2. The activity of the sources was later measured in a 4π -counter.

A separate determination of the activities of Ru^{103}, Ru^{106}, Rh^{103}, and Rh^{106} was carried out with the aid of aluminum filters. It is known that the critical energy of the β spectrum of Ru^{106} is 39.2 kev, whereas the energy of the very strongly converted metastable transition Rh^{103} is 40 kev. Thus, the aluminum filter of 3 mg /cm^2 thickness succeeds in fully absorbing the electron emissions of Ru^{106} and Rh^{103}, and passes only the β emissions of Ru^{103} and Rh^{106}.

The radiation emitted by Ru^{103} shows a complicated β spectrum, but the spectrum is basically soft. Thus, 89.3% of the β particles have a cutoff $E_{max} = 220$ kev; 7% have $E_{max} = 105$ kev; 0.7% have $E_{max} = 390$-455 kev; and 3% have $E_{max} = 702$ kev.

The complicated β spectrum of Rh^{106} has a rather hard cutoff. The cutoff energy of the softest component of the spectrum is about 900 kev. Filters of different thickness may therefore be resorted to, to estimate the activity introduced by each of those two isotopes, by way of determining Ru^{103} activity directly, and determining Ru^{106} activity in terms of the activity of its daughter product Rh^{106}. The number of impulses N_3 and N_{60} recorded by the 4π -counter from the preparation covered over by filters of 3 mg/cm^2 thickness and 60 mg/cm^2 thickness, respectively, may be expressed in terms of the absolute β activity of those isotopes $N(Ru^{103})$ and $N(Rh^{106})$:

$$N_3 = k_3 N(Ru^{103}) + k'_3 N(Rh^{106}),$$
$$N_{60} = k_{60} N(Ru^{103}) + k'_{60} N(Rh^{106}),$$

where k_3, k'_3, k_{60}, k'_{60} are coefficients defining the fraction of Ru^{103} and Rh^{106} emissions transmitted through the filters used. It was shown experimentally that the background of

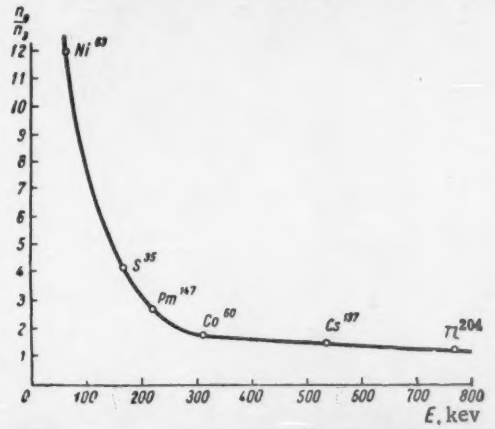

Absorption of β emission of reference preparations covered by filter of 3 mg/cm^2 thickness, plotted versus cutoff energy of their β spectra.

*The results of measurements of the Mo^{99} yield upon fission on U^{235} and Pu^{239} will be published subsequently.

Fissionable isotope	$\frac{Ru^{103}}{Mo^{99}}$	Ru^{103}, %	$\frac{Ru^{106}}{Mo^{99}}$	Ru^{106}, %	$\frac{Ru^{103}}{Ru^{106}}$
Pu^{239}	1,03	5,7±1,0	0,839	4,6±0,8	1,24
U^{235}	0,50	3,2±0,6	0,111	0,71±0,12	4,51

γ rays could be safely neglected in measurements using the filters in 4π-counters. The values of coefficients k_β, k'_β, k_{60}, and k'_{60} were obtained experimentally. Coefficients $k'_\beta = 0.99$ and $k'_{60} = 0.87$ were found from the absorption curve of the β radiation of pure Ru^{106} isotope and the daughter isotope Rh^{106} existing in equilibrium with it. The absorption curve was taken in a 4π-counter with filters of from 3 kg/cm² to 70 mg/cm² thickness.

Since the β spectrum of Ru^{103} is basically a soft spectrum, extrapolation of the absorption curve of β emission of Ru^{103} to zero filter thickness is somewhat difficult. Coefficient k_β was therefore computed by taking into account the decay scheme† from the experimentally obtained relation: the absorption of β emission in aluminum of 3 mg/cm² thickness to the cutoff energy of the β spectrum.

The relationship so arrived at is presented in the figure. The ratio of the number of β particles recorded in the 4π-counter without a filter (n_0) to the number of particles recorded with a filter of 3 mg/cm² thickness in use (n_3) is plotted along the ordinate, the cutoff energy of the simple β spectrum is plotted along the abscissa. The effective ratio n_0/n_3 obtained on the basis of that curve for the complex β spectrum of Ru^{103} is 3.00 ± 0.06. Accordingly, k_β = = 0,333.

The coefficient $k_{60} = 0.0057$ is determined solely by the hard component (E_{max} = 702 kev) of the β spectrum of Ru^{103}. The fraction of that radiation passed through a filter of 60 mg/cm² thickness was determined on the basis of absorption of β emissions of Tl^{204}, having a similar cutoff energy for the β spectrum (E_{max} = 766 kev).

Thus, of the two equations for N_β and N_{60}, $N(Ru^{103})$ and $N(Rh^{106}) = N(Ru^{106})$ may be determined in the preparation, and the absolute activities of Ru^{103} and Ru^{106} may be found in the sample according to the usual formulas, toward the end of the irradiation. The amount of ruthenium in 1 g of solution was determined by optical means.

The absolute β activity of Mo^{99} was determined by measuring the β activity of thick preparations (pellets of $PbMo_4$, weighing 40 mg, on a lead block) by means of a lead-window end-window counter, graduated according to a reference source. The references for that case were thin preparations of Mo^{99} transferred to a thin film, the absolute activity of the preparations being assayed either in a 4π-counter or with an end-window counter with a window thickness of from 5 μg/cm² to 10 μg/cm². To graduate the end-window counters, the previously measured standard was dissolved and reprecipitated by addition of a large quantity of carrier in the form of $PbMo_4$. The precipitate was dried out and pellets weighing 40 mg were prepared from the precipitate, the activity of the pellets being assayed on an end-window counter.

The relative and absolute yields of Ru^{103} and Ru^{106} are given in the Table.

In the calculations, the following values were assigned for the quantities used: Mo^{99} yield on fission of Pu^{239} was (5.5 ± 0.4)%, and on fission of U^{235} (6.4 ± 0.4 %); half life of Ru^{103}: 39.8 days; half life of Ru^{106}: 1 year, and of Mo^{99}: 68.3 hr.

Received December 22, 1958

† B. S. Dzhelepov and L. K. Peker, Decay Schemes of Radioactive Nuclides (Izd. AN SSSR, 1957).

NEUTRON ENERGY DEPENDENCE OF REMOVAL CROSS SECTIONS OF H_2O, B_4C, C, Fe, and Pb

D. L. Broder, A. A. Kutuzov, and A. P. Kondrashov

Up to the present time, a few papers devoted to the study of removal cross sections of fast neutrons for different elements have been published [1-4]. The method of removal cross sections attracts attention owing to the fact that it makes it possible to design shielding consisting of a mixture of water and various elements with comparative ease and accuracy.

The essence of the method consists in finding the effective cross section of an element equivalent to the absorption cross section for fast neutrons. This effective cross section, known as the removal cross section, includes a part of the elastic scattering cross section (that part which contributes large-angle scattering of neutrons i.e., which increases the path of the neutron in the shielding material), plus the cross section of all processes leading to neutron absorption. Inelastic scattering introduces an important contribution to the process of removing neutrons since it is more isotropic in character than elastic scattering, and, in addition, as a result of that process, large losses in neutron energy occur. Naturally, the removal cross section may be varied, depending on the neutron energies, in view of the inconstancy of the elastic and inelastic scattering cross sections and variations in the angular distributions of the scattered neutrons.

In [1-4], the removal cross sections of several substances for neutrons of the fission spectrum and neutrons of initial energy E_n = 2.9 and 6.7 Mev were measured. The fast-neutron removal cross sections at energies E_n = = 4 and 14.9 Mev may be found from an analysis of the findings in [5,6] for several substances (see Table). It must be duly noted that the removal cross sections for Fe, computed on the basis of the findings reported in [5,6], may be lowered by 5-10 %. This is because the experiments described in [5,6] were conducted for uniform water-steel mixtures of not less than 800 mm in thickness.

The removal cross section approach is usually employed in designing hydrogen-containing media, since the energy dependence of the cross section of hydrogen and the large amount of neutron energy spread in response to scattering by hydrogen best satisfy the basic assumptions underlying the approach.

If we abstract from the question of the accumulation of low-energy neutrons, we may attempt to carry over the technique of utilizing the removal cross section to media containing other light elements in place of hydrogen.

The fast-neutron removal cross sections for the neutron energy range of 4 to 14.9 Mev were measured for water, boron carbide, iron, and lead in the present research. Instead of the water usually used in such experiments as the basic component, boron carbide was employed. The neutrons were obtained from the D(d,n) He^3 and T(d,n) He^4 reactions.

The experimental arrangement consisted of tanks of cylindrical design 100 cm in diameter and of a total thickness of 115 cm in the direction of the deuteron beam, with a charge of boron carbide (Fig. 1). The density of the boron carbide charge was 1.1 g/cm^3. The neutron source was placed inside the first tank in a special channel, and lined up adjacent to the wall of the second tank. The third tank served as spare. For measurements of the removal cross sections, the samples investigated replaced the source. Radial channels in the tanks accomodated particle detectors. Channels not used to house detectors were filled with thin-walled duralumin cylinders charged with boron carbide. A fission chamber with Th^{232} (fission threshold of 1.1 Mev) served as fast-neutron detector. The samples investigated were stacks of Cm-3 plates of 9 cm over-all thickness and lead plates of 9 cm and 18 cm over-all thicknesses. Water poured into the tank to a layer thickness of 9.6 cm was also investigated. The dimensions of the plates were 70 x 100 cm. The diameter of the tank with water was 100 cm. Results of the measurements are shown in Fig. 2 and in the Table.

Figure 2 shows data of measurements adduced by various authors and the results of analysis of data presented in [4], in addition to our data. The authors of [4] reported curves of the removal cross section for iron and carbon as a function of distance separating neutron source and detector immersed in the water. The dependence of the

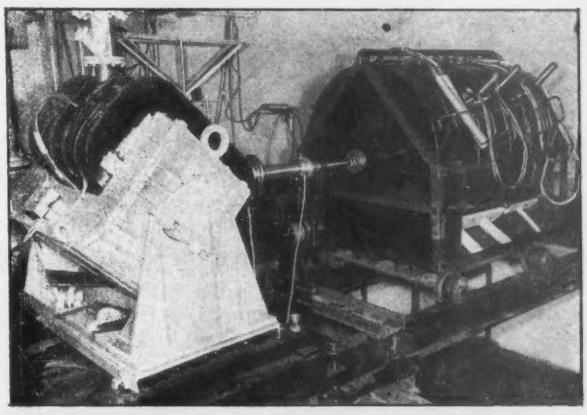

Fig. 1. General view of the experimental arrangement.

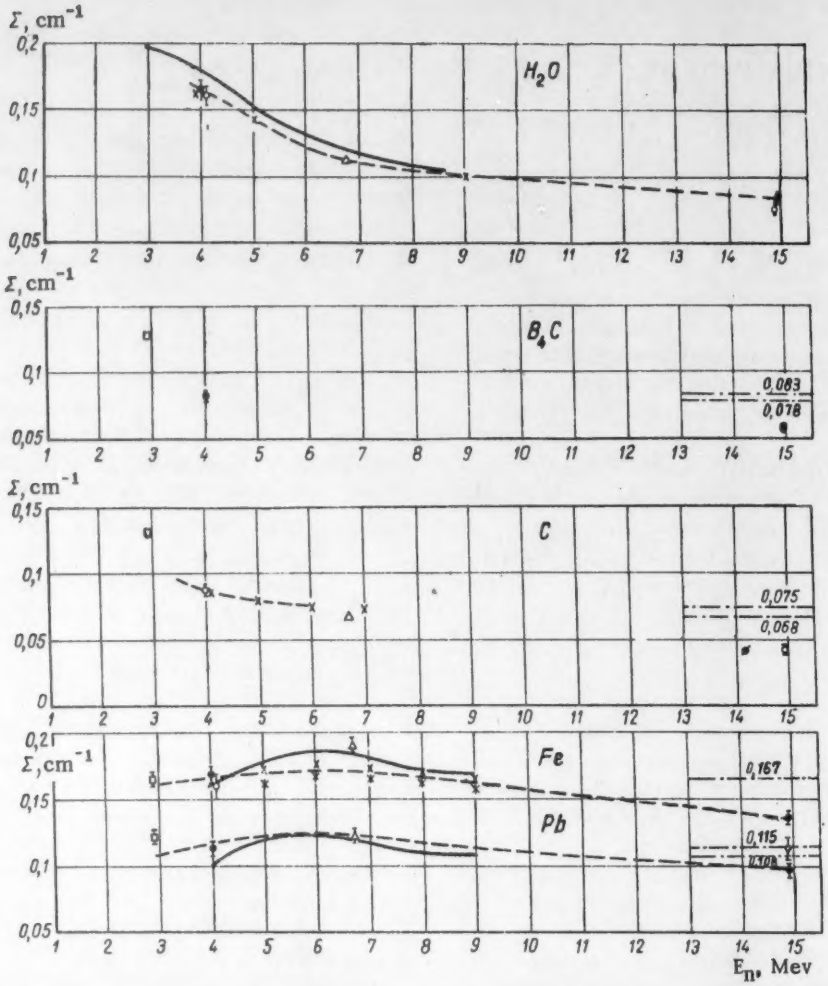

Fig. 2. Neutron energy dependence of removal cross sections for various materials (data presented by various authors). ✳,×) obtained from analysis of results reported in [4]; ●) results of present research for B_4C, the results correspond to reciprocal relaxation lengths); □) is from [3], △) is from [4], ○) is from [5,6], ◐) is from [7], (corresponding to reciprocal relaxation lengths for graphite of 1.67 g/cm³ density); — · — · —) according to data reported in [1,2,4] (for fission-spectrum neutrons); ——) according to data reported in [4]; — — —) according to curve based on experimental points.

energy of the maximum in the spectrum of nonscattered neutrons of the fission source on the distance in the water is known from [1]. On the basis of those data and from a consideration of the curves plotting the dependence of the removal cross sections on the thickness of the water layer, we arrived at an approximate relation for the dependence of the values of the removal cross section for carbon and iron on neutron energy over the range of neutron energies 5-9 Mev (Fig. 2). Those values are naturally, to a certain extent, averaged over a definite energy interval. As is apparent from inspection of Fig. 2 and the Table, the values of the removal cross sections obtained in the present research show close similarity to the corresponding values reported in other papers for H_2O, Fe, and Pb. The cross sections for B_4C and C are equal to the reciprocal values for the relaxation of fast neutrons in those media on thicknesses equal to 8-15 mean-free-path lengths. They may be distinguished from the removal cross sections for those substances measured in a hydrogen-containing medium. In the present research, measurements are also reported for the distribution of fast neutrons in uniform mixtures of iron and lead with boron carbide.

Correlation of all of the values reported for removal cross sections and results of measurements carried out in uniform mixtures of iron and lead with boron carbide, permit the assumption that the removal cross section approach is useful in calculating the fast-neutron distributions in media containing several other light elements instead of

Results of Measurements of Removal Cross Sections for Various Substances.

Substance	Density g/cm³	Data of present research		Data of various authors							
				[1—2]	[3]	[4]		[5]	[6]		
		$E_n = 4$ Mev	$E_n = 14,9$ Mev	Fission spectrum	$E_n = 2,9$ Mev	$E_n = 6,7$ Mev	Fission spectrum	$E_n = 4$ Mev	$E_n = 14,9$ Mev		
H_2O	1	0,165±0,008	0,084±0,004	—	—	0,112	—	0,161±0,008	0,0757±0,0038		
B_4C	1,67	0,083±0,003**	0,058±0,002**	0,078—0,083	0,129*	—	—	—	—		
C	1,67	—	—	0,068±0,004	0,132±0,0017	0,069±0,002	0,075±0,0015	0,088±0,004**	0,0416±0,002**		
Fe	7,83	0,169±0,007	0,137±0,005	0,167±0,007	0,166±0,0033	0,193±0,0076	0,167—0,172	0,160±0,016***	0,113±0,011***		
Pb	11,3	0,113±0,005	0,097±0,005	0,115±0,0098	0,122±0,0049	0,124±0,005	0,108±0,0032	—	—		

*Value obtained by conversion of data in [3] for boron and carbon.

**Values obtained from measured attenuation curves of fast neutrons in boron carbide and graphite [6], and corresponding to reciprocal values of relaxation lengths at distances equal to 8-15 mean free paths in those media.

***Values obtained from measurements with homogeneous water-steel mixtures (28.5%, 44% and 62% iron in volume) [5, 6].

hydrogen. The values of the removal cross sections for H_2O, Fe, and Pb, measured in B_4C, remain close to the values measured in hydrogen-containing media.

In conclusion, the authors welcome the opportunity to express their heartfelt thanks to Prof. A. K. Krasin and Candidate in Physical and Mathematical Sciences V. V. Orlov for their kind and unflagging interest in the research and their valuable advice, and to express their gratitude to G. N. Derigin, N. I. Dudkin, A. P. Klimov, V. G. Liforov, Z. S. Blistanov, A. I. Chusov, and V. S. Tarasenko for their kind assistance.

LITERATURE CITED

1. T. Rockwell, Reactor Shielding Design Manual TID-7004 (March. 1956).
2. B. Price, C. Horton, and K. Spinney, Radiation Shielding, Atomic Energy Research Establishment (U.K., 1957).
3. V. I. Kukhtevich, V. I. Sinitsyn, and S. G. Tsypin, Atomnaya Énergiya No. 5, 565 (1958).*
4. J. Bourgeois, P. Lafore, J. P. Millot, J. Rastain, F. De Vathaire, "Methods and experimental coefficients used in the computation of reactor shielding," Paper No. 1190, Second International Conference on the Peaceful Uses of Atomic Energy (Geneva, 1958).
5. D. L. Broder, Atomnaya Énergiya No. 7, 55 (1957).*
6. D. L. Broder, S. A. Kurkin, A. A. Kutuzov, V. V. Levin, and V. V. Orlov, "Study of spatial and energy distributions of neutrons in various media," Paper No. 2147, Second International Conference on the Peaceful Uses of Atomic Energy (Geneva, 1958).
7. V. Duggal and S. Puri, J. Appl. Phys. 29, 675 (1958).

Received January 21, 1959

*See English translation.

AVERAGE ENERGY OF β PARTICLES AT VARIOUS DEPTHS OF AN ATMOSPHERE-EQUIVALENT MEDIUM

V. P. Kasatkin

In β-radiation dosimetry it is important to know the average energy of the β particles, since this quantity is essential in determining the value of the dosage at a given depth.

We have measured the average energies of the spectrum of an atmosphere-equivalent medium in the fields of the β radiation of W^{185} and Y^{91} sources 1, 25, and 50 cm in diameter.

The spectra were measured with a scintillation spectrometer with a stilbene crystal [1]. A special diaphragm enabled us to detect the spectra of the β particles emitted at angles of 0, 30, and 60° relative to the normal to the surface of the source.

The results of the measurement of the average energy for W^{185} and Y^{91} sources are shown in Figs. 1 and 2. As is evident from the figures, the average β-particle energy decreases with increasing depth of medium. In the use of W^{185}, the decrease in average energy for extended sources (25 and 50 cm) is considerably greater than for sources of small diameter. The average energy of the β particles incident on the crystal at an angle of 60° likewise decreases more rapidly than the average energy corresponding to all of the β particles from a source 50 cm in diameter. At a given depth, the average energy decreases with increasing source diameter.

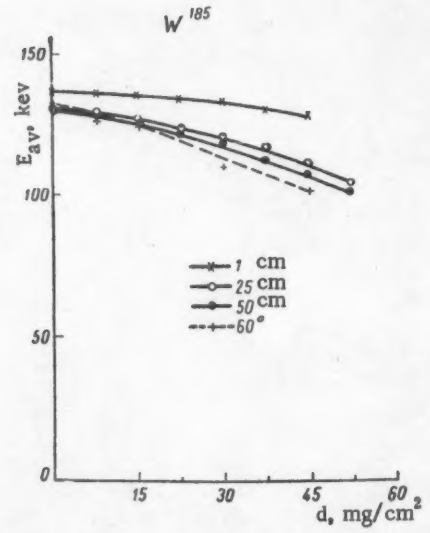

Fig. 1. Average energies of β particles of W^{185} in a medium at various depths.

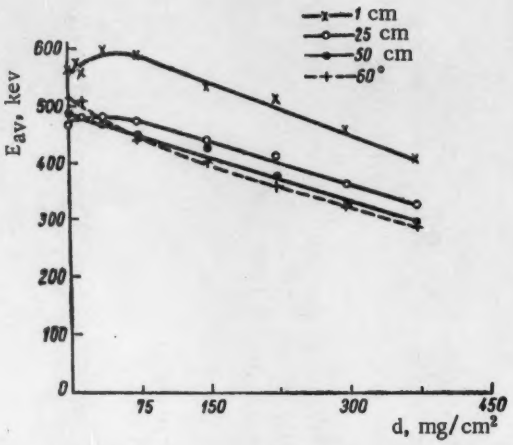

Fig. 2. Average energy of β particles from Y^{91} in a medium at various depths.

The curves for Y^{91} (shown in Fig. 2) have a similar character and are different only in that in the case of sources 1 and 25 cm in diameter, some increase in average energy is observed at small depths of the medium. The rate of decrease in average energy with increasing depth depends somewhat on the source diameter; attention is attracted by the fact that the decrease in average energy in a thickness Δx is considerably less than $(\overline{dE/dx})\,\Delta x$, where $(\overline{dE/dx})$ is the average ionization loss. This explains the considerable absorption and scattering of the slowest electrons in the spectrum.

The results obtained by us for sources 1 cm in diameter are found to agree with previously published data [2] for a point source of P^{32}.

LITERATURE CITED

1. K. K. Aglintsev, V. P. Kasatkin, and V. V. Smirnov, "Investigation of effective electron spectra in beta- and gamma-radiation dosimetry," Proceedings of the International Conference for Applications of Radioisotopes (Paris, September, 1957); "Radioisotopes in scientific research," Proceedings Intern. Conference 1, 109 (1958).
2. G. Brownell, Nucleonics 10, 30 (1952).

Received January 6, 1959

NEW POSITRON ACTIVITIES IN NEUTRON-DEFICIENT ISOTOPES OF LUTETIUM, YTTERBIUM, AND HOLMIUM

A. V. Kalyamin, I. Yu. Levenberg, and V. A. Yakovlev

A 10-minute irradiation of a tantalum target by 660-Mev protons was carried out in the synchrocyclotron of the Laboratory of Nuclear Problems in the Joint Institute for Nuclear Studies. A magnetic β spectrometer* was used to measure the end-point of the positron spectrum and half life of lutetium, ytterbium, and holmium, which were separated by a chemical method from the target.

Positrons with an energy of 1.7 ± 0.2 Mev and a half life of 43 min were found in the lutetium fraction. Within the limits of our experimental accuracy, the half life is the same as the half life of Lu^{167} (55 min [1]), and the end-point energy agrees well with the value of the end-point energy of Lu^{167} (1.76 Mev) predicted by Levy on the basis of a semiempirical rule [2]. In comparing the experimental values of the end-point energies of positron spectra with predicted values, it was assumed that a transition to the ground state of the daughter nucleus occurs in the positron decay.

A positron spectrum with an energy of 2.9 ± 0.15 Mev and a half life of 82 ± 4 min was detected in the Yb fraction. This value of energy agrees very well with the end-point energy value of 3.0 Mev which Levy calculated for Yb^{161}.

In the holmium fraction, the positron spectrum has an energy of 2.1 ± 0.15 Mev and a half life of 50 min, which, according to the Levy systematics, corresponds to Ho^{155} with an energy of 2.15 Mev or Ho^{158} with an energy of 2.3 Mev.

We note that the neutron-deficient isotopes of ytterbium and holmium with other mass numbers have, according to the tables of Levy and Riddel [2], positron spectrum end-point energies which differ by about 1 Mev or more from the ones indicated above.

In the daughter fraction of dysprosium (chromatographically separated from the holmium fraction), the characteristic γ spectrum of Dy^{155} [3] was found, using a scintillation γ spectrometer. This makes more plausible the supposition that the mass number of the new isotope of holmium is 155.

We express our deep gratitude to Professor A. N. Murin for his interest in the work and his part in a discussion of the results.

LITERATURE CITED

1. P. M. Aron, A. V. Kalyamin, A. N. Murin, and V. A. Yakovlev, Izvest. Akad. Nauk SSSR, Ser. Fiz. 22, 817 (1958).
2. H. Levy, Phys. Rev. 106, 1265 (1957); J. Riddel, Table of Levy's Empirical Atomic Masses (Chalk River, Ontario, July, 1956).
3. A. N. Dobronravova, L. M. Krizhanskii, A. N. Murin, and V. N. Pokrovskii, Izvest. Akad. Nauk SSSR, Ser. Fiz. 22, 815 (1958).

Received December 10, 1958

*The β spectrometer was constructed by two co-workers at the Laboratory of Nuclear Problems of the Joint Institute for Nuclear Studies, V. N. Mekhedov and M. Ya. Kuznetsova.

ANNULAR SHIELDING OF CHROMATOGRAPHIC COLUMNS IN WORK WITH RADIOACTIVE ISOTOPES

A. A. Goryunov

In chromatographic work with γ-emitting radioisotopes, an assembled stack of shielding rings proves highly practical, economical, stable, and reliable (Figs. 1 and 2).

The basic components of the shielding are the interchangeable removable lead rings 1 and 2 which are 40 mm in height and 100 mm across, and have lugs and recesses which facilitate overlapping of slots between adjacent rings, and joints between the parts of each ring. The shielding assembly made of rings of that width makes for safe handling of γ emitters with radiation energies ranging up to 1 Mev, in quantities equivalent to as much as 100-200 mg of radium •

Two types of rings are used. The small rings, designed for shielding the chromatographic column 3, have an inner diameter of 100 mm and an outer diameter of 300 mm. A column varying from 8 to 60 mm in diameter may be placed inside the shielding formed from those rings. The inner diameter of the large rings, designed for shielding of the reserve vessel 4 with the radioactive solution, is 160 mm, the outer diameter being 360 mm.

The lines at which the small rings are joined are offset by 120°. The removable section of the ring comprises only 1/3 of the ring. The lines at which the large rings are joined are displaced by 180°. This offsetting of the lines of junction (made with a 15 mm extension overlapping the slot) between rings of different types allows for reliable stability on the part of the stationary section of the shielding, and facilities the removal of small rings without disassembling the entire shielding arrangement where inspection of the column during the experiment or upon termination of the experiment is required. The inner surface and the horizontal planes of the rings are finished with quick-drying shellac giving a firm film covering. The outer surface is painted white.

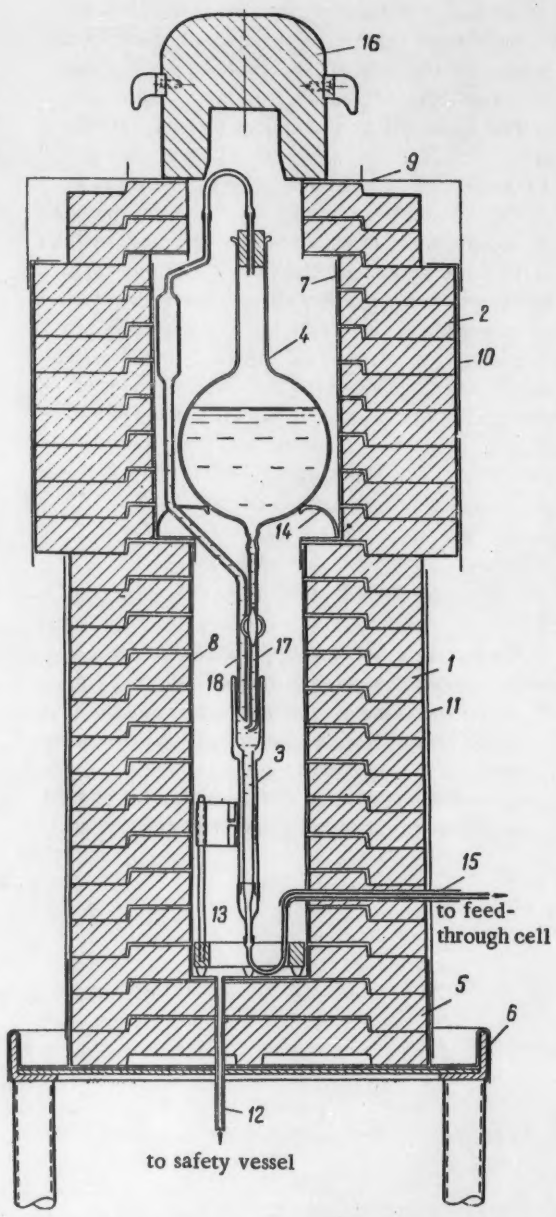

Fig. 1. Plan view through annular lead shielding. 1) Small ring; 2) large ring; 3) chromatographic column (of plastic glass); 4) reserve vessel (glass); 5) lead slab; 6) facing of support leg; 7,8) inner shielding jackets; 9,10,11) outer shielding jackets; 12) safety downcomer tube; 13) clamp for column support; 14) reserve vessel holder; 15) outlet tube; 16) cylinder; 17,18) tubes of semiautomatic feed (of glass).

•Health Rules and Standards for Handling of Radioactive Isotopes [in Russian] (Medgiz, Moscow, 1953).

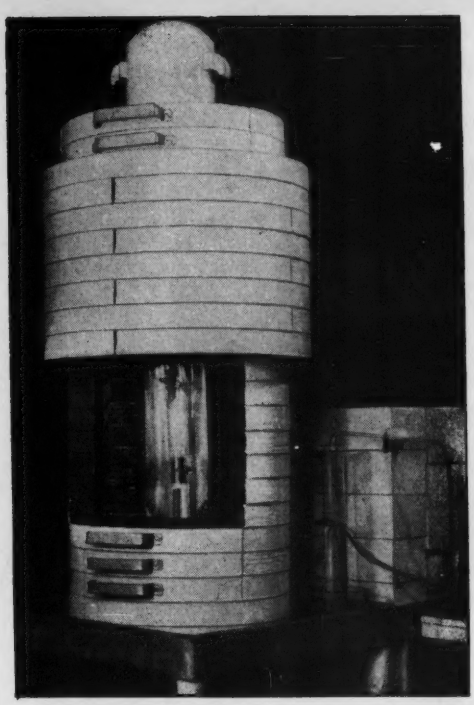

Fig. 2. General view of annular lead shielding. Some of the removable parts of the small rings have been detached.

The entire shielding is assembled on a special metal stand, flanged on the edges and designed to carry a load of 0.5-3 tons.

Depending on the amount of γ emitter to be processed, two to four solid slabs 5, 300 mm in diameter and having the same extensions and recesses as the rings, are first placed in the base of the shielding, prior to assembly. The small rings are stacked on those slabs, with the removable sections placed in the most advantageous position for removal when required. Selecting the necessary height, determined by the column length, the small rings are topped by a steel ring 1-1.5 mm thick, for protection against sagging of the large rings, after which the large rings are stacked such that the lines of junction of the first ring are arranged in alignment with the middle of the removable section of the small rings. The next large ring is so positioned that its line of junction falls perpendicular to the line of junction of the first large ring, etc.

After that, the surface of the lead shielding is faced with thin metal sheet (tin plate serving the purpose best) to avert radioactive contamination of the surface. The facing of parts 7-11 is made sectionally. The lower part of the inner jacketing comprises a cylinder with a bottom, and is cut out at the height of the second or third ring to form a window. The window facilitates mounting of the column in place, and is covered over, before beginning the experiment, with a semicylinder of tin. An opening is made in the bottom of the lining 8, with the safety downcomer tube 12 welded to that opening, for draining the active solutions passed through. This tube then passes through an opening leading through the slabs 5 and connects to an overflow vessel via rubber tubing. The capacity of the overflow vessel must not be less than the capacity of the reserve vessel 4.

The chromatographic column 3 is held in place by a clamp 13, with the aid of a spring-tensioned vise. The reserve vessel 4 is mounted in the shielding with the aid of a ring support 14 made of tin plate. Radial orifices are made in the wall of one of the lower shielding rings to accomodate the outlet duct of the column. Brass tubing 15 is inserted into that orifice, with the outlet tube passed through the orifice. Depending on the method used for monitoring the operating of the column, the outlet tube is connected to a feedthrough cell, placed under an end-window counter, or with a fraction collector.

The removable sections of the small rings are equipped with metal handles. The extension is removed in the upper removable sections, since otherwise the rings could not be inserted into the shielding assembly. The single small through-slit formed in that site is situated in the least active zone (between the column and the reserve vessel), so that it may be left out of account in view of the small activity penetrating through the slit.

After the reserve vessel 4 is filled with the solution to be investigated, one or two small rings are stacked on top of the last large ring in order to reduce the upper surface of the shielding, after which lead bricks or a specially cast lead cylinder 16 are placed on top of the lining 9. When that is done, the shielding is complete.

The shielding assembly so described is designed for shielding a small laboratory chromatographic column designed to carry a charge of 1 g of ion-exchange resin and a reserve vessel of 1 liter capacity, which is an integral part of the semiautomatic feed arrangement operated on the familiar principle of the "inverted vessel." Tubes 17 and 18 function as the control components of the system.

Received January 25, 1958

ON THE EQUILIBRIUM SHIFT BETWEEN RADON AND ITS DECAY PRODUCTS IN THE AIR STREAM

Yu. P. Bulashevich and N. P. Kartashov

The biological effects of radon on the respiratory organs depend on the degree of equilibrium prevailing between randon and its short-lived decay products [1]. Techniques are known for assaying the concentration of those products in the air [2-4]. It is therefore of interest to calculate the shift in equilibrium between radon and its decay products in the air stream for the conditions corresponding to ventilation in mine workings where emanation is present.

Let the rate of emanation of radon from a unit surface area of the walls of the mine stope be constant and equal to q. Then, assuming the rate of convective transport v at all points in the air course to be constant for a radon concentration c averaged over the cross section of the stope, we may formulate the following equation:

$$v\frac{\partial c}{\partial x}+\lambda c=\frac{ql}{s}=Q, \qquad (1)$$

where λ is the decay constant of radon, l is the perimeter of the stope cross section; s is the cross-sectional area of the stope. The x axis is directed along the air course.

The diffusion of radon along the mine gallery may be neglected. The integral of (1) satisfying the constraint c = 0 at x = 0 takes the form:

$$c=\frac{Q}{\lambda}\left[1-\exp\left(-\frac{\lambda}{v}x\right)\right]. \qquad (2)$$

A similar equation is used in radiohydrogeology for estimating radon accumulation in underground waters [4,5]. Since x/v = t is the time taken for a volume element of air to move long the stoping, then the concentration of RaA is found from the equation

$$\frac{dc_A}{dt}+\lambda_A c_A=Q[1-\exp(-\lambda t)]. \qquad (3)$$

Taking into account the fact that $c_A = 0$ at t = 0, we get

$$c_A=Q\left\{\frac{1-\exp(-\lambda t)}{\lambda_A-\lambda}+\frac{\lambda[1-\exp(-\lambda_A t)]}{\lambda_A(\lambda-\lambda_A)}\right\}. \qquad (4)$$

The concentration of RaA, in equilibrium with radon, is determined from the equation

$$c_A^0=\frac{\lambda}{\lambda_A}c. \qquad (5)$$

Dividing (4) term by term into (5), we find the coefficient of dynamic radioactive equilibrium between RaA and Rn:

$$\eta_A=\frac{\lambda_A}{\lambda_A-\lambda}+\frac{\lambda}{\lambda-\lambda_A}\frac{[1-\exp(-\lambda_A t)]}{[1-\exp(-\lambda t)]}. \qquad (6)$$

In similar fashion, we derive the equilibrium coefficient for RaB and RaC:

$$\eta_B=\frac{\lambda_A\lambda_B}{(\lambda_A-\lambda)(\lambda_B-\lambda)}+ \\ +\frac{\lambda\lambda_B[1-\exp(-\lambda_A t)]}{(\lambda_B-\lambda_A)(\lambda-\lambda_A)[1-\exp(-\lambda t)]}+ \\ +\frac{\lambda\lambda_A[1-\exp(-\lambda_B t)]}{(\lambda-\lambda_B)(\lambda_A-\lambda_B)[1-\exp(-\lambda t)]}; \qquad (7)$$

$$\eta_C=\frac{\lambda_A\lambda_B\lambda_C}{(\lambda_A-\lambda)(\lambda_B-\lambda)(\lambda_C-\lambda)}+ \\ +\frac{\lambda\lambda_B\lambda_C[1-\exp(-\lambda_A t)]}{(\lambda-\lambda_A)(\lambda_B-\lambda_A)(\lambda_C-\lambda_A)[1-\exp(-\lambda t)]}+ \\ +\frac{\lambda\lambda_A\lambda_C[1-\exp(-\lambda_B t)]}{(\lambda-\lambda_B)(\lambda_A-\lambda_B)(\lambda_C-\lambda_B)[1-\exp(-\lambda t)]}+ \\ +\frac{\lambda\lambda_A\lambda_B[1-\exp(-\lambda_C t)]}{(\lambda-\lambda_C)(\lambda_A-\lambda_C)(\lambda_B-\lambda_C)[1-\exp(-\lambda t)]}. \qquad (8)$$

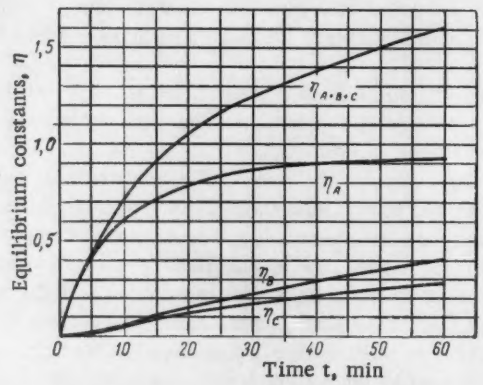

Radioactive equilibrium constants for equilibrium between radon and its decay products. η_{A+B+C} is the total equilibrium constant.

The diagram displays graphs of the equilibrium coefficients plotted against time. If the time of total air turnover is taken, then the coefficients will have reference to the discharge of the ventilation stream. The relatively long half lives of RaB and RaC are the reason for the comparatively low equilibrium coefficients of those elements, within the time interval considered. The concentration of Rn increases practically in proportion to time, over the interval of interest. RaA is the basic decay product of radon, which accumulates in the air course.

Now by using the values of the equilibrium coefficients, we may derive the concentrations of the corres-

ponding decay products, on the basis of the known concentration of Rn:

$$c_1 = \eta_1 c \cdot \mu \mu \text{ curies/liter} \qquad (9)$$

Note that the total equilibrium constant, represented on the diagram, is subject to the constraint $\eta_{A+B+C} \leq 3$.

Calculation of the equilibrium constants in the presence of nonuniform emanation is in principle carried out by the method outlined above. It is evident that as the emating surfaces are displaced toward the beginning of the air course, the equilibrium constants at the exit will be higher than in the case of a uniformly emanating stope.

As the rate of air flow increases, the equilibrium constants and the concentration of decay products of radon drop sharply.

LITERATURE CITED

1. L. S. Ruzer, Atomnaya Énergiya 4, 144 (1958) *
2. C. Yourt, Canad. Mining J. 76, 60 (1955).
3. J. Horley, Nucleonics 11, 12 (1953).
4. V. I. Baranov, Radiometry [in Russian] (Izd. AN SSSR, 1956).
5. A. N. Tokarev and A. V. Shcherbakov, Radiohydrogeology [in Russian] (Gosgeoltekhizdat, 1956).

Received January 6, 1959

*See English translation.

PROPAGATION OF Co^{60} RADIATION IN THE AIR ABOVE THE EARTH

O. I. Leipunskii and V. N. Sakharov

In computing the dosage from powerful γ sources found in the air above the earth, attenuation of the radiation due to the geometric factor (in the first several tens of meters distance from the source) and due to absorption of gammas in the air (with increase in distance) must be taken into account. At distances greater than several hundreds of meters from the source, absorption becomes the deciding factor in the attenuation of the radiation dose. When the source is very powerful and its radiation is quite considerable at distances of several hundreds of meters or several kilometers, calculation of the dose requires knowledge of the laws of attenuation of radiation by the air.

The theoretical derivation of those laws is complicated by multiple scattering of gammas.

The problem of the spatial distribution of gamma-ray dosage has been solved only for the homogeneous medium, while the problem of radiation from a point source located at the interface between two media (e.g. air-earth interface) has not been solved theoretically.

The present paper describes experimental data on the attenuation of the intensity of Co^{60} radiation in the air above the earth at distances of 1-800 meters from the source. The measurements were performed at an altitude of 0.7 meters above the earth, i.e., approximately at half the height of an average human adult. The source was placed at the same height. Sources with activities of about 500, 10, and 1 curie, and also 10 and 1 μ curie, were employed. The total attenuation curve was obtained from separate and interrelated overlapping curves.

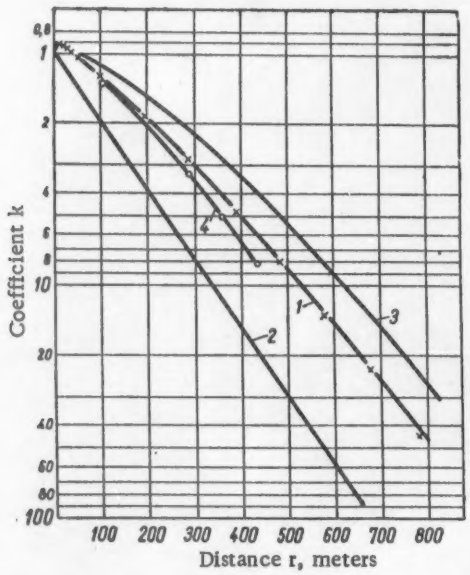

Dependence of the coefficient $\underline{k}$ on distance to the source $\underline{r}$.

The radiation was detected by means of ionization chambers with "air-equivalent" walls, and counters of special design [1]. These counters recorded with equal sensitivity the intensity of the primary radiation source Co^{60} and the scattered radiation, over a wide region of the energy spectrum up to $E_\gamma \approx 80$ kev. There are no precise data on the sensitivity of counters at $E_\gamma < 80$ kev, but it may be assumed that they are insensitive to radiation at $E_\gamma < 50$ kev.

The radiation detector consisted of three combined counters whose axes were arranged in the three mutually perpendicular directions. That design enabled us to circumvent the dependence of detector response on the angle of incidence of the radiation. The sensitivity of the detector setup to intensity of radiation proved to be uniform within 5 % limits in all directions.

The results of the measurements are shown on the diagram in the form of the dependence of the coefficient $\underline{k}$ on the distance to the source $\underline{r}$ (curve 1). Coefficient $\underline{k}$ indicates the number of times the intensity of the radiation is attenuated owing to interaction of the radiation with the air and earth at a temperature 0°C and air pressure 740 mm Hg.

For purposes of comparison, there are also shown in the diagram: 2, the law of attenuation of primary radiation emanating from a source in the air, with scattered radiation neglected; 3, the law of attenuation of a dose of gamma rays from a Co^{60} source immersed in a homogeneous air medium, derived theoretically and in simulation experiments in water [2-4]; 4, data reported in [5], in which case measurements were carried out at distances of 100-400 meters from a source located in the air above the earth.

As is apparent from the diagram, at $\underline{r}$ of the order of several tens of meters, $\underline{k}$ proves to be less than 1; i.e., the intensity of radiation due to interaction with the environment increases. This takes place on account of reflection of radiation from the earth. The intensity of the reflected radiation comprises a maximum of 10-15% of the total radiation intensity at the point of measurement.

At great distances from the source, the measured intensity values proved to be 1.7-1.8 times lower than the

values predicted theoretically or derived from data of simulation experiments in water for the case of a homogeneous air environment. This confirms the assumption entertained by the present authors as to the fact that the dose established in air at great distances from the earth's surface by a point source located at sea level should be approximately half as high as that established at the same distances in a homogeneous air medium. The assumption is based on the following considerations. If the source and the detector are placed on the air-earth interface, then the earth will absorb half of the gammas which, when traversing a pure air medium, would negotiate great distances and become scattered in the air near the point of measurement. Consequently, half of the gammas capable of setting up scattered radiation are absorbed by the earth near the source; and since the radiation consists of scattered gammas, for the most part, at large distances from the source the intensity of the radiation in the presence of the earth should be approximately half that in a homogeneous air environment.

The data obtained on the propagation of radiation in the air surrounding the earth may be used in particular to determine the intensity of radiation above sea level contaminated by radioactive fallout. This problem may be solved by numerical integration, keeping in mind that any surface contamination is composed of a sum of point-source emitters.

The results of calculations of radiation intensity at a height of 1 meter above the center of a portion of the earth of radius R, uniformly contaminated by radioactive materials with a surface density of contamination σ Mev·cm^{-2}·sec^{-1} are in the table. The results are presented in the form of coefficients A for the purpose of computing the intensity J on the basis of the formula

$$J = A \cdot \sigma \quad \text{Mev} \cdot \text{cm}^{-2} \cdot \text{sec}^{-1}$$

in the case of contamination of the surface of the earth by radioactive cobalt. The computations were made for an air temperature of 0°C and air pressure 760 mm Hg.

R, m	25	50	100	200	500	∞
A	1,65	2,0	2,31	2,52	2,64	2,66

In conclusion, the authors take the opportunity to express their acknowledgment to the team of co-workers who made available a powerful source of γ rays and who participated in the measurements.

LITERATURE CITED

1. V. N. Sakharov, Atomnaya Énergiya 3, 61 (1957).*
2. U. Fano, Nucleonics 11, 55 (1953).
3. G. White, Phys. Rev. 80, 154 (1950).
4. V. N. Sakharov, Atomnaya Énergiya 3, 57 (1957).*
5. B. Soole, Proc. Roy. Soc. 230, 343 (1955).

Received December 12, 1958

*See English translation.

ALLOYS OF URANIUM WITH PLATINUM SERIES METALS

Data reported in the literature [1,2] on alloys of uranium with metals of the platinum series are of practical interest, since "fissium", i.e., the residue left over from the fission-product elements following pyrometallurgical processing of the irradiated uranium, consists mainly of ruthenium (33%), rhodium and palladium (10%), and molybdenum (42%) [3]. These data are also important in the study of the behavior of modifications of uranium when fused with other elements.

The Uranium-Ruthenium System. An incomplete phase diagram of this system (see Fig. 1) is based on microscopic and thermographic researches. Transformations in the solid state proceed very slowly. The solubility of ruthenium in α uranium at 633°C comes to 0.1 wt. %, whereas the solubility of uranium in ruthenium at 1500°C is about 0.9 wt. %. Compounds assigned the tentative composition U_3Ru_4, U_2Ru_3 and U_3Ru_5 are probably formed in peritectic fashion, since the liquidus rises without open maxima right up to the melting point of ruthenium (2500°C). The compound URu_3 is formed from a peritectic reaction and has a cubic structure of the Cu_3Au type, with a = 3.988 ± 0.002 A [4].

The Uranium-Rhodium System. The uranium corner of this system is shown in Fig. 2, based on data reported in [1,2]. Up to the compound URh, the diagram is reminiscent of the diagram for ruthenium, except that U_2Rh is formed from a peritectoid rather than a peritectic reaction. The liquidus rises to a peak at 2160°C at 63 wt.% rhodium and then falls to 1500°C at 78 wt. % rhodium. The compound URh_3 has a cubic structure of the Cu_3Au type, with a = 3.991 A [4].

The Uranium-Palladium System (Fig. 3) [5]. The solubility of palladium in α and β uranium is less than 0.3 at.%. The peritectoid temperature at which the solid solution of uranium in palladium forms is assigned arbitrarily (it is higher than 1425°C). The solubility of uranium in palladium is great and fluctuates from 22.2 at. % at 700-900°C to 21.8 at.% at 1400°C. The compound UPd_3 features a hexagonal lattice, varying from a = 5.769 A and c = 9.641 A on the part of uranium, to a = 5.763 A and c = 9.526 A on the part of palladium.

The Uranium-Osmium and Uranium-Iridium Systems [1]. Scanty data have been published about these systems.

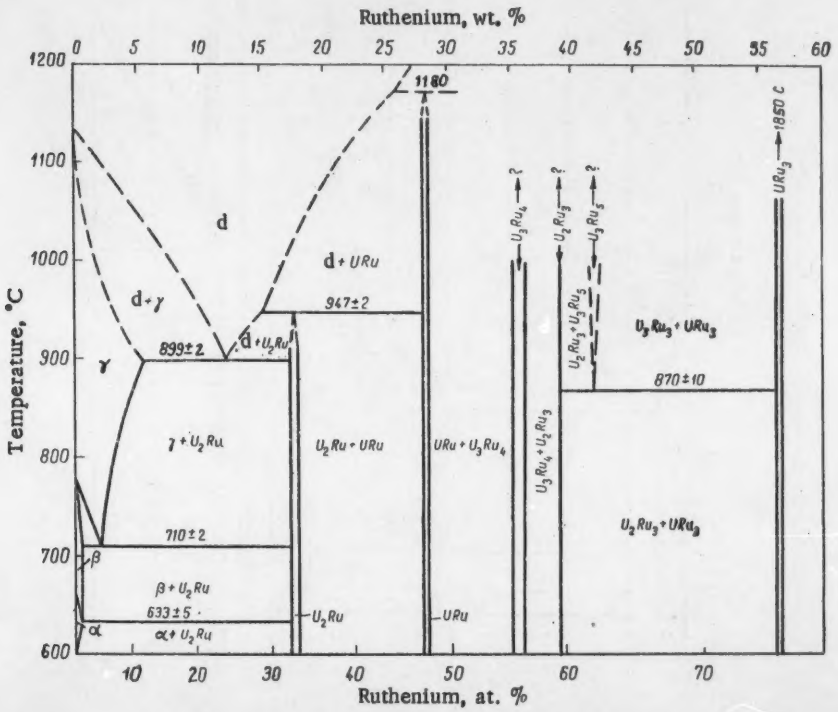

Fig. 1. Phase diagram of uranium-ruthenium system.

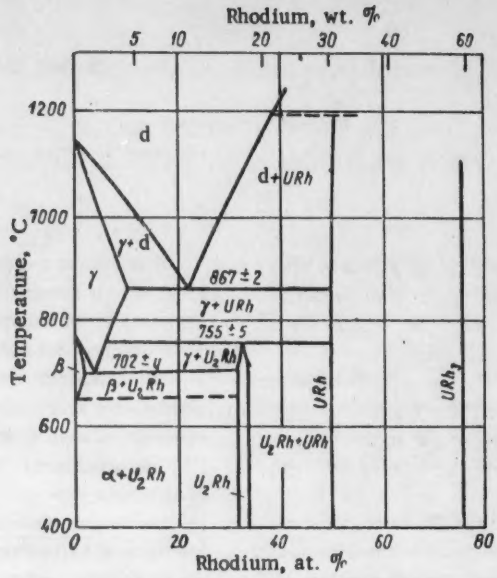

Fig. 2. A part of the uranium-rhodium phase diagram.

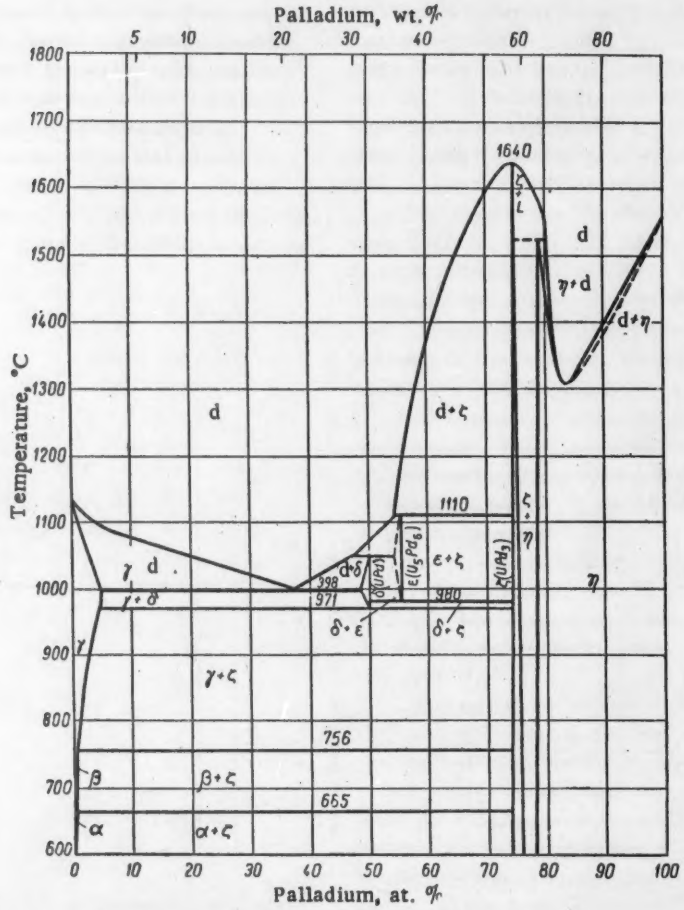

Fig. 3. Phase diagram of the uranium-palladium system.

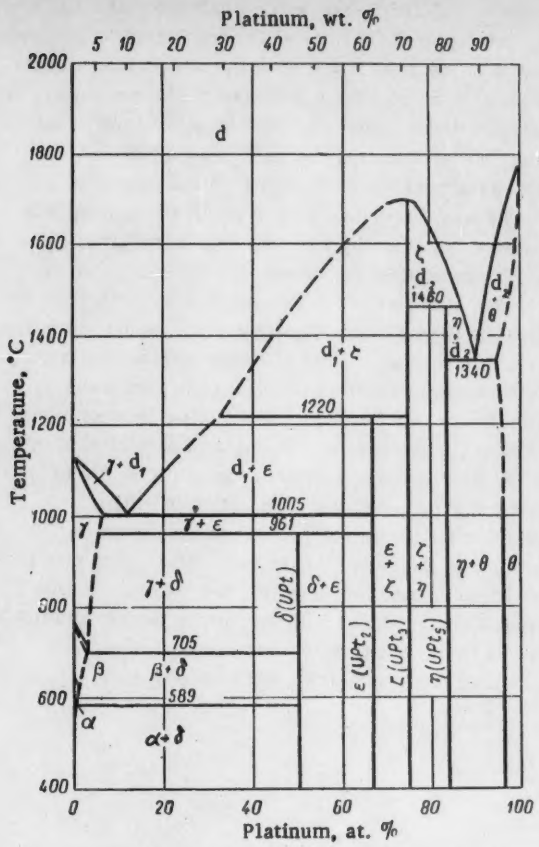

Fig. 4. Tentative phase diagram of uranium-platinum system.

Osmium stabilizes the β and γ phases. The solubility of iridium in uranium at 890°C is of the order of 3 at. %. Compounds UOs_2 and UIr_2 of the $MgCu_2$ type, with face-centered lattices having a = 7.5125 ± 0.0005 A and a = = 7.509A, respectively, have been identified.

The Uranium-Platinum System [1]. A tentative diagram of this system is seen in Fig. 4. The maximum solubility of platinum in γ uranium at the eutectic point is 6.5 at. %, and in β and α uranium, 3.0 at. % and 0.3 at. %. The solubility of uranium in platinum is about 5 at. %. The structures of the compounds UPt_2, having a rhombic lattice with a = 4.12 A, b = 9.69 A, and c = 5.64 A, and UPt_3, having a hexagonal lattice with a = 5.764 A and c = 4.898 A, have been identified.

G. Z.

LITERATURE CITED

1. F. Rough and A. Bauer," Constitution of uranium and thorium alloys," BMI-1300, June 2, 1958.
2. H. Chiswik et al., "Advances in the physical metallurgy of uranium and its alloys," Paper No. 713 (USA) presented at the Second International Conference on the Peaceful Uses of Atomic Energy (Geneva, 1958).
3. L. Koch, Nucleonics 16, 68 (1958).
4. T. Heal and G. Williams, Acta Cryst. 8, 494 (1955).
5. J. Catteral et al., J. Inst. Metals 85, 63 (1956-1957).

BRIEF COMMUNICATIONS

USSR . A new cyclic ion accelerator incorporating a new design, and constituting a further development of the cyclotron, has been put into operation in the Nuclear Problems Laboratory of the Joint Institute for Nuclear Studies at Dubna. As distinct from the conventional cyclotron and synchrocyclotron, the azimuthal magnetic-field strength does not remain constant in this accelerator, but varies with a certain periodicity. The lines of maximum magnetic field strength (the "humps") take the form of Archimedes spirals evolving from the center of the magnet. However, the mean magnetic field (during one period of revolution of an ion) does not fall off radially as in the cyclotron and synchrocyclotron, but increases continuously in order to offset the relativistic mass increase of the ions with increase in energy. Beam defocusing along the vertical and degradation of beam strength, usually due to increase in the mean magnetic field, are eliminated in accelerators of the new type by the focusing action provided by azimuthal variation of the magnetic field.

Proton energies in the new type cyclotrons may be brought up to the same level as in synchrocyclotrons (to 1 Bev), and currents are hundreds of times higher.

A detailed description of the accelerator put into service at Dubna will be published in the next issue of JAE .

USSR . The Ninth Annual Conference on Nuclear Spectroscopy was convened in Kharkov, January 26 to February 2, 1959, and was attended by over 350 scientific workers in research institutes and advanced educational institutions. Over a hundred reports were heard at the Conference, dealing with the results of theoretical and experimental research into the structure of nuclei, α and β decay. A more complete report on

the Conference will appear in the July issue of JAE, and the proceedings of the Conference will be made available in the Bulletin of the Academy of Sciences of the USSR, physical series.

USSR. A simple coincidence circuit with a resolving time of less than 10^{-9} sec has been developed at the Institute of Physics of the Academy of Sciences USSR. Germanium diodes, such as the DG-Ts8, D_2V, or D_2A, which have a low forward resistance, can be used in the circuit. The small resolution time and high efficiency are achieved by virtue of the fact that the diodes are not loaded by a dc bias current. The scheme is based on the differentiation of single isolated pulses when there is no signal present in the second input circuit. Pulses applied to the input of the system simultaneously (within the limits of the resolution time) are not differentiated. The circuit has been used in work on investigations of photoproduction of π^0 mesons in complex nuclei, where a resolution time of $1 \cdot 10^{-8}$ sec is needed, and in investigations of the time characteristics of the FÉU-33 photomultiplier (which requires a resolution time of $\sim 10^{-9}$ sec).

USSR. A simple pulse-amplitude integrator has been developed at the Nuclear Physics Scientific Research Institute of Moscow State University; with this instrument it is possible to total the amplitudes of successively applied pulses and to determine the mean amplitude (for small loading of the detection channel). The device is based on the transformation of the signal into a train of pulses in such a way that the number of pulses in the train N is determined uniquely by the amplitude of the input signal V_a. The totaling of the number of pulses in the trains of the output of the amplitude converter is carried out by a counting device with a capacity of 10^3 and a resolution time of $5 \cdot 10^{-5}$ sec. Used in conjunction with a large 10-channel time analyzer which analyzes the trains by length (by means of a delay circuit in the form of ten successively triggered univibrators) and parallel registration by neon lamps, the system makes it possible to obtain the pulse amplitude distribution in a form convenient for analysis and to determine the mean amplitude of the pulses at the same time. The instrument has been used for recording the mean amplitude of signals characterized by low counting rates (~ 10 min^{-1}) obtained from an ionization chamber used to measure the ionization properties of cosmic radiation.

TERMS AND DEFINITIONS

Fuel Assembly. (Teplovydelyayushchaya sborka) is the basic constructional element of a reactor core and of an assembly of fuel elements (sheet, rod, tubular, etc.). These fuel elements are generally formed into a demountable fuel assembly to make it convenient to reload the fuel in the reactor. In the literature, especially in the foreign literature, these assemblies are frequently referred to as fuel elements and this causes some difficulty in the description of these assemblies because the fuel elements which comprise the assembly require a different designation (for example, fuel sheets, fuel rods, fuel plates, etc.). It is apparent that the word "element" emphasizes the fact that the object is only an element or elementary unit of the whole assembly, which is made up of a complex group of such units and is called the "fuel assembly." Hence, the designation of "fuel assembly" as applied to a group of assembled fuel elements is more accurate.

Operational Down Time. (Operativnoe vremya) is the time period between reactor shutdown and the time when the reactor becomes subcritical because of poisoning (the so-called "iodine pit"). Frequently this time is called the "operational excess reactivity" or "shutdown excess reactivity". All these terms indicate the time period during which operating personnel can remedy any unusual condition which causes or requires shutdown. If the condition is not removed in the operational waiting time, allowing the reactor to be brought back to full power, the reactor cannot be started up again until several hours have elapsed; this is the time required for the iodine pit to be dissipated. The duration of the effect of the iodine pit depends on the reactor and the mode of operation before shutdown. The term " time" is brief and gives the best description of the effect and is preferable.

NEW LITERATURE

E. A. Liberman, Dosimetry of Radiosotopes (Medgiz, 1958) 186 pp, 5 rubles, 45 kopecks.

The salient feature of this monograph is the exposition of problems in the dosimetry of α, β, and γ radiations from the viewpoint of the absorbed dose measured in rads or ergs.

The monograph contains five chapters.

The first chapter provides the basic physical characteristics of radiations emitted by radioactive isotopes. The fundamental laws governing the interactions of ionizing radiations with matter are discussed briefly, and the concept of the dose of x-ray or gamma radiation is approached critically. The fundamental physical characteristics of radiations, determining their biological effects, concepts of linear density of absorbed energy, and linear ionization density, treated in the first chapter, bring the reader up to date on the methods and evaluation of the biological effects of ionizing radiations.

The second chapter is devoted to methods used in measuring ionizing radiations. The characteristics and operating principles of the ionization, scintillation, chemical, and calorimetric methods of measurement are given in highly condensed form. Dose measurement techniques involving the use of the normal ionization chamber are described in more complete form, and an analysis is given of errors encountered in measuring dosage by means of wall (thimble) chambers.

The important section in this chapter is the one dealing with the calibration of scintillation dosimeters in rads where, in particular, we have a description of the method used in calibrating scintillation dosimeters for the measurement of absorbed doses of β radiation emananting from a plane disk source.

The third and fourth chapters are devoted to calculations of the absorbed dose of α, β, γ radiations in matter. These calculations are performed for sources of different geometries, with decay and removal of isotope, etc. taken into account.

The discussion of original contributions of the author on the determination of the absorbed dose of β radiation in matter by measuring x-ray bremsstrahlung is certainly of interest. This section is illustrated by down-to-earth computational examples which impart striking clarity to the material presented.

On the whole, the material in these two chapters supplements and systematizes the knowledge at our disposal in the area of health physics of β radiation, which has been lagging far behind the study of γ-radiation dosimetry in its development.

A number of shortcomings in the treatment of particular questions must be point out, nevertheless.

The summarized and condensed approach sometimes renders reading of the material a bit difficult, and requires from the reader some prior training in the particular area of interest. The question of the connection between the quantity of energy absorbed in the material surrounding a cavity with a gas and ionization in the gas cavity (the Bragg-Gray theory) is dealt with in somewhat muddled fashion.

The monograph is also not immune to a large number of misprints, often resulting in distortion of the meaning. Unfortunate choice of wording is also encountered.

On the whole, we may rest assured that the monograph will prove highly useful not only to biologists and doctors working with radioactive isotopes, but also to physicists and chemists whose work is connected with research on the effects of ionizing radiations on matter.

In Press

M. Benedict and T. Pigford, Nuclear Chemical Engineering (McGraw-Hill, New York) (Russian translation – Atomizdat) 35 folios, 26 rubles.

N. P. Galkin, A. A. Maiorov, and U. D. Veryatin, Processing of Uranium Concentrates (Atomizdat) 12 folios; 7 rubles, 50 kopeks.

The book provides general information on: hydrometallurgical processes used in gleaning uranium from parent ore, reserves of uranium ore, production scales, and areas of application of uranium. Basic emphasis is placed on the technology of processing uranium concentrates to pure salts and metallic uranium.

The book is written for workers in the uranium industry and in research organizations, and may also be used as a textbook for those specialties.

A. G. Grammakov, V. L. Shashkin, and M. B. Shiryaeva, Handbook on Gamma Assay of Uranium Ores (Atomizdat) 4 folios; 2 rubles.

The theoretical fundamentals of radiometric assay of uranium ore are dealt with, and the equipment and procedures used in gamma assay work are described.

The book is written for geophysicists and geologists working in prospecting and exploration of uranium ores. It may also be used as a textbook for students in the fields of geology and geophysics.

The Inexhaustible, Edited by A. K. Krasin (Atomizdat) 5 folios; 1 ruble, 50 kopeks.

Reports by prominent Soviet scientists on various questions affecting the production and use of atomic energy are assembled in this book. These are the reports delivered at the international seminar "Atomic Energy and Youth", which was held in Moscow in 1958, under the auspices of the Committee on Youth Organizations of the USSR.

The book is written in popular style and aimed at a broad audience.

Articles from the Periodical Literature

F. A. Alekseev et al., "The use of the hydrogen isotope tritium in the development of oil fields," Geologiya nefti No. 12, 47 (1958).

S. N. Ardashnikov and N. S. Chetverikov, "Basic dosimetry units in the 'Recommendations' of the International Commission on Radiological Units and Measurements for 1956," (review article) Med. radiologiya No. 1, 12 (1959).

G. I. Blinov et al., "The use of radioactive monitoring and control instruments in the hydrogenation plant," Khimiya i tekhnologiya topliva i masel No. 1, 15 (1959).

E. Z. Bur'yanova, "Bilibinite – a new aqueous silicate of uranium," Zapiski vsesoyuz. mineralog. obshchestva No. 87, Ser. 6, 667 (1958).

G. V. Veinberg, "Isotopic absorption spectrum analysis of cuprous iodide," Optika i spektroskopiya 6, 9 (1959).

V. I. Gol'danskii, "New work on the synthesis of element 102," Priroda No. 1, 118 (1959).

V. K. Zhuravlev, "The effect of ionizing radiations on solid inorganic dielectrics," (review article) Izvest. vyssh. ucheb. zavedenii. Fizika No. 5, 79 (1958).

Yu. S. Zaslavskii, "The present state of the art in the use of radioactive isotopes and radiations in petroleum refining," Khimiya i tekhnologiya topliva i masel No. 1, 17 (1959).

I. A. Zakharova et al., "The Use and Properties of Niobium," Tsvetnye metally No. 1, 73 (1959).

M. A. Kaliko and M. N. Pervyshina, "Study of the surface properties of cracking catalyzers, using the method of adsorbing cesium cations on radioactive cesium," Khimiya i tekhnologiya topliva i masel No. 1, 19 (1959).

E. I. Krylov, "On polynuclear chlorides of niobium and tantalum," Nauchnye doklady vyssh. shkoly, Khimiya i khim. tekhnologiya No. 4, 676 (1958).

B. K. Lakatosh, "The use of radioisotopes in wood processing," Trudy Rostov. n/D inzh. stroit. inst. No. 13, 165 (1958).

L. S. Livshits and L. P. Bakhrakh, "Radiographic study of distribution of niobium in stainless steel," Svarochnoe proizvodstvo No. 1, 31 (1959).

N. P. Mel'nikova and I. A. Shakhzadova, "Synthesis of C^{14}-tagged aromatic hydrocarbons," Khimiya i tekhnologiya topliva i masel No. 1, 40 (1959).

D. I. Nedogovorov et al., "Pilot-plant beneficiation of low-grade placer deposit titanium and zirconium ores in the eastern Ukraine," Tsvetnye metally No. 12, 14 (1958).

A. V. Novoselova, "Beryllium fluoride and fluoroberyllates," Uspekhi khimii 28, 33 (1959).

A. P. Polevodov et al., "Radiation chemical stability of ion exchange resins. Effect of γ and β radiations on cations," Nauchnye doklady vyssh. shkoly, Khimiya i khim. tekhnologiya No. 4, 761 (1958).

V. I. Rogachev, "The use of ionizing radiations in food preservation," Konservnaya i ovoshchesushil'naya promyshlennost' No. 2, 25, (1959).

N. N. Shumilovskii et al., "The theory and practice of the use of relay devices based on the use of radioisotopes," Izvest. Akad. Nauk Latv. SSR No. 10, 11 (1958).

M. N. Fateeva, "What's new in radiodiagnostics?" Med. radiologiya No. 1, 77 (1959).

Ya. N. Fertel'meister et al., "The use of beta radiations for measuring the thickness of a layer of settled coal dust," Ugol' No. 1, 48 (1959).

J. Bellier and M. Tourasse, Nuclear Energy Engr. 13, 85 (1959).

A. Bertinchamps, Science 128, 988 (1958).

R. Beth and C. Lasky, Science 128, 1393 (1958).

H. Brown, J. Nuclear Energy 8, 177 (1959).

S. N. Buckley et al., J. Inst. Metals 87, 150 (1958).

J. Burkett, Nuclear Energy Engr. 13, 104 (1959).

P. Cotterill et al., J. Inst. Metals 87, 159 (1958).

M. Englander, Rev. mét. 55, 1177 (1958).

C. Erginsoy, J. Nuclear Energy 8, 215 (1959).

R. Hanna and B. Rose, J. Nuclear Energy 8, 197 (1959).

M. Hiller, J. Nuclear Energy 8, 187 (1959).

S. Katcoff and D. Williams, J. Inorg. and Nucl. Chem. 7, 194 (1958).

S. Katcoff and D. Williams, J. Inorg. and Nucl. Chem. 7, 189 (1958).

A. Kolb, Phys. Rev. 112, 291 (1958).

P. Kovanic and M. Kulka, Jaderná Energie, 5, No. 1, 6 (1959).

J. Lehmann and H. Aubert, Rev. mét 55, 1188 (1958).

M. MacGregor and R. Booth, Phys. Rev. 112, 486 (1958).

J. Murray, J. Inst. Metals 87, 94 (1958).

G. Parry and L. Graham, J. Inst. Metals 87, 125 (1958).

R. Post, Jaderná Energie, 5, No. 1, 2 (1959).

E. Rae et al., Phys. Rev. 112, 492 (1958).

C. Shiflett et al., J. Inorg. and Nucl. Chem. 7, 210 (1958).

J. Totter et al., Science 128, 1490 (1958).

J. Wallman et al., J. Inorg. and Nucl. Chem. 7, 199 (1958).

SIGNIFICANCE OF ABBREVIATIONS MOST FREQUENTLY ENCOUNTERED IN SOVIET PHYSICS PERIODICALS

AN SSSR	*Academy of Sciences, USSR*
FIAN	*Physics Institute, Academy of Sciences USSR*
GITI	*State Scientific and Technical Press*
GITTL	*State Press for Technical and Theoretical Literature*
GOI	*State Optical Institute*
GONTI	*State United Scientific and Technical Press*
Gosénergoizdat	*State Power Press*
Gosfizkhimizdat	*State Physical Chemistry Press*
Goskhimizdat	*State Chemistry Press*
GOST	*All-Union State Standard*
Gostekhizdat	*State Technical Press*
GTTI	*State Technical and Theoretical Press*
GUPIAÉ	*State Office for Utilization of Atomic Energy*
IFKhI	*Institute of Physical Chemistry Research*
IFP	*Institute of Physical Problems*
IL	*Foreign Literature Press*
IPF	*Institute of Applied Physics*
IPM	*Institute of Applied Mathematics*
IREA	*Institute of Chemical Reagents*
ISN (Izd. Sov. Nauk)	*Soviet Science Press*
IYaP	*Institute of Nuclear Studies*
Izd	*Press (publishing house)*
KISO	*Solar Research Commission*
LÉTI	*Leningrad Electrotechnical Institute*
LFTI	*Leningrad Institute of Physics and Technology*
LIM	*Leningrad Institute of Metals*
LITMiO	*Leningrad Institute of Precision Instruments and Optics*
Mashgiz	*State Scientific-Technical Press for Machine Construction Literature*
MATI	*Moscow Aviation Technology Institute*
MGU	*Moscow State University*
Metallurgizdat	*Metallurgy Press*
MOPI	*Moscow Regional Pedagogical Institute*
NIAFIZ	*Scientific Research Association for Physics*
NIFI	*Scientific Research Institute of Physics*
NIIMM	*Scientific Research Institute of Mathematics and Mechanics*
NII ZVUKSZAPIOI	*Scientific Research Institute of Sound Recording*
NIKFI	*Scientific Institute of Motion Picture Photography*
OIYaI	*Joint Institute of Nuclear Studies*
ONTI	*United Scientific and Technical Press*
OTI	*Division of Technical Information*
OTN	*Division of Technical Science*
RIAN	*Radium Institute, Academy of Sciences of the USSR*
SPB	*All-Union Special Planning Office*
Stroiizdat	*Construction Press*
URALFTI	*Ural Institute of Physics and Technology*

NOTE: Abbreviations not on this list and not explained in the translation have been transliterated, no further information about their significance being available to us —*Publisher.*

SOVIET

research in

ANALYTICAL CHEMISTRY

OF URANIUM

A collection of ten papers from the Consultants Bureau translations of the Soviet Journal of Analytical Chemistry and the famous "Doklady" of the Academy of Sciences (1949-58)... This collection will acquaint the analytical chemist working in this field with Soviet techniques for the determination of uranium in solutions, in ores and the products of their treatments, and in accessory minerals, plus methods for the determination of impurities in uranium.

heavy paper covers — illustrated — $10.00

CONTENTS

- Extraction of Uranyl α-Nitroso-β-naphtholate and Separation of Uranium from Vanadium and Iron.
- The Composition of Uranyl Selenite. A Volumetric Method of Determining Uranium.
- The Composition of the Luminescence Center of Sodium Fluoride Beads Activated by Uranium.
- Rapid Luminescent Determination of Uranium in Solutions.
- Preparation of Slightly Soluble Compounds of Quadrivalent Uranium Using Rongalite.
- Investigation of Complex Compounds of the Uranyl Ion Which are of Importance in Analytical Chemistry.
- Uranyl and Thorium Selenites.
- The Evaporation Method and Its Use for the Determination of Boron and Other Impurities in Uranium.
- Spectrographic Determination of Uranium in Ores and the Products Obtained by Treatment of These Ores.
- Determination of Uranium in Accessory Minerals.

CONSULTANTS BUREAU

227 WEST 17TH STREET NEW YORK 11 N Y

Research by Soviet Experts
Translated by Western Scientists

Soviet Research on the LANTHANIDE AND ACTINIDE ELEMENTS, 1949-1957

An important contribution to the literature of nuclear chemistry, this collection of papers is a comprehensive presentation of Soviet research on the chemistry of lanthanides and actinides. The 106 reports included in this collection appeared in the major Soviet chemical journals translated by Consultants Bureau, as well as in the Soviet Journal of Atomic Energy, 1949-1957.

The five sections, totalling 657 pages, provide broad representation of contemporary Soviet research in this important aspect of nuclear science. This collection should be accessible to all nuclear researchers, whether theoretical or applied.

Each part may be purchased as follows:

Basic Chemistry (25 papers) **$15.00**
Analytical and Separation Chemistry (30 papers) **$20.00**
Nuclear Chemistry (and Nuclear Properties) (32 papers) ... **$22.50**
Geology (10 papers) **$7.50**
Nuclear Fuel Technology (9 papers) **$7.50**
Complete collection **$65.00**

RADIATION CHEMISTRY, PROCEEDINGS OF THE FIRST ALL-UNION CONFERENCE MOSCOW, 1957

More than 700 of the Soviet Union's outstanding research scientists participated in this conference sponsored by the Academy of Sciences and the Ministry of the Chemical Industry. Each of the 56 reports read in the various sessions covers either the theoretical or practical aspects of radiation chemistry, and special attention is given to radiation sources used in radiation-chemical investigations. The general discussions which followed each report and reflected various points of view on the problem under analysis are also included.

Primary Acts in Radiation Chemical Processes
heavy paper covers 5 reports, plus discussion ..... illustrated **$25.00**
Radiation Chemistry of Aqueous Solutions (Inorganic and Organic Systems)
heavy paper covers 15 reports, plus discussion ..... illustrated **$50.00**
Radiation Electrochemical Processes
heavy paper covers 9 reports, plus discussion ..... illustrated **$15.00**
The Effect of Radiation on Materials Involved in Biochemical Processes
heavy paper covers 6 reports, plus discussion ..... illustrated **$12.00**
Radiation Chemistry of Simple Organic Systems
heavy paper covers 9 reports, plus discussion ..... illustrated **$30.00**
The Effect of Radiation on Polymers
heavy paper covers 9 reports, plus discussion ..... illustrated **$25.00**
Radiation Sources
heavy paper covers 3 reports ..... illustrated **$10.00**

Individual volumes may be purchased separately.

NOTE: Individual reports from each volume are available at $12.50 each. Tables of contents sent upon request.

special price for the 7-volume set **$125.00**

Payment in sterling may be made to Barclay's Bank in London, England.

CONSULTANTS BUREAU
227 West 17th Street · New York, N.Y., U.S.A.